Newsletters on Stratigraphy, Vol. 50/2 (2017), 141–185 **Article**
Published online February 2017; published in print April 2017

Correlation of Turonian continental margin and deep-sea sequences in the subtropical Indian Ocean sediments by integrated planktonic foraminiferal and calcareous nannofossil biostratigraphy

Brian T. Huber[1]*, Maria Rose Petrizzo[2], David K. Watkins[3], Shannon J. Haynes[4], and Kenneth G. MacLeod[5]

With 11 figures, 6 tables, 6 plates and 2 appendices

Abstract. Marine mudstone sediments recovered from multiple boreholes drilled in southeast Tanzania yield some of the best preserved Turonian microfossils in the world, and these specimens provide a valuable new perspective on planktonic foraminiferal and calcareous nannofossil evolution, taxonomy, biostratigraphy, and biodiversity. High sedimentation rates and the consistent presence of well-preserved microfossil assemblages throughout the sequence increase the resolution of biostratigraphic data generated allowing for improved correlation within and outside the depositional basin. The late early–middle Turonian Tanzanian record reveals prolonged species stasis with essentially no changes in relative abundance, no extinctions, and no evolutionary appearances for both calcareous plankton groups until the late middle Turonian. This interval is followed in the late Turonian by two species turnovers. The older of these occurs at the top of the mid-Turonian *Helvetoglobotruncana helvetica* Zone, where last occurrences of three planktonic foraminiferal species are followed, within several meters, by first occurrences of five foraminiferal species and an increase in the abundance of dwarfed planktonic forms. Changes in the calcareous nannofossil assemblages at this level are modest and include the extinction of one calcareous nannofossil species and an abrupt but temporary spike in the abundance of another species. There are no obvious changes in lithology, bulk sediment geochemistry, or stable isotope values across this first turnover event. The second, larger species turnover occurs at a hiatus within the late Turonian *Marginotruncana sinuosa-Huberella huberi* Zone and is marked by extinction of three calcareous nannofossil species followed by first appearances of four calcareous nannofossil species. Corresponding with the nannofossil first occurrences is a dramatic increase in the relative abundance of several species of biserial planktonic foraminifera, an increase in average grain size, and a shift in preservation

Authors' addresses:
[1] Department of Paleobiology, MRC-121, National Museum of Natural History, Smithsonian Institution, Washington, DC 20013, USA. huberb@si.edu
[2] Dipartimento di Scienze della Terra "A. Desio", Università degli Studi di Milano, via Mangiagalli 34, 20133 Milano, Italy. mrose.petrizzo@unim.it
[3] Department of Geology, University of Nebraska, Lincoln, Nebraska 68588, USA. dwatkins1@unl.edu
[4] Department of Geological Sciences, University of Missouri-Columbia, Columbia, MO 65211, USA. sjh2c4@mail.missouri.edu
[5] Department of Geological Sciences, University of Missouri-Columbia, Columbia, MO 65211, USA. MacLeodK@missouri.edu
* Corresponding author: huberb@si.edu

www.borntraeger-cramer.de
DOI: 10.1127/nos/2017/0373 0078-0421/2017/0373 $ 11.25

such that foraminiferal tests in overlying samples are infilled with sparry calcite. Revisions to the Turonian foraminiferal and nannofossil biozonations, including replacement of the *Marginotruncana schneegansi* Zone with two zones, the *Falsotruncana maslakovae* Zone overlain by the newly defined *Marginotruncana sinuosa-Huberella huberi* Zone, are proposed following detailed taxonomic and biostratigraphic comparisons. One new planktonic foraminiferal species, *Helvetoglobotruncana microhelvetica* Huber and Petrizzo n. sp., is described. Age-depth models are developed for both sites to identify diachronous vs. reliable bioevents, to estimate sedimentation rates and hiatus durations. Comparison between the Tanzanian calcareous plankton distributions and those in Turonian samples from Ocean Drilling Program Hole 762C (Exmouth Plateau, southeast Indian Ocean) reveals (1) relatively gradual changes at Hole 762C rather than an interval of stasis followed by turnover events in Tanzania and (2) significant diachroneity in the position of many lowest and highest occurrences, resulting in inconsistency in the order of events. Species diachroneity is attributed to dissimilar mesotrophic and oligotrophic environmental settings of the clastic margin vs. pelagic carbonate environments.

Key words. Cretaceous, planktonic foraminifera, calcareous nannofossils, Turonian, biostratigraphy

1. Introduction

The Turonian was a time when global temperatures and sea level reached a maximum for the Cretaceous Period, the equator-to-pole temperature gradient was low and the biogeographic distribution of thermophilic marine calcareous plankton was expanded poleward (Huber et al. 1995, 2002, Watkins et al. 1996, Petrizzo et al. 2000, 2001, Bice et al. 2003, Friederich et al. 2012, Haq 2014). The base of the Turonian, corresponds with the middle of Oceanic Anoxic Event 2 (OAE2), which was 450–600 kyr in duration and is correlated globally by a large positive carbon isotope excursion (Schlanger et al. 1987, Jenkyns et al. 1994, Jenkyns 1999, Tsikos et al. 2004, Jarvis et al. 2006, Voigt et al. 2008, Meyers et al. 2012). OAE2 was probably triggered by intense volcanic eruptions (Turgeon and Creaser 2008, Du Vivier et al. 2014) and changes in circulation patterns (e. g., MacLeod et al. 2008, Martin et al. 2012, Zheng et al. 2013, 2016) leading to abrupt global warming, widespread oceanic dysoxia, and widespread deposition of organic-rich sediments (Schlanger and Jenkyns 1976, Arthur et al. 1987, Jenkyns 2010). Deep water warming and restructuring of the vertical water column during OAE2 may have caused the selective extinction of some deeper dwelling planktonic foraminifera (Premoli Silva and Sliter 1999, Huber et al. 1999, Leckie et al. 2002), and significant changes in the composition of calcareous nannofossil assemblages (Linnert et al. 2010).

The early through middle Turonian has been considered to be a time of stasis among the calcareous plankton communities, with little change in species diversity or taxonomic composition (Premoli Silva and Sliter 1999, Hart 1999, Bown et al. 2004). It was also a time of prolonged extreme global warmth, with oxygen isotope paleotemperature records showing little temporal variation (Voigt et al. 2004, Macleod et al. 2013).

The late Turonian has been characterized as a time of increased speciation and enlargement in test size among the planktonic foraminifera, primarily as a result of diversification of the *Marginotruncana* lineage (e. g., Caron 1985, Premoli Silva and Sliter 1999), but the timing and rate of this speciation event has not been well documented. Among calcareous nannofossil taxa, there was also a late Turonian increase in diversity, but the timing of this taxonomic change has not been well documented. The few oxygen isotope paleotemperature data available for the late Turonian show persistence of extreme global warmth, but the records are discontinuous and not well dated (Huber et al. 2002, Voigt et al. 2004, Friedrich et al. 2012).

Ages of planktonic foraminiferal first and last occurrence events have been reliably calibrated in the early Turonian, but are poorly calibrated in the middle and late Turonian. The Global Boundary Stratotype, Section and Point (GSSP) for the base of the Turonian, located in the Rock Canyon Anticline west of Pueblo, Colorado, has been dated at 93.9 Ma using cyclostratigraphic and radioisotopic chronometry (Meyers et al. 2012). The boundary is placed ~0.3 m.y. after the initial carbon isotope ($\delta^{13}C$) excursion that is used to identify the onset of OAE2 (Joo and Sageman 2014). Although the duration of the Turonian is stated as 4.1 m.y. in the 2012 Geologic Time Scale (GTS 2012, Gradstein et al. 2012), radiometric and astrochronologic age control is limited to the earliest 200 kyr of the stage (Meyers et al. 2012) and few stratigraphically continuous rock records of the stage are available for biostratigraphic study.

Significant differences in the relative timing of Turonian planktonic foraminiferal and calcareous nannofossil bioevents and their inter-correlation have led to uncertainties in the chronostratigraphic framework applied in various studies. For example, the first appearance datum (FAD) of the calcareous nannofossil *Quadrum gartneri* Prins and Perch-Nielsen (in Manivit et al. 1977), is within or just above the uppermost portion of the positive $\delta^{13}C$ excursion that defines OAE2 (Tsikos et al. 2004, Linnert and Mutterlose 2015) and below the FAD of the planktonic foraminifer *Helvetoglobotruncana helvetica* (Bolli 1945), whereas GTS 2012 onsiders these FADs to be synchronous. Similarly, the relative order of the FAD of *Eiffellithus eximius* (Stover 1966) and the last appearance datum (LAD) of *H. helvetica* and the assigned ages also differ considerably among various studies and geological time scale schemes (see discussion in Huber and Petrizzo 2014, p. 46). Accurate identification of these events is important as each of these species is used to identify biozones in standard tropical/subtropical biostratigraphic schemes.

This study focuses on planktonic foraminiferal and calcareous nannofossil distributions in Turonian cores that were drilled in a shelf/slope marine sequence in southeast Tanzania during the Tanzania Drilling Project (TDP). Calcareous microfossil distributions are compared with cores drilled in pelagic carbonate sediments deposited on Exmouth Plateau (subtropical southeast Indian Ocean) at Ocean Drilling Program (ODP) Hole 762C. Turonian microfossils from the TDP sites provide many advantages for study. The tests are commonly preserved as glassy (= optically translucent) tests with wall textures that are nearly indistinguishable from modern specimens, and their shell geochemistry has been effectively unaltered by diagenetic processes (Jimènez Berrocoso et al. 2010, 2012, 2015, Wendler, I. et al. 2011, 2013, MacLeod et al. 2013, Huber and Petrizzo 2014, Haynes et al. 2015). Calcareous nannofossil assemblages include dissolution-susceptible and fragile specimens that have been rarely or never observed elsewhere, resulting in unusually high species diversity in Tanzanian samples (Lees 2007). Calcareous dinoflagellates reveal wall architectures that have not been previously observed (Wendler, J. et al. 2013, Wendler and Bown 2013).

Analysis of the Turonian TDP borehole samples provides an unprecedented opportunity to integrate the relative order of species occurrences for planktonic foraminiferal and calcareous nannofossil assemblages that lived in a turbid, mesotrophic setting with assemblages that lived in a deep sea oligotrophic on the opposite side of the Indian Ocean. The main objectives of this paper are to: (1) clarify taxonomic uncertainties among planktonic foraminifera and calcareous nannofossils that have been a source of confusion and inconsistent age ranges in the literature; (2) integrate the Turonian distribution data for select species of both plankton groups from the TDP and ODP sites to determine which species are most reliable for correlating between the continental margin and pelagic carbonate depositional settings; and (3) establish a more reliable integrated biostratigraphic framework for global correlation of Turonian marine sediments. A forthcoming companion paper will present more detailed observations on the taxonomy and evolution of the Turonian planktonic foraminifer and calcareous nannofossil assemblages.

2. The Tanzania Drilling Project

The Tanzania Drilling Project (TDP) was initiated in 2002 to recover stratigraphically continuous records of microfossil lagerstätte using portable, land-based drilling rigs with maximum penetration depths of 100–200 m. The first phase of TDP coring (2002–2006) drilled 20 drill sites with a focus mostly on recovery of Cenozoic sediments, but one site (TDP 15) located in the Kilwa District (Fig. 1), targeted Turonian sediments. Interpretations of the regional stratigraphy and geology and the initial results from this phase of field reconnaissance and drilling were published in Pearson et al. (2001, 2004, 2006) and Nicholas et al. (2006, 2007). The second phase of TDP coring (2007–2009) was devoted to field mapping and drilling of Cretaceous sediments at 19 sites, 10 of which cored Turonian sediments. Nine of the Turonian sites were drilled near Lindi village and one (TDP 38) was drilled in the Kilwa District (Fig. 1). Initial results of the drilling and field work and interpretations of the regional geology and stratigraphy were published in Jiménez Berrocoso et al. (2010, 2012, 2015).

The two primary goals for the Cretaceous TDP were to test the greenhouse ice sheet hypothesis, which proposes links between brief cooling events, sea level changes, and growth of polar ice sheets during greenhouse climates (e.g., Gale et al. 2002, Voigt et al. 2004, Miller et al. 2004, 2005, Bornemann et al. 2008) and to obtain a complete sediment record across the Cenomanian-Turonian boundary (CTB) to characterize biotic and geochemical changes associated with

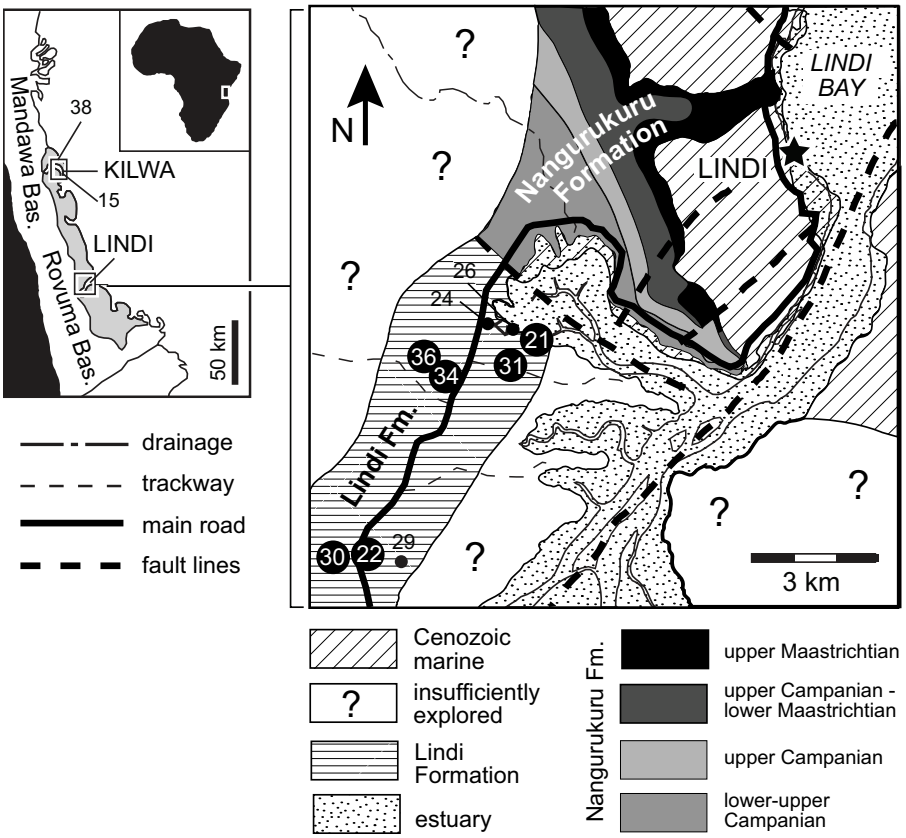

Fig. 1. Coastal geology map showing the distribution of Cretaceous sediments in the Rovuma and Mandawa Basins in eastern Tanzania. Principle TDP site locations discussed in this study are shown as black circles, other sites yielding Turonian sediments shown as unfilled numbers.

OAE2. The remarkably constant oxygen isotope data generated from TDP 31 foraminifera demonstrated that the hot greenhouse climate was not interrupted by growth of a polar ice sheet during the Turonian (MacLeod et al. 2013). Unfortunately, efforts to recover a complete CTB were unsuccessful at all 11 of the Turonian drill sites because of borehole collapse and other drilling complications at eight of the sites and presence of an unconformity or faulted contact at the other sites (Nicholas et al. 2006, Jiménez Berrocoso et al. 2010, 2012, 2015). Until now, age determinations for the oldest Turonian and youngest Cenomanian sediments have remained problematic due to contradictory interpretations of the planktonic foraminifera and calcareous nannofossil biostratigraphies. Absence of laterally continuous lithostratigraphic marker beds has impeded regional correlation of the boreholes.

3. Geologic setting of southeast Tanzania

Extensional tectonics and rifting between Madagascar and East Africa during the Jurassic, caused by the breakup of Gondwana continents, led to the formation of the Mandawa and Ruvuma basins in southern Tanzania (Salman and Abdula 1995, Key et al. 2008). A period of tectonic stability and gradual subsidence of these basins from the late Albian through early Oligocene resulted in accumulation of a thick, relatively homogeneous, clay-dominated succession that is included in the Kilwa Group (Nicholas et al. 2006). This sedimentary succession was deposited in a submarine fan system that was spread over considerable distances on a passive margin. These sediments have a gentle oceanward dip and have been exposed in a continuous band that parallels the Tanzania coastline to the south of Dar es Salaam by post-Miocene uplift (Fig. 1). Mapping of fault traces and structural pop-up structures in the southeast coastal region suggests that a switch from quiescent to compressional tectonics occurred sometime after the Oligocene (Nicholas et al. 2007).

Nicholas et al. (2006) assigned the lower portion of the Kilwa Group to the Nangurukuru Fm., which was described as a claystone unit containing silt and minor sandstone interbeds and was given an age range from the Santonian to Maastrichtian. The base of the Kilwa Group was subsequently extended stratigraphically downward based on the recognition of a Lindi Fm. This unit was described in Jiménez Berrocoso et

al. (2015) and dated as ranging from late Albian to Coniacian in age. The Lindi Fm. is mostly composed of dark, finely laminated claystones and siltstones containing thin sandstone interbeds and less carbonate than the overlying Nangurukuru Fm. (Petrizzo et al. 2017). The base of the Lindi Fm. is in conformable contact with with the underlying Albian lithified, coarse sandstone.

The Lindi Fm. was deposited in the subtropical western Indian Ocean at about 35° S paleolatitude according to the paleogeographic reconstruction of Hay et al. (1999; Fig. 2). An outer shelf to upper slope setting is inferred for the Lindi Fm. based on the predominance of clay and fine silt lithologies, relatively abundant and diverse assemblages of planktonic foraminifera and calcareous nannofossils, sporadic distribution of mollusks, including ammonites, micro-bivalves, and micro-gastropods, and absence of storm-related sedimentary structures (Jiménez Berrocoso et al. 2015). The distance between the TDP boreholes and the nearest Cretaceous shoreline was estimated to be at least 50 km based on the field studies of Kent et al. (1971).

The more organic-rich, laminated intervals in the Turonian sequence suggest deposition under reduced energy and possibly low oxygen conditions, while occasional thin, massive, bioturbated sandstone beds in the Lindi Fm. were probably emplaced during more oxygenated offshore bottom current transport (Jiménez Berrocoso et al. 2015). Studies of the organic biomarker composition of the Cretaceous and Paleogene sediments indicates the organic matter is thermally immature and is mostly composed of terrestrially derived material with very little contribution by marine sources (van Dongen et al. 2006, Haynes et al. 2016). The excellent microfossil preservation has been attributed to shallow burial of impermeable, clay-rich sediments (Pearson et al. 2004) and reduced microbial activity in the sediment column during deposition and early diagenesis (Haynes et al. 2016).

4. Material and methods

Continuous coring of the TDP sites was achieved using a portable drill rig with wireline capability and a maximum penetration depth of ~200 m. The core diameter is 48 mm for Sites 21–35 and 64 mm for Sites 36–40. Each core is usually 1 to 3 m in length and full core-sections are 1 m in length. Standard core sample notation is written in the order site, core, core-section, and centimeter interval.

Turonian planktonic foraminifera and calcareous nannofossils were analyzed for biostratigraphic study primarily from five TDP boreholes drilled 6–12 km southwest of Lindi village (Figs. 1, 3), including TDP sites 22, 30, 31, 34, and 36. Turonian samples from sites 21, 24, 26, 29 (all southwest of Lindi) and sites 38 and 15 (140 and 160 km north of Lindi, respectively) were also examined for planktonic foraminifera during this investigation. Lithologic descriptions, latitude and longitude coordinates, preliminary sedimentologic and biostratigraphic interpretations, and geochemical measurements, including Total Organic Carbon (TOC), and bulk sediment carbonate and organic matter $\delta^{13}C$ and $\delta^{18}O$, were obtained for about 1 sample per 1 to 2 cores and were published in Jiménez Berrocoso et al. (2010, 2012, 2015).

In the present study we distinguish between lowest (LO) and highest (HO) stratigraphic occurrences of planktonic foraminifera and calcareous nannofossils that are used to define biozone boundaries within the sections and first-appearance (FAD) and last-appearance (LAD) datums that are used to define the temporal limits of a bioevent globally.

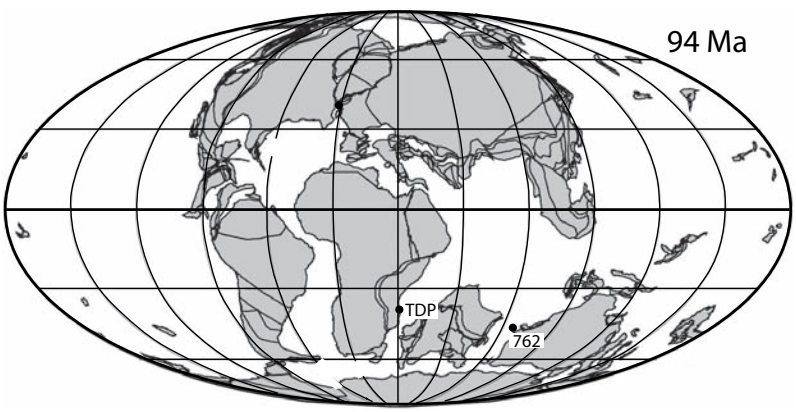

Fig. 2. Paleogeographic map for 94 Ma showing locations of TDP sites and DSDP Site 762 from a reconstruction using the Ocean Drilling Stratigraphic Network (http://www.odsn.de/) and parameters from Hay et al. (1999).

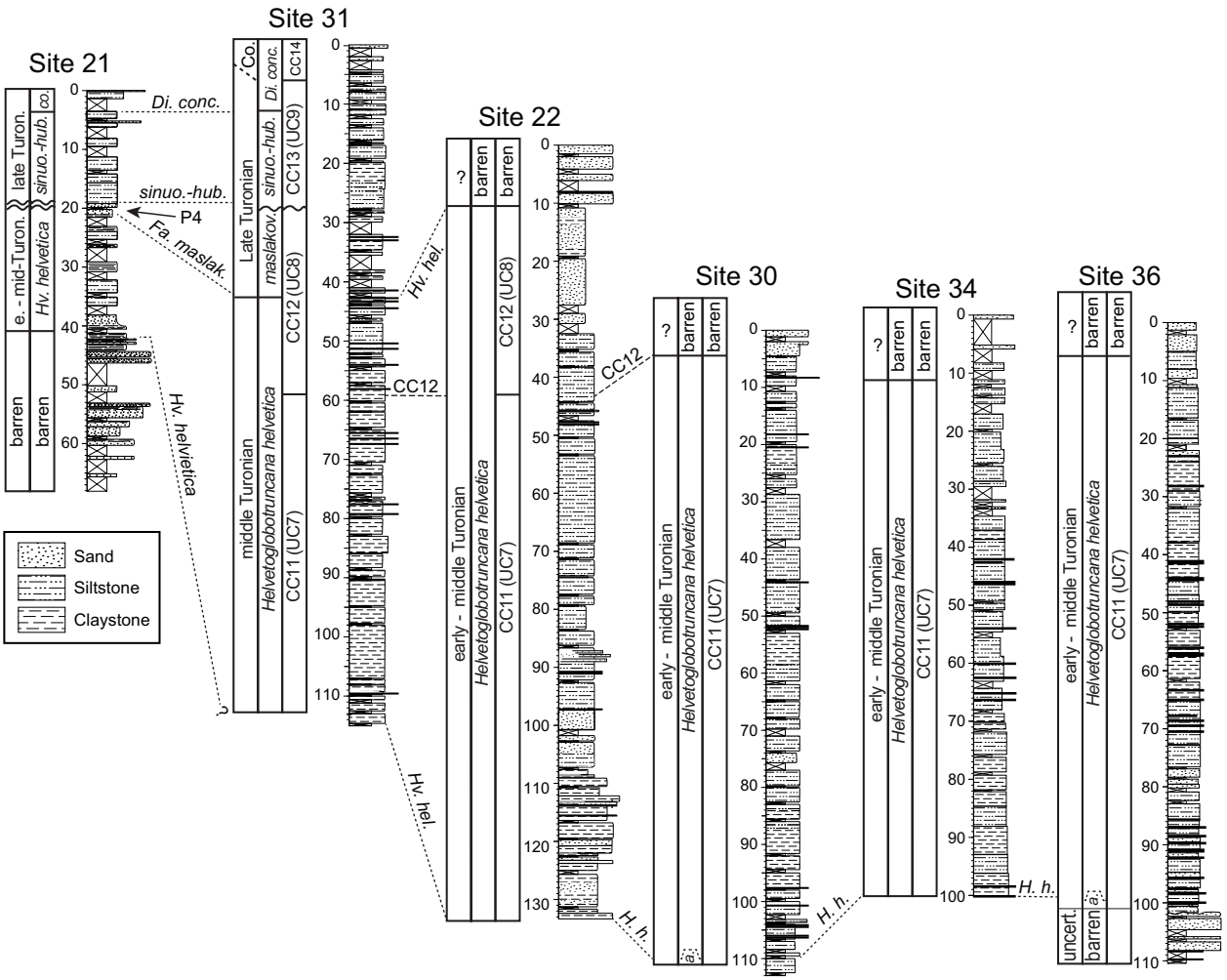

Fig. 3. Correlation of Turonian TDP boreholes in the region of Lindi Village showing (l-r) age, planktonic foraminifera and calcareous nannofossil biozones ("CC" zonation of Perch Nielsen 1985 and "UC" zonation of Burnett 1998), core number, and depth (meters below surface). Abbreviations include: "a" = *Whiteinella archaeocretacea* Zone; "*H. hel*." and "*H. h*." = *Helvetoglobotruncana helvetica* Zone; "*F. maslak*." and "*maslakov*." = *Falsotruncana maslakovae* Zone; "*sinuo.-hub*." = *Marginotruncana sinuosa – Huberella huberi* Zone; "*co*." = *Dicarinella concavata* Zone; "Co." = Coniacian; "uncert." = uncertain. "P4" refers to a fault block containing a Paleocene Zone P4 planktonic foraminiferal assemblage. Dashed lines represent uncertainty discussed in the text; wavy lines represents a hiatus.

Foraminiferal preservation ratings are as follows: E = excellent (sample includes "glassy" shells with no evidence of recrystallization or secondary mineral infilling or overgrowth); G = good ("frosty" shells with minor recrystallization, but no evidence of secondary mineral infilling or overgrowth); M = moderate (opaque shells with minor to significant shell recrystallization, presence of secondary mineral infilling or overgrowth); P = poor (shells strongly recrystallized and infilled or strongly fragmented).

During the Turonian, Ocean Drilling Program (ODP) Hole 762C (Exmouth Plateau, southeast Indian Ocean) was located near 50° S (von Rad et al. 1992, Lawver et al. 1992, Hay et al. 1999) on the northwestern Australian margin in a transitional setting between the Tethyan and Austral bioprovinces (Fig. 2; Howe et al. 2003). Previous biostratigraphic studies of Cretaceous planktonic foraminifera at Hole 762C highlighted a strong Tethyan affinity of the Albian to early Campanian assemblages with some exceptions due to the absence and/or diachronous appearance of some Late Cretaceous subtropical biostratigraphic markers. These anomalous distributions necessitated the use of different zonal markers on Exmouth Plateau for the Turon-

ian–Coniacian stratigraphic interval than in standard Tethyan sections (Wonders 1992, Petrizzo 2000, 2003). A change in composition of the assemblages from a Tethyan to Transitional Bioprovince affinity occurred during the Campanian (Petrizzo 2002, Petrizzo et al. 2011) and the Maastrichtian (Zepeda 1998, Campbell et al. 2004). This prevented application of the standard Tethyan biozonation scheme. The present re-evaluation of Turonian planktonic foraminifera from cores 74X–69X at Hole 762C is designed to check the stratigraphic occurrences of some species according to recent taxonomic revisions and updated species concepts.

Turonian calcareous nannofossils from Hole 762C were examined as part of a preliminary study by Bralower and Siesser (1992). In the present study calcareous nannofossil identification and biostratigraphy was performed using 22 samples from Hole 762C.

4.1 Foraminiferal analyses

Foraminiferal samples averaging 20 cm in length were taken at ~1 m intervals from whole-round TDP cores at all drill sites. Samples were disaggregated and washed through a 63 μm sieve using tap water and then air-dried. Presence-absence observations for biostratigraphically important planktonic species are presented in Table 1 for TDP 31 and a summary of the subsurface depths and core samples for key events determined for the 11 TDP sites that recovered Turonian sediments is presented in Table 2. Preliminary observations of the foraminiferal biostratigraphy published in Jiménez Berrocoso et al. (2010, 2012, 2015) are superseded by results of the present study. Samples for foraminiferal study from ODP Hole 762C were processed according to methodology explained in Petrizzo (2000). Planktonic foraminiferal biozones follow Petrizzo (2000) and have been revised in this study. Presence-absence observations for Hole 762C are presented in Table 3 and a summary of the subsurface depths and core samples for key datums are presented in Table 4.

Taxonomic revisions and biostratigraphic distribution data recently published by Haynes et al. (2015) for biserial planktonic foraminifera and Huber and Petrizzo (2014) for *Helvetoglobotruncana* spp. are incorporated in the present study. Taxonomic concepts for remaining taxa are mostly drawn from Robaszynski et al. (1979, 1984), Caron (1985), and Huber and Leckie (2011). Primary and secondary type images and original species descriptions for all discussed taxa are presented in the Mikrotax Online Taxonomic Atlas (http://www.mikrotax.org/pforams/index.html). All biostratigraphically important species are listed in Appendix 1 along with remarks for taxa that require additional clarification. Species were designated with the suffix "s.l." (= *sensu lato*) or "s.s." (= *sensu stricto*) depending on how close their morphology compared with the original species concept. Species abundance data and paleoenvironmental interpretations of the Turonian portion of the Lindi Fm. and ODP Hole 762C will be presented in a companion paper (Huber et al., in prep.).

Definitions of the Turonian planktonic foraminiferal biozones applied in this study and their ages are summarized below, from oldest to youngest:

Whiteinella archaeocretacea Partial-Range Zone
Definition: Body of strata with *Whiteinella archaeocretacea* from the extinction of Cenomanian *Rotalipora cushmani* to the lowest occurrence of *Helvetoglobotruncana helvetica*.
Author: Bolli, 1966 (by synonymy = *Praeglobotruncana gigantea* Zone)
Age at base: Latest Cenomanian–early Turonian; base 94.30 Ma determined from calibration of the *R. cushmani* extinction in Bed 68 at the Pueblo, Colorado GSSP section (Caron et al. 2006) and the cyclostratigraphic age model of Meyers et al. (2012). Using the age calibration for the base of the overlying *H. helvetica* Zone the duration of this zone is calculated as 0.78 m.y.

Helvetoglobotruncana helvetica Taxon-Range Zone
Definition: Body of strata containing the total range of the nominate taxon.
Author: Sigal, 1955 (by synonymy = *Praeglobotruncana gigantea* Zone)
Age: Late early–middle Turonian; base 93.52 Ma determined by calibration of the *H. helvetica* extinction in Bed 102 at the Pueblo, Colorado GSSP section (Caron et al. 2006) using the cyclostratigraphic age model of Meyers et al. (2012). The age of the top of the zone must be younger than 92.77 Ma (Huber and Petrizzo 2014), which is the calibrated age for the highest occurrence of *H. helvetica* at the top of the outcrop at the Pueblo section where the total stratigraphic range of the species is not recorded (Caron et al. 2006).

Falsotruncana maslakovae Partial-Range Zone
Definition: Body of strata containing *F. maslakovae* from the highest occurrence of *H. helvetica* to the lowest occurrences of *Marginotruncana sinuosa* and/or *Huberella huberi*.

Table 1 Presence/absence data for Turonian mostly non-biserial planktonic foraminiferal at TDP Site 31. See Haynes et al. (2015) for relative abundance data for biserial species and benthic foraminiferal percent abundance data.

TDP 31	Depth (mbs)	Preservation	Planktonic Foram Zone	*D. hagni*	*D. hagni* (small)	*H. helvetica*	*H. microhelvetica*	*H. praehelvetica*	*P. stephani*	*W. aprica*	*D. marianosi*	*D. canaliculata*	*M. caronae*	*Archaeoglobiger.* spp.	*M. pseudolinneiana*	*M. sigali*	*M. amabilis*	*F. maslakovae*	*M. coldreriensis*	*M. coronata*	*M. schneegansi*	*M. angusticarenata*	*M. sinuosa*	*Hu. huberi*	*M. tarfayensis*	*G. asper*	*M. undulata*	*A. cretacea*	*C. fornicata*	*M. flandrini*	*D. concavata*	*P. nuttalli*
1-1, 34-50	0.42	M	*Di. concavata*									x		x	x		x		x	x		x	x	x	x	x	x	x	x	x	x
2-1, 20-34	2.27	M										x		x	x		x		x	x		x	x	x	x	x	x	x	x	x	x
3-1, 32-54	4.63	M/P											x	x	x	x	x		x	x		x	x	x	x	x	x	x	x	x	
4-1, 20-35	5.28	G										x		x	x				x	x		x	x	x			x	x	x		x	
5-1, 7-29	7.18	M										x		x	x	x	x		x	x		x	x	x		x	x	x	x		x	
6-1, 80-105	8.93	M-G								x		x	x	x	x		x		x	x		x	x	x		x	x	x	x		x	
7-1, 75-90	10.83	M-G										x	x	x	x		x		x	x	x		x	x			x		x		x	
8-1, 58-76	11.67	M-G	*Mg. sinuosa - Hu. huberi*											x	x		x		x			x	x	x		x	x					
9-1, 34-51	12.93	M-G												x	x		x		x	x		x	x	x		x	x	x	x			
10-1, 19-39	14.29	M/G							x					x	x		x	x	x	x	x		x	x		x	x		x	x		
10-2, 90-110	16.00	M												x										x								
11-1, 0-20	16.60	M										x	x	x	x		x	x	x	x	x		x	x		x	x	x				
12-2, 43-62	18.53	M							x					x	x		x		x	x	x	x	x	x			x	x	tr			
13-1, 26-40	19.93	M											x	x	x	x	x		x	x			x	x		x	x					
14-2, 5-25	21.15	M											x	x	x		x		x	x		x	x	x	x	x	x	x				
15-1, 69-88	22.49	M										x	x	x	x		x		x	x	x		x	x		x		x	tr			
16-2, 10-20	24.15	M/G							x			x		x	x		x		x	x		x	x	x	x	x	x	x				
17-2, 24-40	25.72	M							x					x	x	x	x		x	x	x		x	x	x	x	x	x	tr			
18-2, 20-40	27.30	M							x				x	x	x	x	x	x	x	x	x	x	x	x	x	x			tr			
19-1, 2-20	28.11	G	*Falsot. maslakovae*									x	x	x	x		x	x	x	x		x	x						tr			
20-1, 36-56	29.46	G							x				x		x		x															
21-1, 45-65	32.55	G							x				x	x	x		x		x										tr			
21-2, 74-94	33.84	G/E		x																												
22-1, 2-20	35.11	G/E							x			x		x	x			x	x													
23-1, 40-60	38.50	G							x			x	x	x	x		x	x	x	x	x								tr			
24-1, 50-70	39.60	G										x		x	x	x	x		x										tr			
25-1, 30-50	41.40	G							x				x	x	x	x	x	x	x	x	x											
26-1, 40-60	43.10	M	*Helvetoglobotruncana helvetica*	x	x	x	x	x			x			x	x	x	x															
26-1, 73-75	43.34	G/E											x	x																		
27-2, 5-25	45.15	G		x	x	x	x	x	x	x		x																				
28-1, 5-25	46.25	G		x	x	x	x	x	x	x	x	cf.																				
29-1, 27-47	47.37	G		x	x	x		x	x	x	x																					
30-1, 40-60	50.65	G		x	x	x	x	x	x	x	x																					
31-1, 34-53	52.52	G		x	x	x		x	x	x	x																					
32-1, 94-109	54.10	G/E		x	x	x	x	x	x	x	x																					
34-1, 45-65	56.55	M		x	x	x	x	x	x	x	x																					
35-1, 50-70	58.10	M		x	x	x	x	x	x	x																						
36-1, 10-29	59.20	G		x		x	x	x	x																							
38-1, 29-49	62.39	G		x	x	x	x	x	x		x																					
39-1, 43-62	65.53	G		x	x	x	x	x	x	x																						
40-1, 29-40	68.48	G		x	x	x	x	x	x																							
42-1, 20-40	73.00	G		x	x	x	x	x	x	x	x																					
44-1, 22-42	76.72	G		x	x	x	x	x	x	x																						
46-1, 3-23	80.13	G/E		x	x	x	x	x	x	x	x																					
47-1, 57-77	83.67	G		x	x	x	x	x	x	x	x																					
48-1, 58-78	86.68	G/E		x	x	x	x	x	x	x	x																					
50-1, 12-30	90.23	G		x	x	x	x	x	x	x	x																					
51-1, 31-51	90.81	G/M		x	x	x	x	x	x	x																						
53-3, 10-30	97.20	M		x	x	x	x	x	x	x	x																					

Table 1 Continued.

54-1, 70-90	98.80	G	x	x	x	x	x	x	x	x																				
55-1, 73-93	99.83	G/M	x	x	x		x	x	x	x																				
56-2, 0-20	101.14	G	x	x	x	x	x	x	x											cf.										
57-1, 70-90	102.04	G	x	x	x	x	x	x	x	x																				
58-1, 54-74	104.88	E	x	x	x	x	x	x																						
59-1, 11-31	107.45	E	x	x	x	x	x	x	x	x																				
60-1, 47-67	108.81	G	x	x	x	x	x	x		x																				
61-1, 14-26	109.50	G	x	x		x	x	x	x	x																				
62-1, 9-29	110.19	G	x	x		x	x	x	x	x																				
63-1, 29-49	111.49	G	x	x		x	x	x	x	x																				
64-1, 45-65	113.55	G	x	x	x	x	x	x	x	x																				
64-2, 37-57	114.47	G	x	x	x	x	x	x	x																					

Table 2 Turonian planktonic foraminiferal and calcareous nannofossil (accompanied by CC zones) lowest and highest occurrences (LOs & HOs) and first and last appearance datums (FADs and LADs) at TDP drill sites. Bioevents in bold are used as control points for the graphic correlation in Figure 10.

Site	Planktonic foraminiferal event	Age (Ma)	Biozone	Stage	Core sample	Min. depth (m)	Max. depth (m)	Mean depth (m)
	Helvetoglobotruncana helvetica HO	>91.51[a]	*H. helvetica*	mid-Turonian	1/2, 15 cm	5.07	5.07	5.07
TDP 15	*Helvetoglobotruncana helvetica* FAD	93.52[a]	*H. helvetica*	mid-Turonian	39/1, 10 cm	85.75	91.65	88.70
	Helvetoglobotruncana praehelvetica LO	---	?*W. archaeocret.*	lower/mid-Turon.	46/1, 70-90 cm	101.60	101.60	101.60
	Dicarinella concavata FAD	91.08[c]	*D. concavata*	upper Turonian	21/1/1, 70-80 cm	0.80	4.82	2.81
	Huberella huberi LO	---	*M. sinuosa-H. huberi*	upper Turonian	21/8/2, 66-76 cm	18.86	19.33	19.10
	Marginotruncana sinuosa LO	---	*M. sinuosa-H. huberi*	upper Turonian	21/8/2, 66-76 cm	18.86	19.33	19.10
TDP 21	*Helvetoglobotruncana helvetica* HO	>91.51[a]	*H. helvetica*	mid-Turonian	21/8/3, 9-23 cm	17.86	19.33	18.60
	Morozovella formosa LO	<54.00[d]	?	Paleocene	21/9/1, 41-51 cm	20.61	21.28	20.95
	Helvetoglobotruncana helvetica FAD	93.52[a]	*H. helvetica*	mid-Turonian	21/14/1, 76-93 cm	36.03	38.78	37.41
	Helvetoglobotruncana praehelvetica LO	---	?*W. archaeocret.*	lower/mid-Turon.	21/15/2, 41-57 cm	39.67	41.59	40.63
	Helvetoglobotruncana helvetica HO	>91.51[a]	*H. helvetica*	mid-Turonian	22/5/1, 68-88 cm	10.26	11.88	11.07
	Eiffellithus eximius (s.l.) FAD	92.99[a]	CC12	mid-Turonian	22/15/2, 22-23 cm	42.05	45.1	43.55
TDP 22	*Helvetoglobotruncana helvetica* FAD	93.52[a]	*H. helvetica*	mid-Turonian	22/49/1, 58-72 cm	128.32	129.07	128.70
	Quadrum gartnerii FAD	<93.55[a]	CC11	lower Turonian	22/51/1, 22-25 cm	131.92	131.92	131.92
	Helvetoglobotruncana praehelvetica LO	---	?*W. archaeocret.*	lower/mid-Turon.	22/51/2, 24-38 cm	132.08	132.08	132.08
	Helvetoglobotruncana praehelvetica LO	---	?*W. archaeocret.*	lower/mid-Turon.	24/4/1&2, 98-102 cm	5.08	8.24	6.66
	Rotaliporids LAD	<94.24[b]	*T. globotruncanoides*	lower-mid-Cenom.	24/5/1, 7-24 cm	5.08	8.24	6.66
TDP 24	*Thalmanninella globotruncanoides* LO	100.5[c]	*T. globotruncanoides*	lower-mid-Cenom.	24/26/1, 67-80 cm	59.80	60.70	60.25
	Planomalina buxtorfi HO	>101.18[c]	*P. buxtorfi*	upper Albian	24/26/2, 67-80 cm	60.70	59.80	60.25
	Planomalina buxtorfi LO	<101.92[c]	*P. buxtorfi*	upper Albian	24/27/3, 67-80 cm	64.72	66.85	65.79
	Helvetoglobotruncana praehelvetica LO	---	?*W. archaeocret.*	lower/mid-Turon.	26/5/1, 61-85 cm	7.35	8.70	8.03
	Rotaliporids HO	<94.24[b]	*T. globotruncanoides*	lower-mid-Cenom.	26/6/1, 61-80 cm	7.35	8.70	8.03
TDP 26	*Thalmanninella globotruncanoides* LO	<100.5[c]	*T. globotruncanoides*	lower-mid-Cenom.	26/21/3, 104-107 cm	55.33	55.78	55.56
TDP 29	*Helvetoglobotruncana helvetica* HO	>91.51[a]	*H. helvetica*	mid-Turonian	29/10/1, 12-35 cm	17.14	20.35	18.75
	Helvetoglobotruncana helvetica LO	<93.41[a]	*H. helvetica*	mid-Turonian	29/20/1, 31-50 cm	41.50	41.50	41.50
	Helvetoglobotruncana helvetica HO	>91.51[a]	*H. helvetica*	mid-Turonian	30/3/1, 14-34 cm	4.25	5.34	4.80
TDP 30	*Helvetoglobotruncana helvetica* FAD	93.52[a]	*H. helvetica*	mid-Turonian	30/45/1, 25-50 cm	110.50	111.15	110.83
	Helvetoglobotruncana praehelvetica LO	---	?*W. archaeocret.*	lower/mid-Turon.	30/46/2, 41-60 cm	111.60	111.60	111.60

Table 2 Continued.

	Pseudotextularia nuttalli LO	---	*D. concavata*	lower Coniacian	31/2/1, 20-34 cm	0.42	4.63	2.53
	***Micula staurophora* FAD (bMst)**	89.77[c]	CC14	lower Coniacian	31/4/1, 4-6 cm	5.05	6.07	5.56
	Dicarinella concavata FAD (bDc)	91.08[c]	*D. concavata*	upper Turonian	31/7/1, 75-90 cm	10.83	11.67	11.25
	***Micula cubiformis* LO (bMc)**	---	CC13	upper Turonian	31/7/1, 54-57 cm	10.55	11.2	10.88
	***Falsotruncana maslakovae* HO (tFm)**	---	*M. sinuosa-H. huberi*	upper Turonian	31/10/1, 19-39 cm	14.29	14.29	14.29
	Contusotruncana fornicata LO (bCf)	---	*M. sinuosa-H. huberi*	upper Turonian	31/10/1, 19-39 cm	14.29	16.00	15.15
	***Huberella huberi* LO (bHh)**	---	*M. sinuosa-H. huberi*	upper Turonian	31/18/2, 20-40 cm	27.30	28.11	27.71
	***Marginotruncana sinuosa* LO (bMsi)**	---	*M. sinuosa-H. huberi*	upper Turonian	31/18/2, 20-40 cm	27.30	28.11	27.71
	***Marthasterites furcatus* FAD (bMf)**	90.24[a]	CC13	upper Turonian	31/18/2, 52-54 cm	27.53	28.01	27.77
TDP 31	***Eiffellithus eximius* (s.s.) LO (bEe)**	---	CC12	upper Turonian	31/18/2, 52-54 cm	27.53	28.01	27.77
	***Lithastrinus septenarius* (s.s.) LO (bLs)**	---	CC12	upper Turonian	31/18/2, 52-54 cm	27.53	28.01	27.77
	Eprolithus moratus HO (tEm)	---	CC12	upper Turonian	31/19/1, 0-2 cm	27.53	28.01	27.77
	***Reinhardtites biperforatus* FAD (bRb)**	90.71[a]	CC12	upper Turonian	31/18/2, 52-54 cm	27.53	28.01	27.77
	Dicarinella hagni LO (tDh)	---	*F. maslakovae*	upper Turonian	31/21/2/74-94 cm	32.55	33.84	33.20
	***Falsotruncana maslakovae* LO (bFm)**	---	*F. maslakovae*	upper Turonian	31/23-1, 40-60 cm	41.40	43.10	42.25
	***Helvetoglobotruncana helvetica* LAD (tHh)**	>91.51[a]	*H. helvetica*	mid-Turonian	31/26/1, 40-60 cm	42.65	43.10	42.88
	Eiffellithus eximius s. Verbeek FAD (bEe*)	92.99[a]	CC12	mid-Turonian	31/35/2, 14-16 cm	58.65	59.52	59.09
	***Quadrum gartnerii* FAD (bQg)**	<93.55[a]	CC11	lower Turonian	31/64/2, 37-57 cm	114.47	114.47	114.47
	***Helvetoglobotruncana helvetica* FAD (bHh)**	<93.52[a]	*H. helvetica*	mid-Turonian	31/64/2, 37-57 cm	114.47	114.47	114.47
TDP 34	*Helvetoglobotruncana helvetica* HO	>91.51[a]	*H. helvetica*	mid-Turonian	34/4/1, 29-49 cm	5.23	8.99	7.11
	Helvetoglobotruncana helvetica FAD	<93.52[a]	*H. helvetica*	mid-Turonian	34/46/2, 76-98 cm	99.98	100.96	100.47
TDP 36	*Helvetoglobotruncana helvetica* HO	>91.51[a]	*H. helvetica*	mid-Turonian	36/2/3, 80-100 cm	6.90	7.90	7.40
	Helvetoglobotruncana helvetica FAD	93.52[a]	*H. helvetica*	mid-Turonian	36/40/2, 1-21 cm	92.11	93.90	93.01
	Helvetoglobotruncana praehelvetica LO	---	?*W. archaeocret.*	lower/mid-Turon.	36/41/3, 0-21 cm	97.11	98.40	97.76
TDP 38	*Helvetoglobotruncana helvetica* HO	>91.51[a]	*H. helvetica*	mid-Turonian	38/2/1, 57-70 cm	0.74	2.64	1.69
	Helvetoglobotruncana helvetica LO	<93.52[a]	*H. helvetica*	mid-Turonian	38/13/1, 0-17 cm	29.09	29.09	29.09

[a] Huber and Petrizzo 2014
[b] This study; use Caron 2006 HO in mid Bed 68 and Meyers et al. 2012 radiometrically calibrated age for bentonite ~0.3 m above
[c] Gradstein et al. 2012
[d] Berggren and Pearson 2005

Author: Modified herein from Wonders (1992), who defined the base at the extinction of *H. helvetica* and the top at the extinction of *F. maslakovae*.

Age: Late Turonian. The age of the base and top of the zone has not been calibrated.

Comments: This zone is proposed to correlate the lower part of the *M. schneegansi* or *M. sigali* Zones, which have been used interchangeably as an interval zone separating strata that spans from the HO of *H. helvetica* to the LO of *D. concavata* (Premoli Silva and Sliter 1995, Robaszynski and Caron 1995). The distinct morphology of *F. maslakovae* and its relatively short stratigraphic range make it a very useful biomarker for subdividing the late Turonian. It's LO was recorded immediately above the extinction of *H. helvetica* by Caron (1981) in the Pont du Fahs type region of Tunisia, in the southeastern subtropical Indian Ocean (ODP Sites 762 and 763: Wonders 1992, Petrizzo 2000), and in the high latitude Indian Ocean (ODP Site 1138: Petrizzo 2001). In the present study, *F. maslakovae* appears immediately above the extinction of *H. helvetica* at TDP 31, and at Hole 762C reveals its LO is in the same sample as the HO of *H. helvetica*.

Marginotruncana sinuosa – Huberella huberi Concurrent-Range Zone

Definition: Body of strata between the lowest occurrences of *Hu. huberi* and/or *M. sinuosa* to the lowest occurrence of *Dicarinella concavata*.

Author: This study.

Age: Late Turonian. The age of the base and top of the zone have not been calibrated.

Comments: This zone partially replaces the *Marginotruncana* spp and *M. marianosi* Zones previously proposed for the Exmouth Plateau record (Wonders 1992, Petrizzo 2000) and the upper part of the *M. schneegansi* or *M. sigali* Zones (Premoli Silva and Sliter 1995,

Table 3 Presence/absence data for Turonian planktonic foraminifera at ODP Hole 762C.

Hole 762C	Depth (mbsf)	Planktonic Foram Zone	*H. helvetica*	*H. praehelvetica*	*W. aprica*	*D. hagni* s.l.	*P. stephani*	*M. coronata*	*M. pseudolinneiana*	*M. sigali* s.l.	*M. simplex*	*D. canaliculata*	*M. angusticarenata*	*M. simplicissima*	*F. maslakovae*	*M. caronae*	*M. coldreriensis*	*M. flandrini*	*A. cretcaea*	*M. sinuosa*	*H. huberi*	*M. schneegansi*	*D. marianosi*	*C. fornicata*	*P. nuttalli*	*D. concavata*
69X-1, 42-44	780.42	*D. concav.*						x	x		x		x	x		x		x	x	x	x		x	x		x
69X-1, 90-92	780.92							x	x		x		x	x		x		x		x	x	x	x	x		x
69X-2, 6-9	781.59							x	x		x		x	x		x		x		x	x		x	x		x
69X-2, 66-68	782.18							x	x		x		x	x		x		x		x	x		x	x	x	x
69X-CC, 16-18	783.18	*M. sinuosa-H. huberi*						x	x	x	x		x	x			x	x	x	x	x		x	x		
70X-1, 11-13	785.13							x	x		x		x	x		x		x		x	x	x		x		
70X-1, 43-45	785.45				x			x	x		x		x	x		x		x		x	x	x	x			
70X-1, 62-64	785.64				x			x	x		x		x	x		x		x		x	x		x			
70X-CC, 11-13	785,96				x			x	x	x	x		x	x		x		x		x	x	x	x			
71X-1, 8-10	790.10				x			x	x	x	x	x	x	x	x	x	x	x	x	x	x					
71X-1, 50-52	790.52				x			x	x	x	x		x	x	x	x	x	x	x	x	x					
71X-1, 121-123	791.23	*Falsotruncana maslakovae*			x			x	x	x	x		x	x	x	x	x	x	x							
71X-2, 5-7	791.57				x				x						x											
71X-2, 51-53	792.03				x			x	x	x	x		x	x	x	x	x	x	x							
71X-2, 122-124	792.74				x			x	x	x	x		x		x			x	x							
71X-CC, 26-28	793.28				x			x	x		x	x		x	x			x	x							
72X-1, 7-9	795.09				x			x	x	x	x		x	x	x	x	x	x								
72X-1, 52-54	795.54				x			x	x	x	x	x	x	x	x	x	x	x	x							
72X-1, 102-104	796.04				x			x	x	x	x	x	x	x	x			x	x							
72X-2, 10-12	796.62				x			x	x	x	x	x	x	x	x			x	x							
72X-2, 50-52	797.02				x			x	x	x	x	x	x	x	x			x	x							
72X-2, 100-102	797.52				x			x	x	x	x	x	x	x	x	x		x	x							
72X-CC, 9-11	798.11				x			x	x	x	x	x	x	x	x	x	x	x	x							
73X-1, 12.5-15	799.62				x		x	x	x	x	x	x	x	x	x	x		x								
73X-1, 76-78	800.26				x			x	x	x	x	x	x	x				x								
73X-1, 127-129	800.77				x			x	x	x	x	x	x	x	x	x										
73X-2, 13-15	801.13				x			x	x	x	x	x		x	x											
73X-2, 76-78	801.76				x		x	x	x	x	x	x	x	x	x	x	x									
73X-2, 125-128	802.25				x		x	x	x	x	x	x	x	x	x	x										
73X-3, 5-7	802.55	*Hv. helvetica*	x		x	x	x	x	x	x	x	x	x	x	x	x										
73X-3,44-47	802.94		x	x	x	x	x	x	x		x	x	x	x												
73X-CC, 15-17	803.30		x	x	x	x		x	x		x	x	x													
74X-1, 30-32	804.80		x			x		x	x																	
74X-1, 101-103	805.51		x	x	x	x																				
74X-2, 30-32	806.30		x	x	x	x	x			x	x	x														
74X-2, 100-102	807.00		x	x	x	x	x	x	x	x	x															

Table 4 Turonian planktonic foraminiferal and calcareous nannofossil (accompanied by CC zones) lowest and highest occurrences (LOs & HOs) and first appearance datums (FAD) at ODP Hole 762C. Bioevents in bold are used as control points for the graphic correlation in Figure 10.

Planktonic foraminiferal event	Age (Ma)	Biozone	Stage	Core sample	Min. depth (m)	Max. depth (m)	Mean depth (m)
Dicarinella concavata FAD	91.08[a]	*D. concavata*	upper Turonian	69X-2, 66-68 cm	782.18	783.18	782.68
Pseudotextularia nuttalli LO		*D. concavata*	upper Turonian	69X-2, 66-68 cm	782.18	783.18	782.68
Contusotruncana fornicata LO	---	*M. sinuosa-H. huberi*	upper Turonian	70X-1, 11-13 cm	785.13	785.45	785.29
***Micula cubiformis* LO**	---	CC13	upper Turonian	70X-1, 80-82 cm	785.80	786.20	786.00
***Micula staurophora* FAD**[a]	89.77[b]	CC13	upper Turonian	70X-CC	785.96	790.25	788.11
Falsotruncana maslakovae HO	---	*M. sinuosa-H. huberi*	upper Turonian	71X-1, 8-10 cm	785.96	790.10	788.03
***Huberella huberi* LO**	---	*M. sinuosa-H. huberi*	upper Turonian	71X-1, 50-52 cm	790.52	791.23	790.88
***Marginotruncana sinuosa* LO**	---	*M. sinuosa-H. huberi*	upper Turonian	71X-1, 50-52 cm	790.52	791.23	790.88
***Marthasterites furcatus* FAD**	90.24[b]	CC13	upper Turonian	72X-1, 75-77 cm	793.11	795.25	794.18
***Eiffellithus eximius* s. Verbeek LO**	---	CC12	upper Turonian	71X, CC	797.52	800.00	798.76
Eprolithus moratus HO	---	CC12	mid-Turonian	73X-1, 125-127 cm	800.00	800.77	800.39
***Lithastrinus septenarius* LO**	---	CC12	mid-Turonian	73X-2, 25-27 cm	801.27	801.56	801.42
***Falsotruncana maslakovae* LO**	---	*F. maslakovae*	upper Turonian	73X-3, 5-7 cm	802.25	802.55	802.40
Eiffellithus eximius s.l. FAD	92.99[a]	mid-Turonian	mid-Turonian	74X-2, 51-53 cm	806.50	807.55	807.03
***Helvetoglobotruncana helvetica* LAD**	>91.51[c]	*H. helvetica*	mid-Turonian	73X-2, 125-128 cm	802.25	802.55	802.40
***Helvetoglobotruncana helvetica* FAD**	<93.52[c]	*H. helvetica*	mid-Turonian	74X-2, 100-102 cm	807.00	807.00	807.00
***Quadrum gartnerii* FAD**	<93.55[a]	CC11	lower Turonian	74X-2, 100-103 cm	809.50	809.70	809.60

[a] Bralower & Seisser 1992
[b] Gradstein et al. 2012
[c] Huber and Petrizzo 2014

Robasynski and Caron 1995). The simultaneous LOs of *M. sinuosa* and *Hu. huberi* at TDP 31 and ODP Hole 762C are here considered a more useful means of correlating upper Turonian sediments with higher resolution across a wider geographic and paleoenvironmental range. Unambiguous identification of *Hu. huberi* requires observation of backward-directed extensions on the later biserial chambers, which may be difficult to observe in moderately to poorly preserved material. Nonetheless, the appearance of this distinctive taxon and its co-occurrence with *M. sinuosa* in the same relative stratigraphic level of the upper Turonian at sites in the Pacific (Georgescu 2007), Atlantic (Georgescu et al. 2011) and Indian (this study) Oceans demonstrates their utility as global biomarker species.

At Hole 762C the HO of *F. maslakovae* may represent an additional marker for the identification of the base of the zone as it coincides with the LOs of *Hu. huberi* and/or *M. sinuosa*. At TDP 31 the HO of *F. maslakovae* occurs stratigraphically higher within this zone.

Dicarinella concavata Lowest Occurrence Interval Zone

Definition: Body of strata from the lowest occurrence of *D. concavata* to the lowest occurrence of *D. asymetrica*.

Author: Sigal, 1955.

Age: Late Turonian–Coniacian; age of base not reliably calibrated, but estimated as 91.08 Ma in GTS 2012; age of top not calibrated, estimated as 86.66 Ma in GTS 2012.

Comments: This biozone, as defined by Sigal, has been successfully applied in the Tethyan pelagic realm in Italy and Tunisia (e.g., Premoli Silva and Sliter 1995, Robasynski and Caron 1995). On the contrary, the biozone was not used by Wonders (1992) and Petrizzo (2000) at Exmouth Plateau because of either the rarity of *D. concavata* or because its LO was recorded above the LO of *D. asymetrica* in the other sites drilled on Exmouth Plateau. From the level of its LO to the top of the section *D. concavata* occurs consistently in low abundance to the top of TDP 31.

4.2 Calcareous nannofossil analyses

At TDP 31 seventy-five samples, ranging in depth from 5 to 115 mbs, were prepared and examined with a sampling resolution of at least one sample per core. Presence/absence data for TDP 31 are reported in Table 5. Sites 22, 30, 34, and 36 were examined at much lower sampling resolution since the sections all overlap stratigraphically. Select bioevents are summa-

Table 5 Presence/absence data for Turonian calcareous nannofossils at TDP 31.

TDP 31	Nannofossil Zone	Depth (m)	Preservation	*Calcicalithina alta*	*Chiastozygus spissus*	*Eiffellithus eximius* (s.s.)	*Eiffellithus eximius* (sensu Verbeek)	*Eprolithus moratus*	*Helicolithus turonicus*	*Liliasterites angularis*	*Lithastrinus septenarius*	*Marthasterites furcatus*	*Micula staurophora*	*Micula* sp. cf. *M. cubiformis*	*Quadrum gartnerii*	*Radiolithus planus*	*Reinhardtites biperforatus*	*Rhagodiscus achylostaurion*	*Rhomboaster svabenickiae*	*Stoverius achylosus*	*Stoverius coronotus*	*Tranolithus minimus*
4-1, 4-6 cm	CC14	5.05	G			X	X				X	X	X	X	X		X				X	X
4-2, 6-8 cm	CC13	6.07	G			X	X				X	X		X	X		X				X	X
5-1, 70-72 cm	CC13	7.71	M			X	X				X	X		X	X		X				X	X
6-1, 6-8 cm	CC13	8.07	G			X	X				X	X			X		X				X	X
7-1, 54-56 cm	CC13	10.55	M			X	X				X	X		X	X		X				X	X
8-1, 19-21 cm	CC13	11.2	M			X	X				X	X			X		X				X	X
9-1, 60-62 cm	CC13	13.11	M			X	X					X			X						X	X
10-1, 11-13 cm	CC13	14.12	G			X	X				X	X			X		X				X	X
10-3, 0-2 cm	CC13	16.01	G			X	X				X	X						X			X	X
12-1, 15-17 cm	CC13	17.16	G			X	X				X	X			X		X		X		X	X
12-3, 16-18 cm	CC13	19.17	G			X	X					X			X						X	X
14-1, 5-7 cm	CC13	20.06	M			X	X				X	X			X		X				X	
15-1, 62-64 cm	CC13	22.13	G			X	X				X	X			X			X			X	
16-1, 0-2 cm	CC13	23.01	G			X	X				X	X					X				X	
17-2, 48-50 cm	CC13	25.89	G			X	X				X	X			X			X			X	X
18-1, 3-5 cm	CC13	26.04	G			X	X				X	X			X			X			X	X
18-2, 2-3 cm	CC13	27.03	G			X	X				X	X					X		X		X	
18-2, 52-54 cm	CC13	27.53	G			X	X				X	X			X		X				X	X
19-1, 0-2 cm	CC12	28.01	G	X			X	X	X	X					X	X					X	
20-1, 0-2 cm	CC12	29.01	G				X	X	X	X					X	X		X	X		X	
21-2, 57-59 cm	CC12	33.58	G				X	X		X					X	X		X	X		X	
21-3, 0-2 cm	CC12	34.01	G				X	X	X						X	X			X			
22-1, 0-2 cm	CC12	35.01	G	X			X	X	X						X	X		X	X			
23-1, 50-52 cm	CC12	38.51	G				X		X						X				X			
24-1, 83-85 cm	CC12	39.74	G				X	X							X	X		X	X	X		
25-1, 2-4 cm	CC12	41.03	M				X	X														
25-1, 52-54 cm	CC12	41.53	G	X			X	X	X						X			X	X	X		
26-1, 7-9 cm	CC12	42.68	G				X	X	X						X	X			X			
26-2, 5-7 cm	CC12	43.66	G				X	X								X		X		X		
27-1, 8-10 cm	CC12	44.09	G					X								X						
27-1, 54-56 cm	CC12	44.55	G				X	X	X						X			X		X		
28-1, 2-4 cm	CC12	46.13	G		X			X							X	X		X		X		
29-1, 0-2 cm	CC12	47.01	G				X	X	X						X			X	X	X		
29-2, 58-60 cm	CC12	48.59	M		X		X	X	X						X			X		X		
30-1, 2-4 cm	CC12	50.18	M													X				X		
30-2, 1-3 cm	CC12	51.17	G				X	X	X						X			X		X		
31-1, 28-30 cm,	CC12	52.37	G		X			X							X			X		X		
32-2, 13-15 cm	CC12	54.22	G	X				X							X	X		X		X		
33-1, 2-4 cm	CC12	55.03	G					X								X		X		X		
33-1, 64-66 cm	CC12	55.65	G	X	X		X	X	X									X		X		
34-1, 88-90 cm	CC12	56.89	G		X			X							X	X		X		X		

Table 5 Continued.

35-1, 0-2 cm	CC12	57.51	G	X	X		X	X	X							X		X		X		
35-2, 14-16 cm	CC12	58.65	G	X	X		X	X	X						X	X		X	X	X		
36-1, 51-53 cm	CC11	59.52	G		X										X	X		X		X		
36-2, 6-8 cm	CC11	60.07	G		X			X	X						X			X		X		
37-1, 9-11 cm	CC11	60.6	M		X			X	X						X	X		X	X	X		
38-2, 6-8 cm	CC11	63.02	G		X			X	X							X		X		X		
39-1, 61-63 cm	CC11	65.62	G					X							X			X		X		
39-3, 3-5 cm	CC11	67.04	G	X	X			X							X	X		X	X	X		
40-1, 8-10 cm	CC11	68.22	M					X							X	X		X	X	X		
40-3, 8-10 cm	CC11	70.22	G	X				X								X		X		X		
42-1, 14-16 cm	CC11	72.85	G		X			X	X						X	X		X		X		
43-2, 4-6 cm	CC11	75.05	G	X				X								X		X		X		
44-1, 3-5 cm	CC11	76.44	M					X								X		X		X		
45-2, 53-55 cm	CC11	78.54	G		X			X	X						X			X	X	X		
46-2, 8-10 cm	CC11	81.09	G	X	X			X								X		X		X		
47-1, 53-55 cm	CC11	83.54	M		X			X	X						X	X		X		X		
48-1, 58-60 cm	CC11	86.59	G	X	X				X							X		X		X		
49-1, 60-62 cm	CC11	89.61	M					X												X		
50-1, 10-12 cm	CC11	90.21	G		X			X							X	X				X		
51-1, 50-52 cm	CC11	90.91	G		X			X	X						X	X		X		X		
52-1, 50-52 cm	CC11	92.51	G															X				
53-1, 51-53 cm	CC11	95.52	G		X			X	X							X		X		X		
54-1, 55-57 cm	CC11	98.56	G		X			X	X							X		X		X		
55-1, 48-50 cm	CC11	99.49	G	X	X			X	X						X	X		X		X		
56-1, 10-12 cm	CC11	100.15	G	X	X			X	X							X		X		X		
57-1, 52-54 cm	CC11	101.77	G		X			X	X							X		X	X	X		
58-1, 0-2 cm	CC11	104.25	G	X	X			X							X	X		X		X		
59-1, 53-55 cm	CC11	107.78	G	X	X			X								X		X				
60-1, 74-76 cm	CC11	108.99	P																			
61-1, 46-49 cm	CC11	109.78	G		X											X		X				
62-1, 51-53 cm	CC11	110.52	G												X							
63-1, 10-12 cm	CC11	111.12	G		X			X								X		X		X		
63-2, 38-40 cm	CC11	112.49	G		X			X	X									X		X		
64-2, 58-60 cm	CC11	114.59	G	X	X			X								X		X		X		

rized for the TDP sites in Table 2. Smear slides were prepared from raw sediment following procedures described in Watkins and Bergen (2003). Biostratigraphic placement of samples uses the "CC" Zonation of Perch-Nielsen (1985) with placements adjusted following the quantitative analysis of Corbett et al. (2014) and the geochronological assignments in Ogg and Gradstein (2015). A list of authors and dates for calcareous nannofossil species discussed in this study is presented in Appendix 2.

Census counts and biostratigraphic examination were performed using a polarizing light microscope at 1000x. For each census count, all specimens in multiple sets of ten fields of view (FOV) were identified and counted until the total count per sample exceeded 450 specimens or 400 FOV had been counted. This procedure was adopted to minimize closure in the data set. The total specimen count per sample was divided by the number of FOV necessary to generate that count, yielding a ratio of specimen/FOV (#/FOV) which is used as a relative measure of the relative degree of clastic dilution of the biogenic component. Results of the normalized FOV counts are shown in Figure 4. In addition to the census count, each sample slide was scanned for at least 400 FOV to identify any species that were not included in the census count. Specimens

of *Zeugrhabdotus* spp. that are smaller than 4 µm could not be consistently differentiated and were counted as the combined taxon "small *Zeugrhabdotus*".

5. Biostratigraphic results

5.1 TDP Planktonic foraminiferal distributions

In Turonian samples planktonic foraminifera generally occur in few (5–10 %) to common (10–30 %) abundance relative to total foraminiferal contentat all sites, with planktonic abundance ranging from between 30 % to 80 % and averaging ~50 % of the total foraminiferal assemblage (Haynes et al. 2015, 2016). Preservation in the lower and middle Turonian is best at sites 22, 29, 30, and 31, with most levels yielding optically translucent and hollow shells; preservation is good to moderate at sites 21, 24, 26, 34 and 36, and it is poor to moderate at sites 15 and 38. Preservation in the upper Turonian, which was recovered only at Sites 21 and 31, is moderate to poor with nearly all shells showing infilling by secondary calcite.

The biggest change from the preliminary biostratigraphic reports in Jiménez Berrocoso et al. (2010, 2012, 2015) is discovery of rare *H. helvetica* specimens in samples from as much as 86 m below the originally reported levels, resulting in thinning or elimination of the lower Turonian *W. archaeocretacea* Zone at most sites. Difficulty with reliable identification of the base of the *H. helvetica* Zone, due to morphologic variability of the nominate taxon and rarity of *sensu stricto* forms in its early range (Huber and Petrizzo 2014), results in a tentative assignment of the *W. archaeocretacea* Zone at six of the 11 drill sites (Fig. 3, Table 2). Absence of evidence within the *W. archaeocretacea* Zone for enrichment of $\delta^{13}C$ values obtained from bulk carbonate and organic carbon measurements (Jiménez Berrocoso et al. 2010, 2012, 2015) at the TDP drill sites indicates that if the zone is present, it either postdates the OAE2 carbon isotope excursion interval or the carbon isotope excursion was not preserved in the Tanzanian clastic margin record.

5.1.1 TDP Site 31

Site 31 recovered the most complete middle–upper Turonian record with 71.6 m of the *H. helvetica* Zone overlain by 11.4 m of the *F. maslakovae* Zone, 16.5 m of the *M. sinuosa*/*Hu. huberi* Zone and 10.8 m of the *D. concavata* Zone (Table 1; Fig. 3). Range plots of non-biserial and biserial planktonic foraminifera from Site 31 are presented in Figures 5 and 6, respectively. Below 28 m (cores 19–64), most foraminiferal tests have no cement infilling and show good to excellent preservation, whereas above 28 m (cores 1–18) nearly all tests are infilled with secondary calcite, but preservation of the external test surface is generally good.

The interval from 43.1 m (TDP 31-26-1, 40–60 cm) to the bottom of the borehole at 114.5 m (TDP 31-64-2, 37–57 cm) is assigned to the *H. helvetica* Zone based on the presence of the nominate taxon, which is very rare in its lower range and becomes increasingly common upwards (Huber and Petrizzo 2014). The zone has an average of 53 % benthic species and 10 % biserial species with minor variations above and below these values (Fig. 20 in Haynes et al. 2015). Assemblages within the zone include abundant *W. baltica* and common *H. praehelvetica*, *P. stephani*, and *D. hagni* (including "dwarf" *D. hagni* morphotypes). A small, new

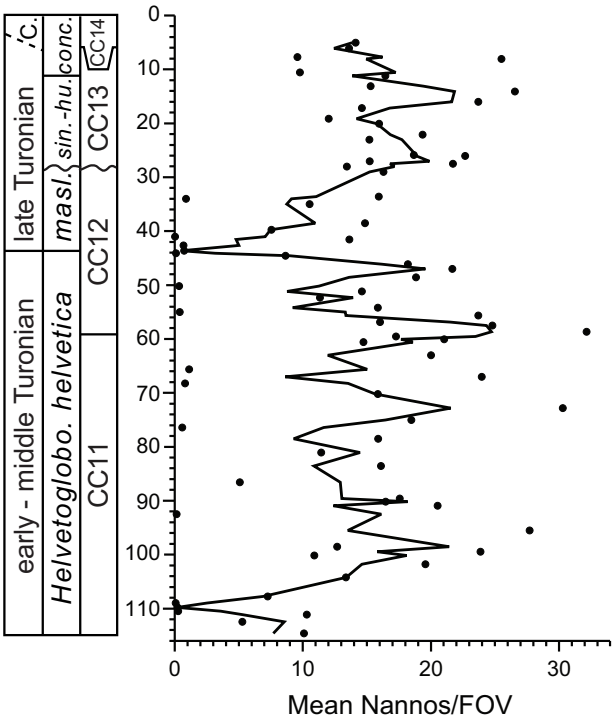

Fig. 4. Census counts of TDP 31 calcareous nannofossils normalized to a ratio of specimens/FOV (see methods for explanation) with a 3-point moving average line added for data smoothing. See Fig. 3 caption for explanation of columns. Abbreviations include: ar. = *Whiteinella archaeocretacea* Zone; *masl*. = *Falsotruncana maslakovae* Zone; *sin-H*. = *Marginotruncana sinuosa – Huberella huberi* Zone; "*D. con*." = *Dicarinella concavata*. See Figure 3 caption for additional explanation.

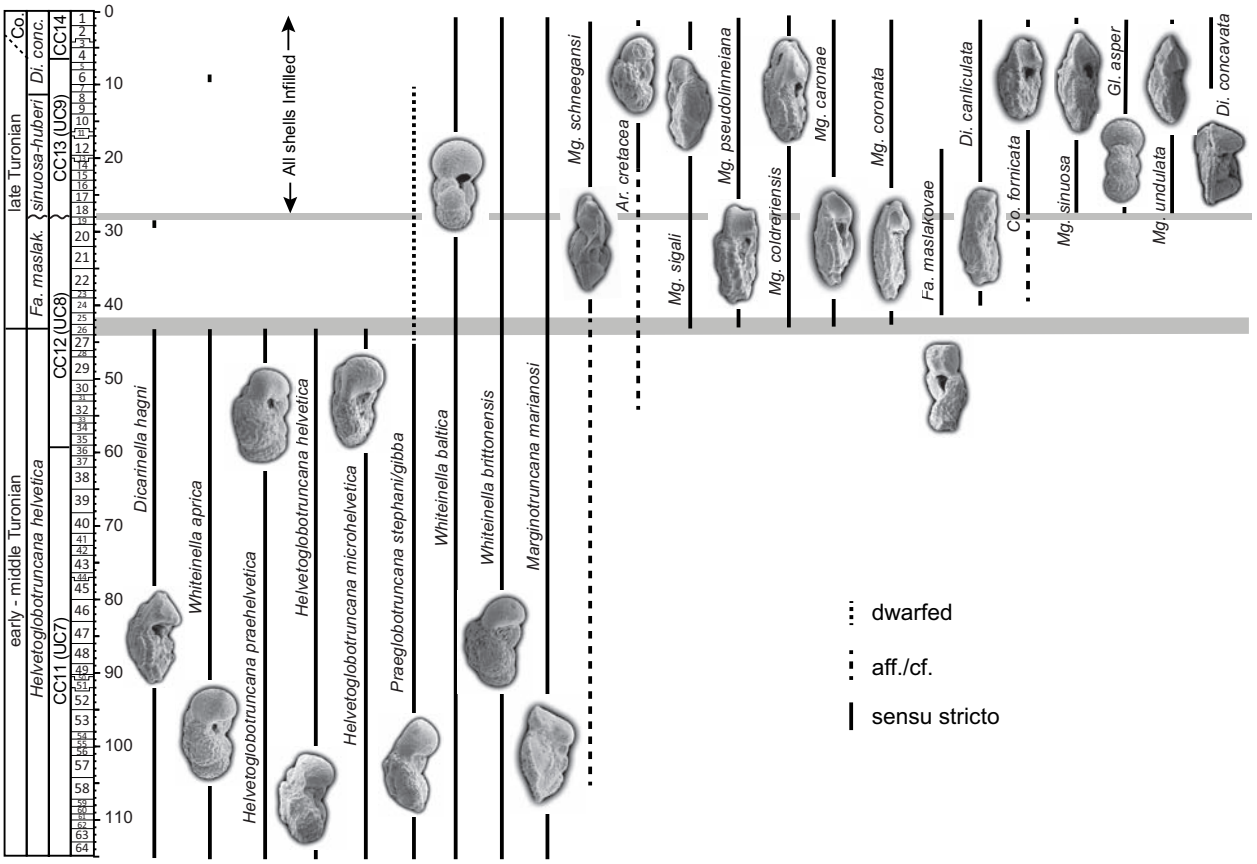

Fig. 5. Stratigraphic ranges of select non-biserial planktonic foraminifera at TDP Site 31 (solid lines), range where only dwarfed morphotypes occur (vertical dotted lines), and range where similar (cf. = similar; aff. = related) morphotypes occur (vertical dashed lines). Horizontal gray lines denote intervals of planktonic foraminiferal species turnover. See Figure 3 caption for additional explanation.

species, *H. microhelvetica* n. sp. occurs throughout the zone in low to moderate abundance (see description in Appendix 1). Species of *Marginotruncana* are restricted to the uppermost two samples of the *H. helvetica* Zone and include *M. caronae*, *M. pseudolinneiana*, and *M. sigali*. Species of the planispiral genus *Globigerinelloides* occur as single specimens in very few samples. Four biserial planktonic species range throughout the zone and show little variation in their relative proportions (Fig. 6; Haynes et al. 2015).

A taxonomic turnover occurs across the *H. helvetica*-*F. maslakovae* zonal boundary. The top of the *H. helvetica* Zone (43.10 m) is marked by the simultaneous extinctions of *H. praehelvetica*, *H. helvetica*, and *H. microhelvetica*, and last consistent occurrences of *W. aprica* and *D. hagni* (Fig. 5, Table 1). This extinction level is followed in the next overlying sample (TDP 31-25-1, 30–50 cm) by the LOs of *F. maslakovae* and several marginotruncanids (*M. coldreriensis*, *M. coronata*, and *M. schneegansi*). An increase in abundance of small forms of *Marginotruncana* and *Praeglobotruncana* also occurs at this level. Three biserial species, including *Laeviheterohelix reniformis*, *Pl. reussi*, *Pl. praenuttalli*, also have their LOs within a 2.5 m interval spanning this zonal boundary (Haynes et al. 2015).

A second, less significant species shift occurs across the zonal boundary between the *F. maslakovae* Zone and *M. sinuosa*/*Hu. huberi* Zone (midpoint depth 27.7 m). The most profound change occurs among the biserial taxa with a dramatic rise in the percent biserial species and the LOs of *Hu. huberi* (Fig. 6; Haynes et al. 2015). This shift is accompanied by the LOs of *M. tarfayaensis* and *M. undulata*, an increased abundance of *Globigerinelloides* (particularly *G. asper*), and an abrupt switch from excellent test preservation (glassy, no shell infilling) in samples below to moderate or poor preservation in samples above. The LO of *Pseudotextularia nuttalli* occurs at the top of the sec-

tion in TDP 31-2-1, 20–34 cm), providing a useful datum for correlation with TDP 39 (Petrizzo et al. 2017).

5.1.2 TDP Site 21

The borehole at TDP 21 was drilled with the intention of recovering a continuous Coniacian–Turonian sequence, but drilling terminated prematurely at 68.10 m because of unconsolidated sands that caused poor core recovery and yielded no biostratigraphic control within the lowermost 26 m (Fig. 3). The upper 4.8 m of the section is assigned to the *D. concavata* Zone and the interval from 19.3–4.8 m is placed in the *M. sinuosa*/*Hu. huberi* Zone. The *H. helvetica* Zone ranges from 41.6–19.3 m, with the nominate taxon occurring in nearly all fossil-bearing samples except the lowermost one (TDP 21-15-2, 41–57 cm), which yielded a depauperate assemblage containing few *H. praehelvetica*. A faulted sediment block containing a Zone P4 Paleocene foraminiferal assemblage occurs at 20.6 m (TDP 21-9-1, 41–51 cm) is bounded by a *H. helvetica* Zone assemblages below and a *M. sinuosa*/*Hu. huberi* Zone assemblage above (Jiménez Berrocoso et al. 2010).

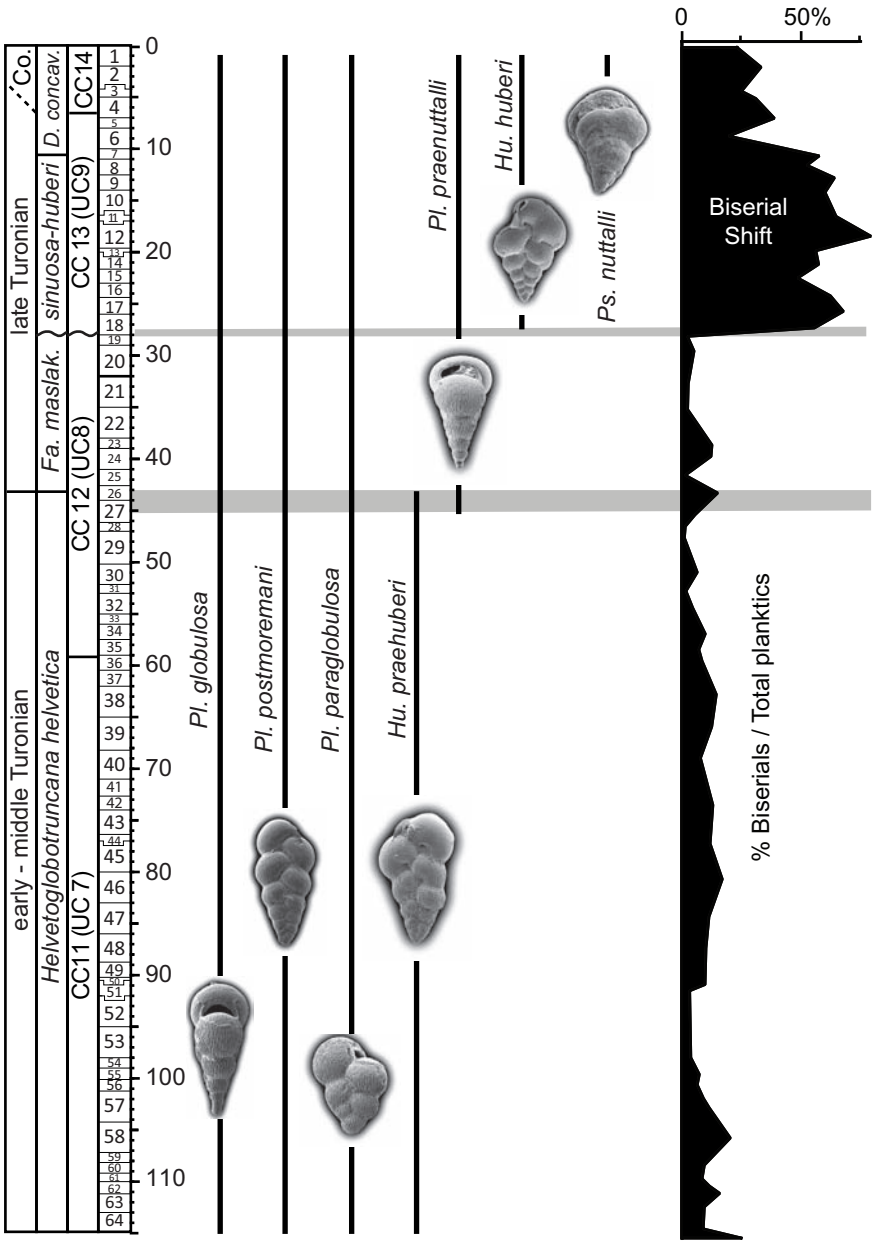

Fig. 6. Stratigraphic ranges of biserial planktonic foraminifera and biserial percent abundance at TDP Site 31. Gray bars are shown where significant biotic shifts occur. Distribution data are from Haynes et al. (2015). See Figures 3 and 5 captions for further explanation.

5.1.3 TDP Sites 22, 30, 34, and 36

Apart from barren intervals at the uppermost levels, the sequences cored at TDP Sites 22 and 34 are placed in the *H. helvetica* Zone (Table 2). Sites 30 and 36 are also assigned to the *H. helvetica* Zone except for the barren uppermost samples and lowermost samples that are barren of foraminifera or lack the nominate taxon. As at Site 31, no species extinctions or LOs were recorded within the *H. helvetica* Zone at any of the four sites.

5.1.4 TDP Sites 24 and 26

Drilling across the Cenomanian-Turonian boundary interval was achieved only at TDP Sites 24 and 26. At both sites the youngest sediments are tentatively assigned to the lower Turonian *W. archaeocretacea* Zone (~4 m thick), due to the absence of *H. helvetica*, and the underlying sediments are assigned to the lower-middle Cenomanian *Thalmanninella globotruncanoides* Zone, due to the absence of the nominate taxa for the *Th. reicheli* and *Rotalipora cushmani* Zones (see Ando et al. 2015).

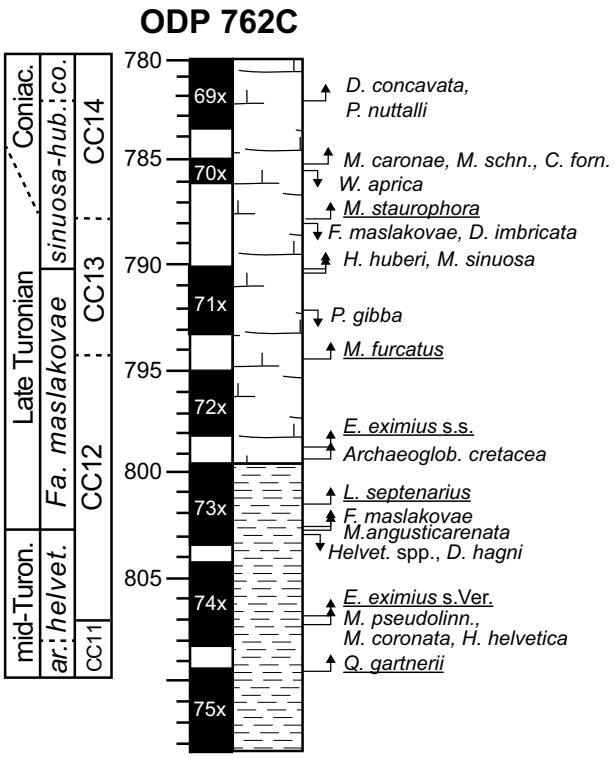

Fig. 7. Planktonic foraminiferal and calcareous nannofossil lowest (up arrows) and highest (down arrows) midpoint occurrence (LOs and HOs) depths at ODP Hole 762C. Calcareous nannofossil datums are underlined. Dashed (uncertain) Turonian/Coniacian boundary placed between the base of Zone CC14 and the LO of *P. nuttalli* following correlations of Hardenbol et al. (1998) and Robszynski and Caron (1995). Dashed line at base of *D. concavata* Zone reflects likelihood that its LO is stratigraphically higher at Exmouth Plateau than at Tethyan localities (Wonders 1992, Petrizzo 2000), and dashed line at base of *H. helvetica* Zone indicates uncertainty because of poor sample preservation (Falzoni et al. 2016b). See Figure 3 caption for further explanation.

5.2 ODP Hole 762C planktonic foraminiferal distributions

Biostratigraphic results from Hole 762C are shown relative to the core depths and lithology in Figure 7, presence/absence observations are presented in Table 3 with key datums listed in Table 4. The *H. helvetica* Zone is assigned from the bottom of the studied interval (807.00 mbsf; meters below seafloor) to 802.55 mbsf based on the consistent presence of nominate taxon, the *F. maslakovae* Zone is assigned to the interval between the *H. helvetica* extinction and the lowest occurrence of *M. sinuosa* and *Hu. huberi* at 790.52 mbsf, and the *M. sinuosa*/*Hu. huberi* Zone is assigned from the latter level to the LO of *D. concavata* at 782.18 mbsf.

The *D. concavata* Zone extends from the latter level to the top of the studied sequence.

The lower limit of this biozone is placed with some uncertainty due to the documented delayed appearance of *D. concavata* at Exmouth Plateau (Wonders 1992, Petrizzo 2000) and because of its rarity and/or absence in other localities in the eastern Indian Ocean (DSDP Site 258, Herb 1974, Herb and Scheibnerova 1977). It is noteworthy that the LO of *Ps. nuttalli* is documented as a single specimen at 782.18 mbsf in Hole 762C, which is the same sample as the LO of *D. concavata* (Table 3).

5.3 TDP sites vs ODP Hole 762C planktonic foraminiferal distributions

There are several important similarities and differences in species distributions within the *H. helvetica* Zone between the TDP sites and Hole 762C. The main similarities include the (1) dominance of the assemblages by whiteinellids, helvetoglobotruncanids, and *D. hagni*, (2) simultaneous disappearance at the top of the zone of the latter two taxonomic groups; (3) HO of normal-sized *P. stephani* within the *H. helvetica* Zone at both sites; (4) appearance of small archaeoglobigerinids in low abundance in the upper *H. helvetica* Zone and increase in size and abundance in the overlying zones; (5) increased size and abundance of mar-

ginotruncanids in the upper Turonian samples; and (6) abrupt increase in abundance of biserial planktonic foraminifera occur near the base of the *M. sinuosa*/*Hu. huberi* Zone.

Notable differences between the TDP sites and Hole 762C include: (1) essentially no extinctions or first occurrences were recorded in the *H. helvetica* Zone at the TDP sites, whereas the *H. helvetica* Zone at Hole 762C contains first occurrences of large marginotruncanids (*M. pseudolinneiana*, *M. coronata*, *M. angusticarenata* and *M. tarfayaensis*), and of *F. maslakovae*, *F. loeblichae*, *M. simplicissima*; (2) *M. hoezli*, and *Globigerinelloides* spp. are consistently present at Site 762 but are absent or very rare at the TDP sites; (3) the LO of *P. gibba* occurs well above the LO of *H. helvetica* at Site 762 compared to Site 31; and (4) small, indeterminate forms of *Dicarinella*, *Marginotruncana*, and *Praeglobotruncana* become a conspicuous component of the upper Turonian assemblages at TDP 31, but these forms were not identified at Hole 762C.

5.4 Calcareous nannofossils

5.4.1 TDP Site 31

Samples between 59.52 and 114.60 m (cores 36–64) contain *Quadrum gartnerii*, *Lucianorhabdus maleformis*, and *Eiffellithus turriseiffelii* and rare *E. perchnielseniae* without *E. eximius* or *Helenea chiastia*. This association indicates lower to middle Turonian Zone CC11. As in many other localities, *Q. gartnerii* is quite rare in the lower part of its range, but it becomes more common higher in the section. *L. maleformis* occurs throughout CC11 at TDP 31, which may be the result of the superior nannofossil preservation at this site.

Sample TDP 31-35-2, 6–8 cm (58.65 m) contains the LO of *E. eximius* sensu Verbeek (Table 3). This form, herein designated *E. eximius* (s. Ver.), is identical to the *E. eximius* of most authors (see below), and its FAD marks the base of middle Turonian Zone CC12. There are several potentially useful biohorizons within Zone CC12 in TDP 31. The top of Core 28 (46.13 m)

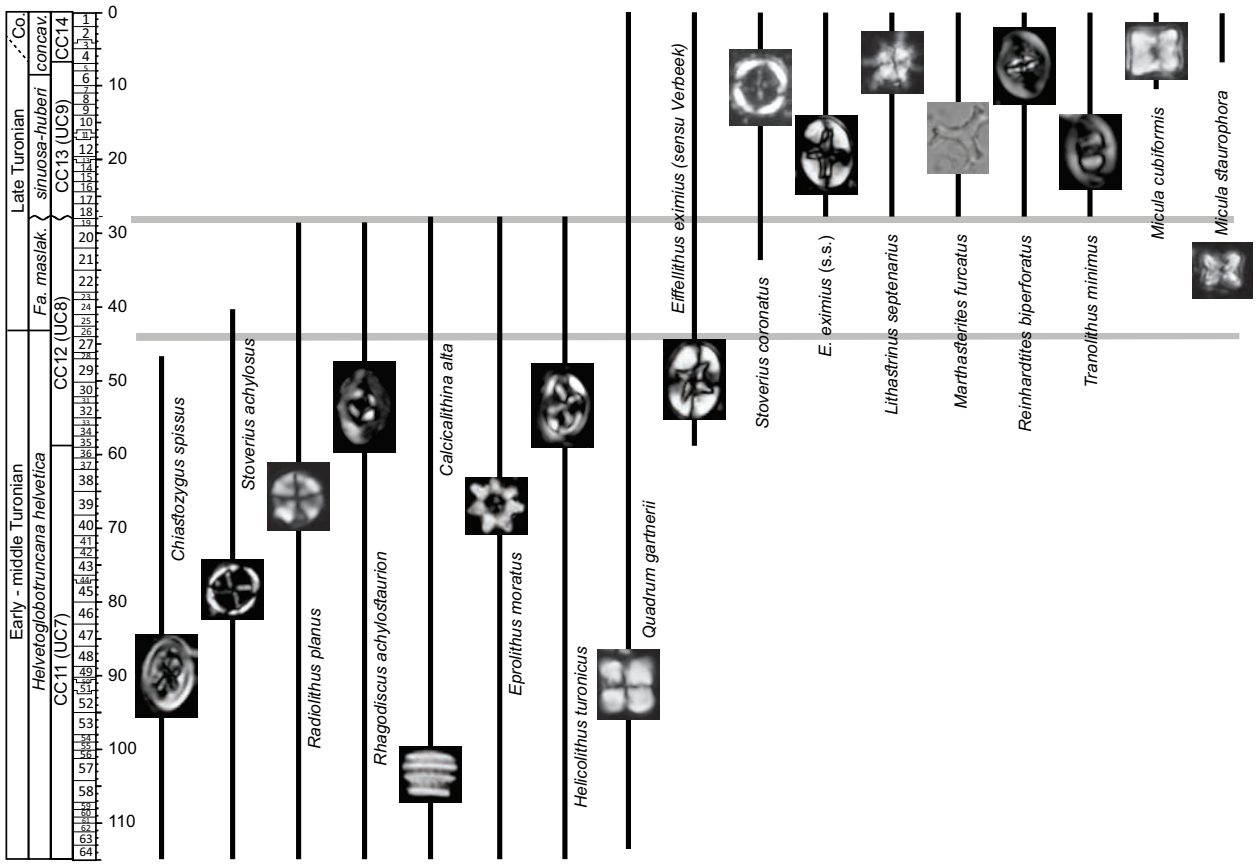

Fig. 8. Stratigraphic ranges of select calcareous nannofossil species at TDP Site 31. See Figure 3 caption for further explanation.

is the LAD of *Chiastozygus spissus*. This species is rare in most samples below ~55 m, but becomes sporadic in occurrence in the upper part of its range (~46–55 m). Sample TDP 31-24-1, 83–85 cm (39.74 m) contains the LAD of *Stoverius achylosus* and sample TDP 31-21-2, 57–59 cm (33.58 m) contains the FADs of *Liliasterites angularis* and *S. coronatus*. A significant reduction in nannofossils/FOV occurs between 44.55 and 41.03 mbs (Fig. 4), suggesting that substantial clastic dilution of the pelagic rain accompanied the planktonic foraminiferal turnover discussed above. There is no turnover in nannofossil assemblages at this level.

There is a significant turnover of nannofossil taxa between Cores 18 and 19, within the interval between 27.5–28.0 m (Fig. 8). The top of Core 19 (28.01 m) contains the LAD of several taxa including *Eprolithus moratus*, *Radiolithus planus*, *Lilliaster angularis*, and *Helicolithus turonicus*. The base of Core 18 (27.53 m) records the FAD of several taxa including *Marthasterites furcatus*, *E. eximius* (s.s.), *Lithastrinus septenarius*, *Reinhardtites biperforatus*, and *Tranolithus minimus*.

The FAD of *M. furcatus* at 27.53 m marks the base of upper Turonian Zone CC13. Corbett et al. (2014) found that quantitative analysis by Ranking and Scaling (RASC) of 26 sections placed the averaged FAD of *M. furcatus*, *R. biperforatus*, and *L. septenarius* as closely spaced events in the late Turonian. The FAD of morphotypes of *E. eximus* with a true axial cross (= *E. eximius* s.s. = sensu Stover; see below) corresponds with the FADs of other upper Turonian forms, which is in agreement with observations in Corbett et al. (2014). Core 10 (16.01 m) has the LAD of *Rhagodiscus achylostaurion*. This species is very rare near the top of its range (~16–25 m in the section), with a last consistent occurrence at about Core 27 (44.6 m). Core 7 (10.55 m) has the FAD of forms similar to *M. cubiformis*, indicating that the upper part of the section (5–10.6 m) is close to, but still below the Turonian–Coniacian boundary. These forms, denoted as *Micula* sp. cf. *M. cubiformis*, are substantially smaller than typical *M. staurophora* (whose FAD marks the base of CC14), lack the strongly developed diagonal elements in *M. adumbrata*, and lack the well-developed central area structure typical of *M. cubiformis* (Fig. 8). As such, these small forms appear to have been precursors to the typical *Micula* species characteristic of Coniacian and higher Cretaceous strata.

The uppermost sample examined (Core 4-1, 5.05 m) contains very rare (< 0.01 %) specimens of *M. staurophora* as well as *Micula* sp. cf. and *M. cubiformis*. These occurrences indicate assignment of the uppermost sample to Zone CC14, and suggest an earliest Coniacian age age at the top of the drilled section (Robaszynski and Caron 1995, Hardenbol et al. 1998).

5.4.2 Other TDP sites

Samples from TDP Site 22 were examined from the interval from 11.88–131.92 m (cores 5–51; Table 2). The lower part of the succession (45.05–131.93 m; cores 16–51) contains well-preserved nannofossil assemblages that include *E. moratus*, *Q. gartnerii*, and *S. achylosus* but lack of *E. eximius* (s. Ver.) and *H. chiastia*, indicates lower to middle Turonian Zone CC11. The FAD of *E. eximius* (s. Ver.) in sample TDP 22-15-2, 53 cm at 42.05 m indicates the base of mid-Turonian Zone CC12. This zone spans to top of the sampled interval and contains *E. moratus* and *Q. gartnerii* without having *E. eximius* or *H. chiastia*. Such an association indicates lower to middle Turonian Zone CC11.

5.4.3 ODP Hole 762C

Samples from ODP Hole 762C were examined from 70X-1, 80 cm through 75X-1, 45 cm (Table 6). Nannofossils were poorly-preserved throughout this interval with substantial dissolution and overgrowth evident, which frequently precluded species level identification of specimens. As a result, only relatively robust species could be traced reliably for biostratigraphic purposes. Samples at the base of this interval (74X-3, 4 cm – 75X-1, 45 cm) contain *E. moratus* and *Q. gartnerii* but lack *E. eximius*, indicating lower Turonian Zone CC11. The FAD of *E. eximius* (s. Ver.) occurs in sample 74X-2, 51–53 cm, delineating the base of the upper lower to middle Turonian Zone CC12. The FAD of *M. furcatus* in sample 71X-CC indicates the base of upper Turonian Zone CC13. At Hole 762C *M. furcatus* is rare, and specimens are generally difficult to recognize confidently due to the substantial diagenetic overprint. Single questionable specimens of *M. furcatus* were observed in the two samples below 71X-CC, but poor preservation precluded definite identification. As a result, the base of Zone CC13 is questionably placed. *Reinhardtites biperforatus* could not be identified with confidence in the Site 762 material due to poor preservation.

Bralower and Siesser (1992) placed the base of CC14, and the Turonian–Coniacian boundary, at the bottom of Core 70X based on the occurrence of *M. staurophora* in the core catcher sample (70X-CC). Re-examination of

Table 6 Presence/absence data for Turonian calcareous nannofossils at ODP Hole 762C.

ODP 762	Depth (mbs)	Nannofossil Zone	*Chiastozygus spissus*	*Eiffellithus eximius* (s.s.)	*Eiffellithus eximius* (s. Ver.)	*Eprolithus moratus*	*Helicolithus turonicus*	*Lithastrinus septenarius*	*Marthasterites furcatus*	*Micula cubiformis*	*Micula staurophora*	*Quadrum gartneri*	*Stoverius achylosus*	*Stoverius coronatus*
70-1, 80	785.80	CC14		X	X			X	X	X		X		X
70, CC	785.96										X			
71-1, 25	790.25	CC13		X	X			X	X			X		X
71-2, 35	791.45			X				X	X			X		X
71, CC	793.11			X	X			X	X			X		X
72-1, 25	795.25	CC12		X	X			X	?			X		X
72-1, 75	795.75			X	X			X	?			X		X
72-2, 50	797.00			X	X			X				X		X
72-2, 102	797.52			X	X			X				X		X
73-1, 51	800.00				X			X				X		X
73-1, 127	800.77				X	X		X				X		X
73-2, 50	801.56				X	X		X				X		X
73-2, 77	801.77				X	X	X					X		X
73-2, 124	802.25				X	X						X		X
73-3, 26	802.75				X	X	X					X		
73-CC	803.20				X	X						X		
74-1, 50	805.00				X	X						X	X	
74-1, 101	805.50				X	X						X	X	
74-2, 5	806.05					X	X					X	X	
74-2, 51	806.50		X		X	X	X					X	X	
74-3, 4	807.55	CC11				X	X					X	X	
75-1, 20	809.70		X			X						X	X	
75-1, 45	809.95													

core catcher samples using the fine-fraction residue extracted from ultrasonically cleaned foraminifera confirms the presence of *M. staurophora*. However, the overlying sample (70X-1, 80 cm) does not contain *M. staurophora*. Despite this absence and the possibility of downhole contamination of the core catcher due to core disturbance (Haq et al. 1990), we follow Bralower and Siesser's (1992) placement of the base of CC14 between Sample 70X-CC and the top of Core 71X.

5.4.4 Taxonomic remarks on *Eiffellithus eximius* morphotypes and biostratigraphic implications

The species *Eiffellithus eximius* was named by Stover (1966, as *Clinorhabdus eximius*) for forms with cross-bars aligned with the cardinal axes of the elliptical rim (+). During the initial development of a comprehensive zonation for the Cretaceous, Verbeek (1977) noted the gradual evolution of *E. eximius* (axial cross) from *E. turriseiffelii* (with a "diagonal cross" in which the cross-bars form an angle of approximately 45° with the cardinal axes of the ellipse) through progressive rotation of the cross-bar alignment during the Turonian (Fig. 9). Verbeek (1977) chose to separate the two species by designating specimens with cross-bars within 20° of the cardinal axes as *E. eximius*. This convention was widely accepted, and the middle Turonian FAD of these forms [*E. eximius* sensu Verbeek; = *E. eximius* (s. Ver.)] was incorporated into the Cretaceous zonation of Sissingh (1977), the NC zonation of Roth (1978) and the widely used CC zonation of Perch-Nielsen (1985). In the latter zonation, the FAD

of *E. eximius* (s. Ver.) serves as the datum to separate CC11 from CC12.

Subsequent taxonomic and biostratigraphic work have indicated the possibility of additional temporal resolution from this evolutionary transition. Shamrock and Watkins (2009) separated out forms with cross-bars at angles from 20 to 40° from the cardinal axes as *E. perchnielseniae* and documented their FAD in the upper Cenomanian. Corbett et al. (2014) used a strict definition of *E. eximius*, including only forms with "a nearly perfectly straight axial cross" (p. 42) and noted that it had a lower upper Turonian first occurrence. This decision had the effect of greatly lengthening the interval assigned to CC11 at the expense of CC12.

Most of the evolutionary transition to *E. eximius* is well represented in the TDP 31 material (Fig. 10). Although rare near its FAD, *E. eximius* (s. Ver.) is consistent in occurrence for most of its range and, because of its relatively robust construction, is identifiable even in moderately preserved material. The transition to *E. eximius* (s.s.) is obscured by a brief hiatus between Cores 18 and 19, but it is a common component of the TDP 31 assemblages of CC13. The upper Turonian FAD of *E. eximius* (s.s.) in TDP 31 corroborates the placement of this form by Corbett, et al. (2014). This taxonomic distinction appears to be a valuable addition to the nannofossil biostratigraphic sequence.

The stratigraphic distribution of *Eiffellithus* spp. as a percentage of the total nannofossil assemblage (Fig. 10) indicates that species within the genus do not become more abundant as additional species (including *E. eximius* morphotypes) appear in the section. Indeed, the average percent abundance of the assemblages decreases from about 7.8% in CC11 to about 7.5% in CC12 and to about 6% in CC13. This change suggests that the progressive evolution of the *E. eximius* morphotypes took place at the expense of niche space previous occupied by the diagonal cross forms (*E. turriseiffelii* and *E. casulus*).

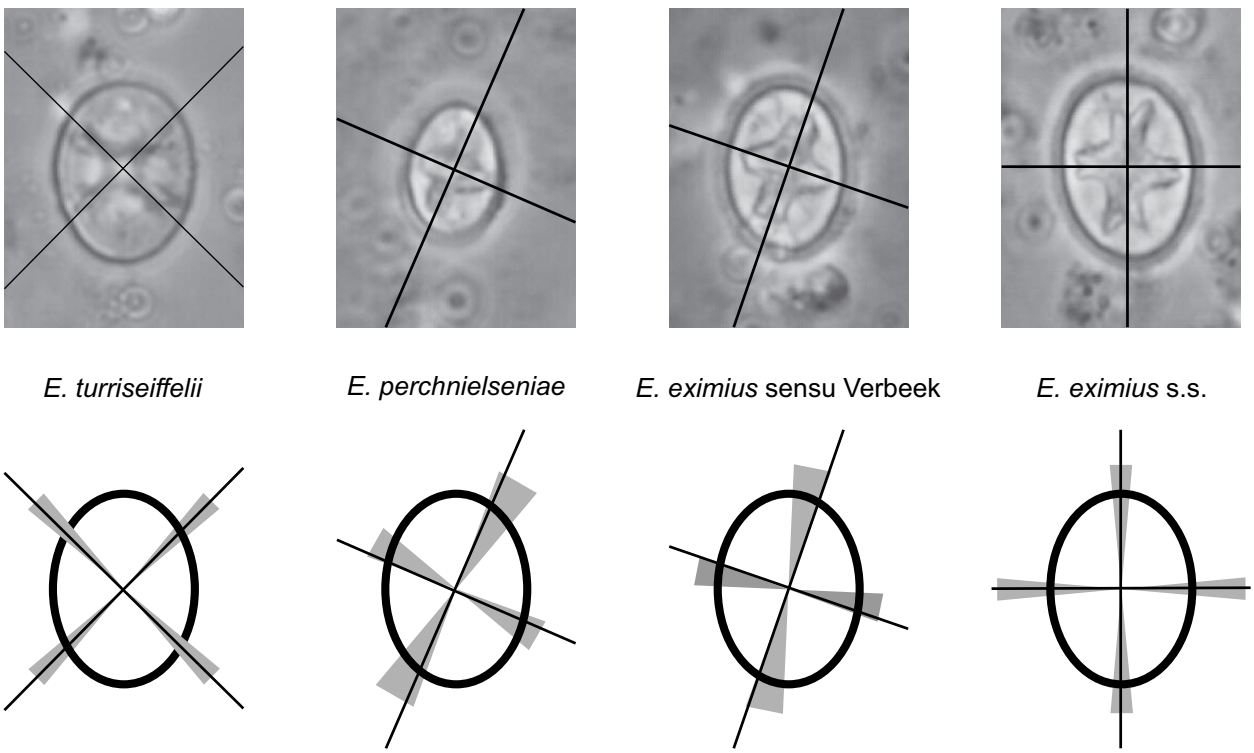

Fig. 9. Comparison of morphotypes in the evolution of *E. eximius* from *E. turriseiffelii* illustrating the progressive rotation of the cross-bars. Orthogonal lines on photographs and line drawing indicate orientation of cross-bars. Shaded areas on line drawings indicate permissible range of variation for cross-bar orientation for each morphotype.

6. Discussion

6.1 TDP borehole correlation

Integration of planktonic foraminiferal and calcareous nannofossil biostratigraphic distributions from TDP borehole samples enables a better means of correlating between the TDP sites than has been achieved previously. The chronostratigraphic framework for the Turonian TDP boreholes is discussed below.

6.1.1 Cenomanian/Turonian boundary interval

Results demonstrate that none of the TDP sites penetrated into the lowermost Turonian, as biostratigraphic markers for the Turonian portions of the *W. archaeocretacea* Zone and Zone CC10 are absent. Carbon isotope data from single species analyses of benthic and planktonic foraminifera from Sites 22 and 31 (MacLeod et al. 2013) and bulk carbonate and organic carbon analyses from these and the other Turonian sites (Jiménez Berrocoso et al. 2010, 2012, 2015) show no relative $\delta^{13}C$ enrichment that correlates with the OAE2 interval. Samples are tentatively assigned to the *W. archaeocretacea* Zone at sites 24, 26, 30, and 36 because of the extreme rarity of *H. helvetica* Zone in its lowermost range (Huber and Petrizzo 2016).

Absence of markers for the stratigraphic interval spanning all of calcareous nannofossil Zone CC10 and from the planktonic foraminiferal *Thalmanninella reicheli* through the *W. archaeocretacea* Zone (Ando et al. 2015) demonstrates that at least 2.7 m.y. of the upper Cenomanian–lower Turonian sediment record is missing at all sampled locations between Dar es Salaam and Lindi Village. Whether this stratigraphic gap was caused by regional faulting or a regional unconformity cannot be resolved in the absence of high-resolution shallow seismic data and additional coring across the CTBI from the shallow to deeper parts of the Mandawa and Ruvuma Basins.

6.1.2 Middle Turonian in TDP boreholes

The scarcity of bioevents within the middle Turonian *H. helvetica* Zone at all TDP sites is remarkable. This period of stasis among the calcareous planktonic assemblages is accompanied by high stability in the biserial planktonic foraminiferal assemblages (Haynes et al. 2015; Fig. 6), benthonic foraminiferal assemblages (Wendler et al. 2016), palynomorphs (Haynes et al. 2016), organic carbon biomarkers (Haynes et al. 2016), sediment grain size (Wendler et al. 2016), and $\delta^{18}O$ and $\delta^{13}C$ signatures of benthonic and planktonic foraminifera (MacLeod et al. 2013, I. Wendler et al. 2013). It is puzzling that several marginotruncanid species that have been identified within the *W. archaeocretacea* Zone and *H. helvetica* Zone at Hole 762C and elsewhere (e. g., Gubbio, Italy: Premoli Silva and Sliter 1995, Tunisia: Robaszynski et al. 1990, Kerguelen Plateau: Petrizzo 2001; southeast France: Falzoni et al. 2016) are absent from the TDP sites.

Identification of *Eiffelithus eximius* (s. Ver.) in the upper *H. helvetica* Zone at TDP Sites 22 and 31 establishes how the two sites are correlated and reveals that the youngest sediments at the other *H. helvetica* Zone sites predate Zone CC12. The need for taxonomic separation of this species is demonstrated by the consistent offset between its LO and that of its descendent species *E. eximius* (s.s.), as observed at TDP 31 and ODP Hole 762C. This distinction clarifies discrepancies in ages assigned to the bottom and top of the zone in different versions of the geological time scale (e. g., Gradstein et al. 2004 vs. Gradstein et al. 2012) and different opinions on whether the base of the zone correlates below or above the top of the *H. helvetica* Zone (Huber and Petrizzo 2014).

6.1.3 Species turnover across *H. helvetica*/*F. maslakovae* zonal boundary

The planktonic foraminiferal turnover across the *H. helvetica*/*F. maslakavae* zonal boundary at TDP 31 is not matched at any other continental margin or deep-sea site that has been studied and does not correspond with a change in co-occurring calcareous nannofossil assemblages. At Hole 762C the extinctions of *H. helvetica* and *D. hagni* occur in the same sample, but the HO of *H. praehelvetica* and LOs of *F. maslakovae* and several species of *Marginotruncana* (e. g., *M. pseudolinnieana*, *M. coronata*, *M. angusticarenata*) are just below or well below the top of the zone, and the HOs of *W. aprica* and *P. gibba* are significantly above the top of the zone. Biostratigraphic studies of Turonian sections in the Bottaccione Gorge (Premoli Silva and Sliter 1995) and central Tunisia (Robaszynski et al. 1990) place the HO of *H. praehelvetica* and LOs of *M. pseudolinnieana* and *M. coronata* below the top of the *H. helvetica* Zone, but there is a lack of agreement between these studies in the relative timing of the HOs of *P. stephani*; in neither report do *P. gibba* and *D. hagni* show coincident HOs.

Two possibilities are considered to explain the planktonic foraminiferal turnover at the top of the *H. helvetica* Zone at 42.65 mbs in TDP 31. One explanation is the possible presence of a disconformity

causing truncation of species ranges at the top of the *H. helvetica* Zone and/or the base of the *F. maslakovae* Zone. Several reasons suggest a major hiatus is unlikely, including (1) consistency in correlation between sites 31 and 762 for the relative stratigraphic levels of the base of Zone CC12, the top of the *H. helvetica* Zone, and the LO of *F. maslakovae*; (2) the absence of species turnover among the calcareous nannofossils; and (3) absence of a discernable change in lithology or paleoenvironment.

Our preferred explanation is that oceanographic conditions in the Tanzanian marginal marine setting abruptly changed across the species turnover level. This could have resulted from a lateral shift of surface water environments or a temporal shift in regional climatic conditions at the time of the *H. helvetica* extinction. Understanding why some marginotruncanid species would have been excluded from TDP Site 31 until after the *H. helvetica* extinction will require further investigation.

6.1.4 Species turnover across *F. maslakovae* – *M. sinuosa*/*Hu. huberi* zonal boundary

The interval separating cores 18 and 19 at TDP 31 (28.11 mbs), which straddles the *F. maslakovae* – *M. sinuosa*/*Hu. huberi* and CC12/CC13 zonal boundaries, denotes a dramatic change in the planktonic foraminiferal and calcareous nannofossil and assemblages in the sediment lithology. To summarize, the sample from the top of Zone CC12 (core 19) contains the highest level of preservation where glassy foraminiferal shells without cement infilling are observed and the HOs of four calcareous nannofossil species (*E. moratus*, *R. planus*, *L. angularis*, and *He. turonicus*) are documented. The overlying sample (core 18) contains the LOs of five calcareous nannofossil species [(*M. furcatus*, *E. eximius* (s.s.), *L. septenarius*, *R. biperforatus*, and *T. minimus*) and one planktonic foraminiferal species (*Hu. huberi*)] accompanied by an abrupt increase in the percentage of biserial planktonic foraminifera (Haynes et al. 2015; Fig. 6) and sediment grain size (Wendler et al. 2016), a shift in benthonic foraminiferal assemblages (Wendler et al. 2016) and a diagenetic shift with consistent cement infilling of foraminiferal tests from core 18 to the top of the borehole.

The stratigraphic juxtaposition of range end-points (i.e., range "pile-up") within this interval suggests a disconformity or presence of a fault. According to Ogg and Gradstein (2015), the FAD of *R. biperforatus* should occur approximately 0.47 Ma prior to the FAD of *M. furcatus*. Co-occurrence of these two biochrons at 27.7 mbs indicates that the "pre-*M. furcatus*" range of *R. biperforatus* is missing at the disconformity, and suggests a hiatus of ~ 400 k.y. The observed changes in planktonic and benthonic foraminiferal assemblages, calcareous nannofossil assemblages, and lithology across this interval suggest that a major shift in the depositional environment must have occurred during the missing time interval. The timing of this event approximately corresponds with a "major cycle boundary" identified as "KTu4" at 91.8 Ma within the upper Turonian *M. schneegansi* Zone in the Cretaceous sea level curve of Haq (2014), but the estimated sea level rise of 70 m is not supported by lithologic and biostratigraphic observations (Haynes et al. 2016). Problems of correlation of this sequence boundary and uncertainty whether this is a global eustatic event are discussed in Haq and Huber (2016). Study of additional sections that span this event are needed to better understand the biotic and lithologic changes observed across this zonal boundary at TDP 31.

6.1.5 Coniacian/Turonian boundary

In the absence of a ratified GSSP section for the Coniacian/Turonian boundary there is no formally accepted criterion for identifying the base of the Coniacian Stage. Planktonic foraminiferal workers generally place the boundary within the lower *D. concavata* Zone (e. g., Premoli Silva and Sliter 1995) and/or near the LO of *Ps. nuttalli* (Robaszynski and Caron 1995, Hardenbol et al. 1998), while most calcareous nannofossil workers place the boundary at or just below the FAD of *M. staurophora* (e. g., Burnett 1998; 2008). At TDP 31, the presence of *M. staurophora* in the uppermost 5.05 m and *Ps. nuttalli* in the upper 2.27 m provides justification for placing the Coniacian/Turonian boundary between those datum events. Moreover, identification of both bioevents at TDP 31 enables correlation with TDP 39 (Petrizzo et al. 2017) where *M. staurophora* and *D. concavata* both occur at the bottom of the borehole and the FAD of *Ps. nuttalli* is10 m stratigraphically higher (Jiménez Berrocoso et al. 2015).

At Hole 762C, the identification of *M. staurophora* at 785.96 mbsf (Sample 70X-CC) and co-occurrences of *Ps. nuttalli* and *D. concavata* at 782.18 mbsf (Sample 69X-2, 66–68 cm) suggests that the Coniacian/Turonian boundary should be placed between those biostratigraphic datums (Fig. 7).

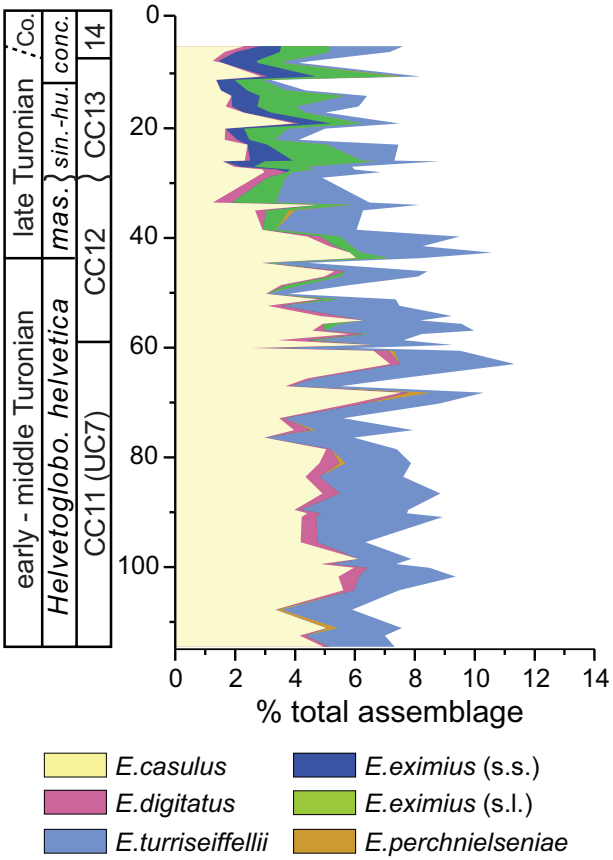

Fig. 10. Stratigraphic distribution of *Eiffellithus* species as a percentage of the total assemblage. Note that the total abundance of *Eiffellithus* does not increase during the speciation of the *E. eximius* morphotypes. See Figure 3 caption for further explanation.

6.2 Chronostratigraphic framework and reliability of species datum events

Establishing an accurate and reliable chronostratigraphic framework for the Turonian TDP 31 and ODP 762 sequences is hindered by the absence of radiometric, magnetostratigraphic, cyclostratigraphic or chemostratigraphic age control points in both sections and lack of a formal definition and accurate age determination for the Turonian/Coniacian Stage boundary (Gradstein et al. 2012). Age control for the sequences is hindered by the fact that previously assigned ages for planktonic foraminiferal and calcareous nannofossil datum events younger than the time interval spanning OAE2 have not been reliably calibrated (Huber and Petrizzo 2014).

Correlation of bulk organic and carbonate $\delta^{13}C$ values from TDP 31 with carbon isotopic events identified in pelagic carbonate sequences elsewhere is not

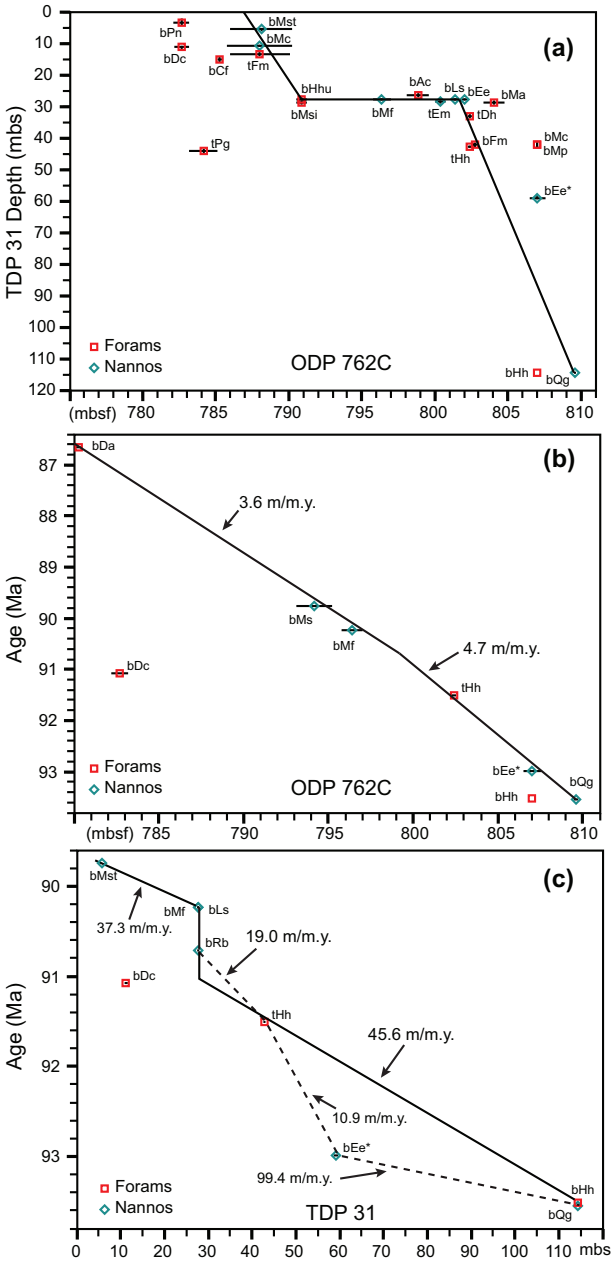

Fig. 11. Graphic correlation and age-depth plots for TDP 31 and ODP Hole 762C. (a) Line of correlation defined by planktonic foraminifera and calcareous nannofossils listed in Tables 2 and 4 for both sites using genus-species abbreviations and "b" for "base" and "t" for "top" of zone datums as listed in Table 2; (b) age-depth curve for TDP 31 using ages and bioevents listed in Table 2; (c) age-depth curve for ODP 762 using ages and bioevents listed in Table 4.

feasible because of the influence of likely time-averaged terrestrial organic matter and presence of diagenetic cements with a strong signal of remineralized organic matter in some samples (Haynes et al. 2016),

causing negative $\delta^{13}C$ excursions that are many times larger than any events recorded for pelagic chalk sequences used in global scale $\delta^{13}C$ correlations. Moreover, the $\delta^{13}C$ records from monospecific analyses of benthonic and planktonic foraminifera show essentially no change throughout all but the uppermost *H. helvetica* Zone at TDP sites 22 and 31 (MacLeod et al. 2013, I. Wendler et al. 2013).

Determination of a best-fit line of correlation (LOC) between TDP 31 and ODP 762 using planktonic foraminiferal and calcareous nannofossil bioevents provides a means for comparing sedimentation histories at the two sites (Fig. 11a). The preferred LOC is drawn as a solid line through the bioevents that are deemed to be most reliable. The events are listed in bold in Table 1 for Site 31. Multiple calcareous nannofossil and planktonic foraminiferal bioevents occur at the same depth at Site 31 and identify a hiatus there that is the equivalent of 11 m of section at Hole 762C. FADs that are delayed at Site 31 relative to Hole 762C plot to the right of the LOC and include the planktonic foraminifera *M. angusticarenata*, *M. coronata*, and *M. pseudolinneiana* as well as the calcareous nannofossil *E. eximius*. FADs that are delayed at Hole 762C plot to the left of the LOC and include *C. fornicata*, *D. concavata*, and *Ps. nuttalli*. The highest occurrence of *P. gibba* is positioned much lower at Site 31 than at Hole 762.

Age-depth plots (ADPs) using planktonic foraminiferal and calcareous nannofossil bioevent ages from Gradstein et al. (2012) are presented in Figure 11b for ODP 762 and in Figure 11c for TDP 31. In both diagrams the FAD of *D. concavata* is positioned considerably below the interpolated LOC, suggesting that the 91.08 Ma age estimate used for this datum is too old by at least 1.2 m.y. At Hole 762C absence of *H. helvetica* from samples just below its recorded LO is probably an artifact of poor preservation (Falzoni et al. 2016b) and it is therefore not used to anchor the LOC. The datums used to define the LOC for Hole 762C suggest a continuous rate of sedimentation ranging between 4.7 and 3.6 m/m.y. (Fig. 11b).

The LOC for Site 31 is anchored at the bottom of the borehole using the FADs of *Q. gartneri* and *H. helvetica* (Fig. 11c). Rarity of sensu stricto forms of *H. helvetica* in samples from the lowermost part of the borehole suggests that the recorded lowest occurrence is very close to its evolutionary first appearance (Huber and Petrizzo 2014). The preferred LOC is drawn through the FAD and LAD of *H. helvetica*, resulting in an estimated sedimentation rate of 45.6 m./m.y. If the FAD of *E. eximius* (s. Ver.) is used to define the LOC then the sedimentation rate would need to shift from 99.4 m/m.y. below this datum to 10.9 m/m.y. above, which is considered unlikely given the the absence of changes in sediment grain size and consistency in the relative abundance of benthic and planktonic foraminiferal and calcareous nannofossil relative abundances across this entire interval (Wendler et al. 2016, Huber et al. in prep.). Using the preferred sedimentation rate the duration of the hiatus at the base of the CC13 and the *M. sinuosa*/*Hu. huberi* Zone is estimated as 0.8 m.y. Above the hiatus the sedimentation rate is calculated as 37.3 m/m.y., which is similar to the underlying sequence.

As has been shown in previous studies, (e. g., Haq and Worsley 1982) the applicability of datum events for establishing a chronostratigraphic framework is limited by the geographic distribution and environmental tolerance of taxa. Much of the biochron diachroneity between the TDP sites and Hole 762C was probably influenced by the inability of some species to tolerate growth or effectively compete across the range of oceanic settings represented by the two sites. The presence of dwarfed morphotypes assigned to *Praeglobotruncana*, *Dicarinella* and *Marginotruncana* may provide a further indication that the environmental conditions on the Tanzanian contintental margin was not optimal for some calcareous plankton species (Huber et al., in prep.). Additional factors that can explain inconsistences in the species distributions include rarity and sporadic distribution of species within part or all of their stratigraphic range and uncertainty of species identifications due to (1) ecophenotypic variation, (2) gradual (anagenetic) evolutionary changes in morphologies, (3) imperfect preservation, and (4) inaccurate identification. The most reliable species for correlation of the two sites, shown in bold in Tables 2 and 4, include those that have the most consistent stratigraphic ordering at both the deep sea and nearshore locations. Until the ages of these biochrons have been directly calibrated using radiochronology, astrochronology and/or other geochronologic methods in both deep-sea and nearshore settings, use of previously assigned age estimates should be done with caution and with acknowledgement of age uncertainties of as much as 1.2 m.y., as has been found for the first appearance datum of *D. concavata*.

7. Conclusions

The Tanzania Drilling Project drilled a composite Turonian sediment record that spans over 4 m.y. from the late early Turonian (at or just below the base of the *H. helvetica* Zone; lower Zone CC11) and extends through the early Coniacian (*D. concavata* Zone; Zone CC14). Unfortunately, no sediments from the earliest Turonian interval including Oceanic Anoxic Event 2 were recovered at any of the 11 Turonian sites.

Extraordinarily good microfossil preservation in nearly all TDP 31 samples enables development of an integrated planktonic foraminiferal and calcareous nannofossil biostratigraphy for establishment of a more reliable chronostratigraphic framework for correlating the boreholes within the depositional basin and characterizing taxonomic and evolutionary changes that occurred during this a time. Primary results from this integrated biostratigraphic study include the following: (1) the middle Turonian *H. helvetica* Zone can be characterized as a time of species stasis with little change in taxonomic composition throughout the nearly 2.5 m.y. time interval; (2) an abrupt shift in the taxonomic composition of planktonic foraminiferal assemblages occurs at 42.8 mbs in TDP 31, at the top of the *H. helvetica* Zone, with the extinction of three species of *Helvetoglobotruncana*, temporary disappearance of *D. hagni*, and *W. aprica*, followed by dominance by species of *Marginotruncana*. However, this was not accompanied by any change in the calcareous nannofossil species composition; (3) a calcareous nannofossil species turnover at 27.7 mbs in TDP 31 is coincident with planktonic foraminiferal changes that include an abrupt increase in the percentage of biserial planktonic species and a minor species turnover, an increase in sediment grain size, and an abrupt diagenetic shift. Age models developed using the microfossil bioevents suggest a hiatus spanning from 0.4 to 0.8 m.y. at this level; and (4) the late Turonian is characterized by increased species diversification among both microfossil groups, affording a greater number of bioevents that improve the reliability of biostratigraphic and chronostratigraphic correlation.

Comparison between the Tanzanian calcareous plankton distributions and those in Turonian samples from Ocean Drilling Project Hole 762C reveals a number of stark contrasts. These include: (1) absence of evidence for evolutionary stasis during the early–middle Turonian at Hole 762C; (2) significant differences between the sites in the relative timing of species first and last occurrences; and (3) the dramatic shift from helvetoglobotruncanid- and dicarinellid-dominated foraminiferal assemblages within the *H. helvetica* Zone to marginotruncanid-dominated assemblages above at TDP 31 occurs more gradually and earlier by at least 2 m.y. at Hole 762C. These differences are attributed to oceanographic settings; specifically TDP 31 records events in a mesotrophic clastic margin setting, whereas the Hole 762C record reflects changes in an oligotrophic pelagic carbonate. Additional complications due to the influence of regional paleoclimatic and other paleoceanographic factors are likely.

A number of the taxonomic and biostratigraphic observations from this study have resulted in improved understanding of some species concepts, refinements in the chronostratigraphic framework for intra- and extra-basinal correlation of the Turonian TDP sites, and revisions in some biozone definitions. However, age calibrations are needed for most of the Turonian planktonic foraminiferal and calcareous nannofossil biochrons in order to establish a reliable age framework for the remarkably well preserved biotic assemblages and paleoenvironmental records that been obtained from the TDP boreholes.

Acknowledgements. Thanks are extended to the Tanzania Petroleum Development Corporation, particularly Joyce Singano, Amina Mweneinda, Emma Msaky, and Frank Mayagilo, for logistical and technical support, the Tanzanian Commission for Science and Technology for permission to carry out the field research program, and the TDP team, especially Alvaro Jimenez Berrocoso, Ines Wendler, Jens Wendler, Jackie Lees, for assistance with fieldwork in Tanzania and subsequent discussions. Assistance with sample picking by Loren Petruny, Erin Jacobs, Carlos Rodriguez-Russo, and Sarah Ehlinger and assistance with SEM imaging and image editing by JoAnn Sanner are gratefully acknowledged. Fieldwork and the drilling program were funded by National Science Foundation grant EAR 0642993to KGM and BTH and a Smithsonian Walcott Fund grant to BTH. Financial support to MRP was provided by PUR 2008 (Università degli Studi di Milano). We are grateful to Christian Linnert and Danuta Peryt for their helpful reviews.

References

Ando, A., Huber, B. T., MacLeod, K. G., Watkins, D. K., 2015. Early Cenomanian "hot greenhouse" revealed by oxygen isotope record of exceptionally well-preserved foraminifera from Tanzania. Paleoceanography 30, 2015PA002854.

Arthur, M. A., Schlanger, S. O., Jenkyns, H. C., 1987. The Cenomanian-Turonian Oceanic Anoxic Event, II. Paleoceanographic controls on organic-matter production and preservation. In: Brooks, J., Feet, A. J. (Eds.), Marine Pe-

troleum Source Rocks. Geological Society Special Publication No. 26, London, p. 401–420.

Banner, F.T., Blow, W.H., 1960. Some primary types of species belonging to the superfamily Globigerinaceae. Contributions from the Cushman Foundation for Foraminiferal Research 11, 1–41.

Barr, F.T., 1972. Cretaceous biostratigraphy and planktonic foraminifera of Libya. Micropaleontology 18, 1–46.

Bermúdez, P.J., 1952. Estudio sistematico de los Foraminiferos rotaliformes. Boletin de Geologia 2, 7–152.

Bice, K.L., Huber, B.T., Norris, R.D., 2003. Extreme polar warmth during the Cretaceous greenhouse? The paradox of the late Turonian $\delta^{18}O$ record at DSDP Site 511. Paleoceanography 18, 1031, doi:1010.1029/2002PA000848.

Bolli, H.M., 1945. Zur Stratigraphie der oberen Kreide in den höheren helvetischen Decken. Eclogae Geologicae Helvetiae 37, 217–328.

Bolli, H.M., 1966. Zonation of Cretaceous to Pliocene marine sediments based on planktonic foraminifera. Boletin Informativo Asociacion Venezolana de Geología, Minería y Petroleo 9, 3–32.

Bornemann, A., Norris, R.D., Friedrich, O., Beckmann, B., Schouten, S., Sinninghe Damsté, J.S., Vogel, J., Hofmann, P., Wagner, T., 2008. Isotopic evidence for glaciation during the Cretaceous Supergreenhouse. Science 319, 189–192.

Bown, P.R., Lees, J.A., Young, J.R., 2004. Calcareous nannoplankton evolution and diversity through time. In: Thierstein, H.R., Young, J.R. (Eds.), Springer-Verlag, Berlin, p. 481–508.

Bralower, T.J., Bergen, J.A., 1998. Cenomanian–Santonian calcareous nannofossil biostratigraphy of a transect of cores drilled across the Western Interior Seaway. In: Dean, W.E. and Arthur, M.A. (Eds.), Stratigraphy and paleoenvironments of the Cretaceous Western Interior Seaway. SEPM Concepts in Sedimentology and Paleontology, p. 59–77.

Bralower, T.J., Siesser, W.G., 1992. Cretaceous calcareous nannofossil biostratigraphyof Sites 761, 762, and 763, Exmouth and Wombat Plateaus, northwest Australia. In: Haq, B.U., von Rad, U. et al. (Eds.), Proceedings of the Ocean Drilling Program, Scientific Results, Ocean Drilling Program, College Station, TX, p. 529–556.

Brotzen, F., 1934. Foraminiferen aus dem Senon Palastinas. Zeitschrift des Deutschen Palastina-Vereins, 28–72.

Burnett, J.A., 1997. New species and new combinations of Cretaceous nannofossils and a note on the origin of Petrarhabdus (Deflandre) Wise & Wind. Journal of Nannoplankton Research 19, 133–146.

Burnett, J.A., 1998. Upper Cretaceous. Calcareous Nannofossil Biostratigraphy, British Micropalaeontological Society Series. In: Bown, P.R. (Ed.), London, Chapman & Hall/Kluwer Academic Press, 132–199.

Campbell, R.J., Howe, R.W., Rexilius, J.P., 2004. Middle Campanian–lowermost Maastrichtian nannofossil and foraminiferal biostratigraphy of the northwestern Australian margin. Cretaceous Research 25, 827–864.

Caron, M., 1976. Revision des types de Foraminiferes planctoniques decrits dans la region du Montsalvens (Prealpes fribourgeoises). Eclogae Geologicae Helvetiae 69, 327–333.

Caron, M., 1981. Un nouveau genre de Foraminifere planctonique du Cretace: Falsotruncana nov. gen. Eclogae Geologicae Helvetiae 74, 65–73.

Caron, M., 1985. Cretaceous planktonic foraminifera. In: Bolli, H.M., Saunders, J.B., Perch-Neilsen, K. (Eds.), Plankton Stratigraphy. Cambridge University Press, Cambridge, p. 17–86.

Caron, M., Dall'Agnolo, S., Accarie, H., Barrera, E., Kauffman, E.G., Amédro, F., Robaszynski, F., 2006. High-resolution stratigraphy of the Cenomanian–Turonian boundary interval at Pueblo (USA) and Wadi Bahloul (Tunisia): stable isotope and bio-events correlation. Géobios 39, 171–200.

Corbett, M.J., Watkins, D.K., Pospichal, J.J., 2014. Quantitative Analysis of Calcareous Nannofossil Bioevents of the Late Cretaceous (Late Cenomanian–Coniacian) Western Interior Seaway and their Reliability in Established Zonation Schemes. Marine Micropaleontology 109, 30–45, doi:10.1016/j.marmicro.2014.04.002.

Cushman, J.A., Ten Dam, A., 1948. *Globigerinelloides*, a new genus of the Globigerinidae. Contributions from the Cushman Foundation for Foraminiferal Research 24, 42–43.

d'Orbigny, A.D., 1840. Memoires Societe Geologique de France. Mem. Soc. Geol. Grance 4, Plates 1–4.

Deflandre, G., Fert, C., 1954. Observations sur les coccolithophoridés actuels et fossiles en microscopie ordinaire et électronique. Annales de Paléontologie 40, 115–176.

Deflandre, G., 1959. Sur les nannofossiles calcaires et leur systématique. Revue de Micropaleontologie 2, 127–152.

Douglas, R.G., 1969. Upper Cretaceous planktonic foraminifera in northern California. Part 1 – Systematics. Micropaleontology 15, 151–209.

Doeven, P.H., 1983. Cretaceous nannofossil stratigraphy and paleoecology of the Canadian Atlantic Margin. Bulletin of the Geological Survey of Canada 356, 1–70.

Douglas, R.G., Rankin, C., 1969. Cretaceous planktonic foraminifera from Bornholm and their zoogeographic significance. Lethaia 2, 185–217.

Du Vivier, A.D.C., Selby, D., Sageman, B.B., Jarvis, I., Gröcke, D.R., Voigt, S., 2014. Marine $^{187}Os/^{188}Os$ isotope stratigraphy reveals the interaction of volcanism and ocean circulation during Oceanic Anoxic Event 2. Earth and Planetary Science Letters 389, 23–33.

Ehrenberg, C.G., 1840. Über die Bildung der Kreidenfelsen und des Kreidemergels durch unsichtbare Organismen. K. Akad. Wiss. Berlin, Physik. Abh. (1838).

Ehrenberg, C.G., 1854. Mikrogeologie. Leipzig, L. Voss, pp. 1–374.

Falzoni, F., Petrizzo, M.R., Jenkyns, H.C., Gale, A.S., Tsikos, H., 2016a. Planktonic foraminiferal biostratigraphy and assemblage composition across the CenomanianeTuronian boundary interval at Clot Chevalier (Vocontian Basin, SE France). Cretaceous Research 59, 69–97.

Falzoni, F., Petrizzo, M.R., Clarke, L.C., MacLeod, K.G., Jenkyns, H.J., 2016b. Long-term Late Cretaceous carbon and oxygen-isotope trends and planktonic foraminiferal

turnover: a new record from the southern mid-latitudes. GSA Bulletin 128, doi:10.1130/B31399.1.

Forchheimer, S., 1972. Scanning electron microscope studies of Cretaceous coccoliths from the Köpingsberg Borehole No. 1, SE Sweden. Sveriges Geologiska Undersökning; Series C, #668, 65, 1–141.

Friedrich, O., Schiebel, R., Wilson, P. A., Weldeab, S., Beer, C. J., Cooper, M. J., Fiebig, J., 2012. Influence of test size, water depth, and ecology on Mg/Ca, Sr/Ca, $\delta^{18}O$ and $\delta^{13}C$ in nine modern species of planktic foraminifers. Earth and Planetary Science Letters 319–320, 133–145.

Gale, A. S., Hardenbol, J., Hathway, B., Kennedy, W. J., Young, J. R., Phansalkar, V., 2002. Global correlation of Cenomanian (Upper Cretaceous) sequences: Evidence for Milankovitch control on sea level. Geology 30, 291–294.

Gandolfi, R., 1942. Ricerche micropaleontologiche e stratigraphfiche sulla Scaglia e sul flysch Cretacici dei Dintorni di Balerna (Canton Ticino). Rivista Italiana Paleontologia 48, 1–160.

Gandolfi, R., 1957. Notes on some species of *Globotruncana*. Contributions from the Cushman Laboratory for Foraminiferal Research 8, 59–65.

Gardet, M., 1955. Contribution à l'étude des coccolithes des terrains néogènes de l'Algérie. Publications du Service de la Carte Géologique de l'Algérie (Nouvelle Série) 5, 477–550.

Gartner, S., 1968. Coccoliths and related calcareous nannofossils from Upper Cretaceous deposits of Texas and Arkansas. The University of Kansas Paleontological Contributions, Article 48 (Protista 1), 1–56.

Georgescu, M. D., 2007. A new planktonic heterohelicid foraminiferal genus from the Upper Cretaceous (Turonian). Micropaleontology 53, 212–220.

Georgescu, M. D., Huber B. T., 2009. Early evolution of the Cretaceous serial planktic foraminifera (late Albian–Cenomanian). Journal of Foraminiferal Research 39, 335–360.

Georgescu, M. D., Quinney, A. E., Anderson, K. D., 2011. New data on the taxonomy, evolution and biostratigraphical significance of the Turonian–Coniacian (Late Cretaceous) planktic foraminifer *Huberella* Georgescu 2007. Micropaleontology 57, 247–254.

Gradstein, F. M., Ogg, J. G., Schmitz, M. D., Ogg, G. M., 2012. The Geologic Time Scale 2012. Elsevier, Amsterdam, The Netherlands.

Gradstein, F. M., Ogg, J. G., Smith, A. G., 2004. A Geologic Time Scale 2004. Cambridge University Press, Cambridge, p. 589.

Hagn, H., Zeil, W., 1954. Globotruncanen aus dem Ober-Cenoman und Unter-Turon der Bayerischen Alpen. Eclogae Geologicae Helvetiae 47, 1–60.

Haq, B. U., 2014. Cretaceous eustasy revisited. Global and Planetary Change 113, 44–58.

Haq, B. U., Huber, B. T., 2016. Anatomy of a eustatic event during the Turonian (Late Cretaceous) hot greenhouse climate. Science China Earth Sciences.

Haq, B. U., von Rad, U., O'Connell, S. et al., 1990. Proceedings of the Ocean Drilling Program. Ocean Drilling Program, College Station, Texas, 826 pp.

Haq, B. U., Worsley, T. R., 1982. Biochronology – Biologic events in time resolution, their potential and limitations. In: Odin, G. S. (Ed.), Numerical Dating in Stratigraphy. J. Wiley, New York, p. 19–33.

Hardenbol, J., Thierry, J., Farley, M. B., Jacquin, T., de-Graciansky, P. C., Vail, P. R., 1998. Mesozoic and Cenozoic sequence chronostratigraphic framework of European basins. In: de Graciansky, P. C., Hardenbol, J., Thierry, J., Vail, P. R. (Eds.), Mesozoic and Cenozoic sequence stratigraphy of European basins, Special Publication, Society for Sedimentary Geology. Society for Sedimentary Geology. Tulsa, OK. p. 3–13.

Hart, M. B., 1999. The evolution and biodiversity of Cretaceous Foraminiferida. Geobios 32, 247–255.

Hay, W. W., DeConto, R., Wold, C. N., Wilson, K. M., Voigt, S., Schulz, M., Wold-Rossby, A., Dullo, W.-C., Ronov, A. B., Balukhovsky, A. N., Söding, E., 1999. Alternative global Cretaceous paleogeography. In: Barrera, E., Johnson, C. (Eds.), Evolution of the Cretaceous Ocean-Climate System. Geological Society of America Special Paper 332, Boulder, CO, pp. 1–47.

Haynes, S. J., Huber, B. T., MacLeod, K. G., 2015. Evolution and phylogeny of mid-Cretaceous (Albian–Coniacian) biserial planktic foraminifera. Journal of Foraminiferal Research 45, 42–81.

Haynes, S. J., MacLeod, K. G., Huber, B. T., Warny, S., Kaufman, A. J., Pancost, R. D., Jiménez Berrocoso, Á., Petrizzo, M. R., Watkins, D. K., Zhelezinskaia, I., 2016. Southeastern Tanzania depositional environments, marine and terrestrial links, and exceptional microfossil preservation in the warm Turonian. Geological Society of America Bulletin, doi:10.1130/B31432.1.

Herb, R., 1974. Cretaceous planktonic foraminifera from the eastern Indian Ocean. In: Davies, T. A., Luyendyk, B. P. et al. (eds.), Initial Reports of the Deep Sea Drilling Project, Volume 26: Washington, D.C., U.S. Government Printing Office, p. 745–769.

Herb, R., Scheibnerova, V., 1977. Synopsis of Cretaceous planktonic foraminifera from the Indian Ocean. In: Heirtzler, J. R., Bolli, H. M. et al. (eds.), Indian Ocean Geology and Biostratigraphy, American Geophysical Union, p. 399–415.

Hill, M. E., 1976. Lower Cretaceous calcareous nannofossils from Texas and Oklahoma. Palaeontographica Abteilung B, 156, 103–179.

Hofker, J., 1956. Die Globotruncanen von Nordwest-Deutshland und Holland. Neues Jahrbuch für Geologie und Paläontologie, Abhandlungen 103, 312–340.

Howe, R. W., Campbell, R. J., Rexilius, J. P., 2003. Integrated uppermost Campanian–Maastrichtian calcareous nannofossils and foraminiferal biostratigraphic zonation of the northwestern margin of Australia. Journal of Micropalaeontology 22, 29–62.

Huber, B. T., Hodell, D. A., Hamilton, C. P., 1995. Mid- to Late Cretaceous climate of the southern high latitudes: Stable isotopic evidence for minimal equator-to-pole thermal gradients. Geological Society of America Bulletin 107, 1164–1191.

Huber, B.T., Leckie, R.M., 2011. Planktic foraminiferal species turnover across deep-sea Aptian/Albian boundary sections. Journal of Foraminiferal Research 41, 53–95.

Huber, B.T., Leckie, R.M., Norris, R.D., Bralower, T.J., CoBabe, E., 1999. Foraminiferal assemblage and stable isotopic change across the Cenomanian–Turonian boundary in the subtropical North Atlantic. Journal of Foraminiferal Research 29, 392–417.

Huber, B.T., Norris, R.D., MacLeod, K.G., 2002. Deep sea paleotemperature record of extreme warmth during the Cretaceous. Geology 30, 123–126.

Huber, B.T., Petrizzo, M.R., 2014. Evolution and taxonomic study of the Cretaceous planktonic foraminifer Genus *Helvetoglobotruncana* Reiss, 1957 Journal of Foraminiferal Research 44, 40–57.

Jarvis, I., Gale, A.S., Jenkyns, H.C., Pearsce, M.A., 2006. Secular variation in Late Cretaceous carbon isotopes: a new $\delta^{13}C$ carbonate reference curve for the Cenomanian–Campanian (99.6–70.6 M). Geological Magazine 143, 561–608.

Jenkyns, H.C., 1999. Mesozoic anoxic events and paleoclimate. Zbl. Geol. Paläont. Teil 9, 943–949.

Jenkyns, H.C., 2010. Geochemistry of oceanic anoxic events. Geochemistry, Geophysics, Geosystems 11; Q03004, doi: 03010.01029/02009GC002788.

Jenkyns, H.C., Gale, A.S., Corfield, R.M., 1994. Carbon- and oxygen-isotope stratigraphy of the English Chalk and Italian Scaglia and its palaeoclimatic significance. Geological Magazine 131, 1–34.

Jiménez Berrocoso, Á., MacLeod, K.G., Huber, B.T., Lees, J.A., Wendler, I., Bown, P.R., Mweneinda, A.K., Isaza Londoño, C., Singano, J.M., 2010. Lithostratigraphy, biostratigraphy and chemostratigraphy of Upper Cretaceous sediments from southern Tanzania: Tanzania Drilling Project Sites 21–26. Journal of African Earth Sciences 57, 47–69, doi:10.1016/j.jafrearsci.2009.07.010.

Jiménez Berrocoso, Á., Huber, B.T., MacLeod, K.G., Petrizzo, M.R., Lees, J.A., Wendler, I., Coxall, H., Mweneinda, A.K., Falzoni, F., Birch, H., Singano, J.M., Haynes, S.J., Cotton, L., Wendler, J., Bown, P.R., Robinson, S.A., Gould, J., 2012. Lithostratigraphy, biostratigraphy and chemostratigraphy of Upper Cretaceous and Paleogene sediments from southern Tanzania: Tanzania Drilling Project Sites 27–35. Journal of African Earth Sciences 70, 36–57, doi:10.1016/j.jafrearsci.2012.05.006.

Jiménez Berrocoso, Á., Huber, B.T., MacLeod, K.G., Petrizzo, M.R., Lees, J.A., Wendler, I., Coxall, H., Mweneinda, A.K., Falzoni, F., Birch, H., Haynes, S.J., Bown, P.R., Robinson, S.A., Singano, J.M., 2015. The Lindi Formation (upper Albian–Coniacian) and Tanzania Drilling Project Sites 36–40 (Lower Cretaceous to Paleogene): Lithostratigraphy, biostratigraphy and chemostratigraphy. Journal of African Earth Sciences 101, 282–308, doi:10.1016/j.jafrearsci.2014.09.017.

Joo, Y.J., Sageman, B.B., 2014. Cenomanian to Campanian carbon isotope chemostratigraphy from the Western Interior Basin, U.S.A. Journal of Sedimentary Research 84, 529–542.

Kent, P.E., Hunt, J.A., Johnstone, D.W., 1971. The geology and geophysics of coastal Tanzania. Institute of Geological Sciences Geophysical Paper No.6, HMSO, London.

Key, R.M., Smith, R.A., Smelor, M., Sæther, O.M., Thorsnes, T., Powell, J.H., Njange, F., Zandamela, E.B., 2008. Revised lithostratigraphy of the Mesozoic–Cenozoic succession of the onshore Rovuma Basin, northern coastal Mozambique. South African Journal of Earth Sciences 111, 89–108.

Klaus, J., 1960. Etude biometrique et statistique de quelques espèces de Globotruncanides 1. Les espèces du genre *Praeglobotruncana* dans le Cenomanien de la Breggia (Tessin, Suisse meridionale). Eclogae Geologicae Helvetiae 53, 304.

Korchagin, V.I., 1982. Sistematika Globotrunkanid. Byull. Mosk. Ova. Ispyt. Prir., Otd. Geol. 57, 114–161.

Kuhry, B., 1970. Some observations on the type material of *Globotruncana elevata* (Brotzen) and *Globotruncana concavata* 'Brotzen'. Revista Española de Micropaleontolgía, 2, 291–304.

Lamolda, M., 1977. Three new species of planktonic foraminifera from the Turonian of northern Spain. Micropaleontology 23, 470–477.

Lawver, L.A., Gahagan, L.M., Covvin, M.F., 1992. The development of paleoseaways around Antarctica. In: Kennett, J.P., Warnke, D.A. (Eds.), The Antarctic Paleoenvironment: A Perspective on Global Change, Antarctic Research Series. American Geophysical Union, Washington, D.C., pp.7–30.

Leckie, R.M., Bralower, T., Cashman, R., 2002. Oceanic Anoxic Events and plankton evolution: Exploring biocomplexity in the mid-Cretaceous. Paleoceanography 17, doi:10.1029/2000PA000572.

Lees, J.A., 2007. New and rarely reported calcareous nannofossils from the Late Cretaceous of coastal Tanzania: outcrop samples and Tanzania Drilling Project Sites 5, 9 and 15. Journal of Nannoplankton Research 29, 39–65.

Lees, J.A., 2008. The calcareous nannofossil record across the Late Cretaceous Turonian/Coniacian boundary, including new data from Germany, Poland, the Czech Republic and England. Cretaceous Research 29, 40–64.

Lehmann, R., 1963. Étude des Globotruncanidés du Crétacé supérieur de la province de Tarfaya (Maroc occidental). Notes du Service Géologique du Maroc 21, 133–179.

Linnert, C., Mutterlose, J., 2015. Boreal early Turonian calcareous nannofossils from nearshore settings – implications for paleoecology, Palaios 30: 728–742.

Linnert, C., Mutterlose, J., Erbacher, J., 2010. Calcareous nannofossils of the Cenomanian/Turonian boundary interval from the Boreal Realm (Wunstorf, northwest Germany). Marine Micropaleontology, 74, 38–58.

Loeblich, A.R., Jr., Tappan, H., 1961. Cretaceous planktonic foraminifera: Part I-Cenomanian. Micropaleontology 7, 257–304.

Loeblich, A.R., Jr., Tappan, H., 1988. Foraminiferal Genera and Their Classification (Volume I–II). New York, Van Nostrand Reinhold C., 970 pp.

MacLeod, K.G., Huber, B.T., Jiménez Berrocoso, A., Wendler, I., 2013. A stable and hot Turonian without glacial $\delta^{18}O$ excursions indicated by exquisitely preserved Tanzanian foraminifera. Geology 41, 1083–1086.

MacLeod, K.G., Martin, E.E., Blair, S.W., 2008, Nd isotopic excursion across Cretaceous ocean anoxic event 2 (Cenomanian–Turonian) in the tropical North Atlantic. Geology, 36, 811–814; doi:10.1130/G24999A.1

Manivit, H., Perch-Neilsen, K., Prins, B., Verbeek, J.W., 1977. Mid Cretaceous calcareous nannofossil biostratigraphy. Kon. Nederl. Akad. Wet. B80, 169–181.

Marianos, A.W., Zingula, R.P., 1966. Cretaceous planktonic foraminifers from Dry Creek, Tehama County, California. Journal of Paleontology 40, 328–343.

Martin, E.E., MacLeod, K.G., Jiménez Berrocoso, Á., Bourbon, E., 2012. Water mass circulation on Demerara Rise during the Late Cretaceous based on Nd isotopes. Earth and Planetary Science Letters, 327–328, 111–120, doi:10.1016/j.epsl.2012.01.037

Masters, B.A., 1980. Re-evaluation of selected types of Ehrenberg's Cretaceous planktonic foraminifera. Eclogae Geologicae Helvetiae 73, 95–107.

Meyers, S.R., Siewert, S.E., Singer, B.S., Sageman, B.B., Condon, D.J., Obradovich, J.D., Jicha, B.R., Sawyer, D.A., 2012. Intercalibration of radioisotopic and astrochronologic time scales for the Cenomanian–Turonian boundary interval, Western Interior Basin, USA. Geology 40, 7–10, doi:10.1130/G32261.32261.

Miller, K.G., Kominz, M.A., Browning, J.V., Wright, J.D., Mountain, G.S., Katz, M.E., Sugarman, P.J., Cramer, B.S., Christie-Blick, N., Pekar, S.F., 2005. The Phanerozoic record of global sea-level change. Science 310, 1293–1298.

Miller, K.G., Sugarman, P.J., Browning, J.V., Kominz, M.A., Olsson, R.K., Feigenson, M.D., Hernández, J.C., 2004. Upper Cretaceous sequences and sea-level history, New Jersey Coastal Plain. Geological Society of America Bulletin 116, 368–393.

Mornod, L., 1950. Les Globorotalides du Cretace superieur du Montsalvens (Prealpes fribourgeoises). Eclogae Geologicae Helvetiae 42, 573–595.

Nicholas, C.J., Pearson, P.J., Bown, P.R., Dunkley Jones, T., Huber, B.T., Karega, A., Lees, J.A., McMillan, I.K., O'Halloran, A., Singano, J.M., Wade, B.S., 2006. Stratigraphy and sedimentology of the Upper Cretaceous to Paleogene Kilwa Group, southern coastal Tanzania. Journal of African Earth Sciences 45, 431–466.

Nicholas, C.J., Pearson, P.N., McMillan, I.K., Ditchfield, P.W., Singano, J.M., 2007. Structural evolution of southern coastal Tanzania since the Jurassic. Journal of African Earth Sciences 48, 273–297.

Ogg, J., Gradstein, F.M., 2015. Time Scale Creator version 6.2. https://engineering.purdue.edu/Stratigraphy/tscreator/index/index.php.

Pearson, P.N., Ditchfield, P.W., Singano, J., Harcourt-Brown, K.G., Nicholas, C.J., Olsson, R.K., Shackleton, N.J., Hall, M.A., 2001. Warm tropical sea surface temperatures in the Late Cretaceous and Eocene epochs. Nature 413, 481–487.

Pearson, P.N., Nicholas, C.J., Singano, J.M., Bown, P.R., Coxall, H.K., van Dongen, B.E., Huber, B.T., Karega, A., Lees, J.E., Msaky, E., Pancost, R.D., Pearson, M., Roberts, A.P., 2004. Paleogene and Cretaceous sediment cores from the Kilwa and Lindi areas of coastal Tanzania: Tanzania Drilling Project Sites 1–5. Journal of African Earth Sciences 39, 25–62.

Pearson, P.N., Nicholas, C.J., Singano, J.M., Bown, P.R., Coxall, H.K., van Dongen, B.E., Huber, B.T., Karega, A., Lees, J.A., MacLeod, K.G., McMillan, I.K., Pancost, R.D., Pearson, M., Msaky, E., 2006. Further Paleogene and Cretaceous sediment cores from the Kilwa area of coastal Tanzania: Tanzania Drilling Project Sites 6–10. Journal of African Earth Sciences 45, 279–317.

Perch-Nielsen, K., 1968. Der Feinbau und die Klassifikation der Coccolithen aus dem Maastrichtien von Danemark. Biologiske Skrifter. Kongelige Danske Videnskabernes Selskab 16, 1–96.

Perch-Nielsen, K., 1979. Calcareous nannofossils from the Cretaceous between the North Sea and the Mediterranean. Aspekte der Kreide Europas, IUGS Series A, 6, 223–272.

Perch-Nielsen, K., 1984. Validation of new combinations. Newsletter of the International Nannoplankton Association 6, 42–46.

Perch-Nielsen, K., 1985. Mesozoic calcareous nannofossils. In: Bolli, H.M., Saunders, J.B., Perch-Nielsen, K. (Eds.), Plankton Stratigraphy, 1, pp. 329–426.

Perch-Nielsen, K., 1986. New Mesozoic and Paleogene calcareous nannofossils. Eclogae Geologicae Helvetiae 79, 835–847.

Peryt, D., 1980. Planktic foraminifera zonation of the Upper Cretaceous in the middle Vistula River valley, Poland. Palaeontologia Polonica 41, 1–123.

Pessagno, E.A.J., 1967. Upper Cretaceous planktonic foraminifera from the western Gulf Coastal Plain. Palaeontographica Americana 5, 245–445.

Petrizzo, M.R., 2000. Upper Turonian–lower Campanian planktonic foraminifera from southern mid-high latitudes (Exmouth Plateau, NW Australia): biostratigraphy and taxonomic notes. Cretaceous Research 21, 479–505.

Petrizzo, M.R., 2001. Late Cretaceous planktonic foraminifera from Kerguelen Plateau (ODP Leg 183): new data to improve the Southern Ocean biozonation. Cretaceous Research 22, 829–855.

Petrizzo, M.R., 2002. Palaeoceanographic and palaeoclimatic inferences from Late Cretaceous planktonic foraminiferal assemblages from the Exmouth Plateau (ODP Sites 762 and 763, eastern Indian Ocean). Marine Micropaleontology 45, 117–150.

Petrizzo, M.R., 2003. Late Cretaceous planktonic foraminiferal bioevents in the Tethys and in the Southern Ocean record: An overview. Journal of Foraminiferal Research 33, 330–337.

Petrizzo, M.R., Falzoni, F., Premoli Silva, I., 2011. Identification of the base of the lower-to-middle Campanian *Globotruncana ventricosa* Zone: Comments on reliability and global correlations. Cretaceous Research 32, 387–405.

Petrizzo, M.R., Jiménez Berrocoso, A., Falzoni, F., Huber, B.T. MacLeod, K.G., 2017. The Coniacian–Santonian sedimentary record in southern Tanzania (Ruvuma Basin, East Africa): planktonic foraminiferal evolutionary, geochemical and palaeoceanographic patterns. doi:10.1111/sed.12331. Sedimentology.

Plummer, H.J., 1931. Some Cretaceous foraminifera in Texas. University of Texas Bulletin 3101, 109–203.

Porthault, B., In: Donze, P., Porthault, B., Thomel, G., Villoutreys, O. de, 1970. Le Sénonien inférieur de Puget-Théniers (Alpes-Maritimes) et sa microfaune. Geobios 3, 81–82.

Premoli Silva, I., Sliter, W.V., 1994. Cretaceous planktonic foraminiferal biostratigraphy and evolutionary trends from the Bottacione section, Gubbio, Italy. Palaeontographia Italica 82, 1–89.

Premoli Silva, I., Sliter, W.V., 1999. Cretaceous paleoceanography: Evidence from planktonic foraminiferal evolution. In: Barrera, E., Johnson, C.C. (Ed.), Evolution of the Cretaceous Ocean-Climate System, Special Paper 332. Geological Society of America, Boulder, Colorado, pp. 301–328.

Reichel, M., 1950. Observations sur les *Globotruncana* du gisement de la Breggia (Tessin). Compte Rendu de la Societe Paleontologique Suisse 42, 596–617.

Reiss, Z., 1957. The Bilamellidea, nov. superfam., and remarks on Cretaceous globorotaliids. Contributions to the Cushman Foundation of Foraminiferal Research 8, 127–145.

Reinhardt, P., 1965. Neue Familien für fossile Kalkflagellaten (Coccolithophoriden, Coccolithineen).

Reuss, A.E., 1854. Beitrage zur Charakteristik der Kreideschichten in den Ostalpen, besonders im Gosauthale und am Wolfgangsee. Denkschr. Akad. Wein. Math. nat. cl.: 63–73, 155, 156.

Robaszynski, F., Caron, M., 1995. Foraminifères planctoniques du Crétacé: commentaire de la zonation Europe-Mediterranée. Société géologique de France 166, 681–692.

Robaszynski, F., Caron, M., Dupuis, C., Amedro, F., Donoso, G.M., Linares, D., Hardenbol, J., Gartner, S., Calandra, F., Deloffre, R., 1990. A tentative integrated stratigraphy in the Turonian of central Tunisia: formations, zones and sequential stratigraphy in the Kalaat Senan area. Bulletin des Centres de Recherches Exploration-Production Elf-Aquitaine 14, 213–384.

Robaszynski, F., Caron, M., Gonzales Donoso, J.M., Wonders, A.A.H. (eds.), a.t.E.W.G.o.P.F., 1984. Atlas of Late Cretaceous globotruncanids. Revue de Micropaléontologie 26, 145–305.

Robaszynski, F., Caron, M., (coordinators – European Working Group on Planktonic Foraminifera), 1979. Atlas of Mid Cretaceous Planktonic Foraminifera (Boreal Sea and Tethys). C.N.R.S., Paris.

Robaszynski, F., González-Donoso, J.M., Linares, D., Amedro, F., Caron, M., Dupuis, C., Dhondt, A.V., Gartner, S., (2000). Le Crétacé supérieur de la région de Kalaat Senan, Tunisie Centrale. Litho-biostratigraphie intégrée: Zones d'ammonites, de foraminifères planctoniques et de nannofossiles du Turonien supérieur au Maastrichtien. Bulletin des Centres de Recherches Exploration-Production Elf-Aquitaine 22, 359–490.

Roth, P.H., 1978. Cretaceous nannoplankton biostratigraphy and oceanography of the Northwestern Atlantic Ocean. Initial Reports of the Deep Sea Drilling Project 44, 731–759.

Salman, G., Abdula, I., 1995. Development of the Mozambique and Ruvuma sedimentar basins, offshore Mozambique. Sedimentary Geology 96, 7–41.

Scheibnerová, V., 1962. Upper Cretaceous, middle Turonian – Klippen belt of West Carpathians in Slovakia, Czechoslovakia. Slovensk. Akad. Vied, Bratislava, Geol. Sbornik 13, 225.

Schlanger, S.O., Jenkyns, H.C., 1976. Cretaceous Oceanic Anoxic Events: Causes and consequences. Geologie en Mijnbouw 55, 179–184.

Schlanger, S.O., Arthur, M.A., Jenkyns, H.C., Scholle, P.A., 1987. The Cenomanian-Turonian Oceanic Anoxic Event, I. Stratigraphy and distribution of organic carbon-rich beds and the marine $\delta^{13}C$ excursion. In: Brooks, J., Fleet, A.J. (Eds.), Marine Petroleum Source Rocks. Geological Society Publication No. 26, London, pp. 371–399.

Shafik, S., 1979. Validation of *Chiastozygus fessus* and *Reinhardtites biperforatus*, International Nannoplankton Association Newsletter 1, C-5.

Shamrock, J.L., Watkins, D.K., 2009, Evolution of the Cretaceous calcareous nannofossil genus *Eiffellithus* and its biostratigraphic significance. Cretaceous Research 30, 1183–1102.

Sigal, J., 1952. Apercu stratigraphique sur la micropaleontologie du Crétacé. Monographies Regionales 1, 3–43.

Sigal, J., 1955. Notes micropaléontologiques nord-africaines. 1. Du pélagiques. C. r. Somm. Soc. geol. Fr. 8, 157–160.

Sissingh, W., 1977. Biostratigraphy of Cretaceous calcareous nannoplankton. Geologie en Mijnbouw 56, 37–50.

Stover, L.E., 1966. Cretaceous coccoliths and associated nannofossils from France and the Netherlands. Micropaleontology 12, 133–167.

Stradner, H., 1963. New contributions to Mesozoic stratigraphy by means of nannofossils. Proceedings of the Sixth World Petroleum Congress, Section 1 Paper 4, 167–183.

Stradner, H. & Steinmetz, J., 1984. Cretaceous calcareous nannofossils from the Angola Basin, Deep Sea Drilling Project Site 530. Initial Reports of the Deep Sea Drilling Project, 75, 565–649.

Trujillo, E.F., 1960. Upper Cretaceous foraminifera from near Redding, Shasta County, California. Journal of Paleontology 34, 290–346.

Tsikos, H., Jenkyns, H.C., Walsworth-Bell, B., Petrizzo, M.R., Forster, A., Kolonic, S., Erba, E., Premoli Silva, I., Baas, M., Wagner, T., Sinninghe Damsté, J.S., 2004. Carbon-isotope stratigraphy recorded by the Cenomanian–Turonian Oceanic Anoxic Event: Correlation and implications based on three key localities. Journal of the Geological Society, London 161, 711–719.

Turgeon, S.C., Creaser, R.A., 2008. Cretaceous oceanic anoxic event 2 triggered by a massive magmatic episode. Nature 454, 323–326.

van Dongen, B.E., Talbot, H.M., Schouten, S.P., Pearson, P.N., Pancost, R.D., 2006. Well preserved Palaeogene and Cretaceous biomarkers from teh Kilwa area, Tanzania. Organic Geochemistry 37, 539–557.

Varol, O., Girgis, M., 1994. New taxa and taxonomy of some Jurassic to Cretaceous calcareous nannofossils. Neues Jahrbuch für Geologie und Paläontologie Abhandlungen 192, 221–253.

Verbeek, J., 1977, Calcareous nannoplankton biostratigraphy of middle and Upper Cretaceous deposits in Tunisia, southern Spain, and France, Utrecht. Micropaleontology Bulletin 16, 1–157.

Voigt, S., Erbacher, J., Mutterlose, J., Weiss, W., Westerhold, T., Wiese, F., Wilmsen, M., Wonik, T., 2008. The Cenomanian Turonian of the Wunstorf section (North Germany): global stratigraphic reference section and new orbital time scale for Oceanic Anoxic Event 2. Newsletters on Stratigraphy 43, 65–89.

Voigt, S., Gale, A.S., Flögel, S., 2004. Midlatitude shelf seas in the Cenomanian-Turonian greenhouse world: Temperature evolution and North Atlantic circulation. Paleoceanography 19, PA4020, doi:10.1029/2004PA001015.

von Rad, U., Exon, N.F., Haq, B.U., 1992. Rift-to-drift history of the Wombat Plateau, northwest Australia: Triassic to Tertiary Leg 122 results. Proceedings of the Ocean Drilling Program Scientific Results 122, 765–800.

Voorwijk, G.H., 1937. Foraminifera from the Upper Cretaceous of Habana, Cuba. K. Ned. Akad. Wet., Proc. Sec. Sci. 40, 190–198.

Watkins, D.K., Bergen, J.A., 2003. Late Albian adaptive radiation in the calcareous nannofossil genus *Eiffellithus*. Micropaleontology 49, 231–252.

Watkins, D.K., Wise, S.W., Jr., Pospichal, J.J., Crux, J.A., 1996. Upper Cretaceous calcareous nannofossil biostratigraphy and paleoceanography of the Southern Ocean, Microfossils and Oceanic Environments. British Micropalaeontological Society, University of Wales, Aberystwyth Press, pp.355–381.

Wendler, I., Huber, B.T., MacLeod, K.G., Wendler, J.E., 2011. Early evolutionary history of *Tubulogenerina* and *Colomia*: New species from exceptionally preserved Turonian sediments in East Africa. Journal of Foraminiferal Research 41, 384–400.

Wendler, I., Huber, B.T., MacLeod, K.G., Wendler, J.E., 2013. Stable oxygen and carbon isotope systematics of exquisitely preserved Turonian foraminifera from Tanzania – Understanding isotopic signatures in fossils. Marine Micropaleontology 102, 1–33.

Wendler, I., Wendler, J.E., Clarke, J.A., 2016. Sea-level reconstruction for Turonian sediments fromTanzania based on integration of sedimentology, microfacies, geochemistry and micropaleontology. Palaeogeography, Palaeoclimatology, Palaeoecology 441, 528–564.

Wendler, J.E., Bown, P.R., 2013. Exceptionally well-preserved Cretaceous microfossils reveal new biomineralization styles. Nature Communications, 4, 2052, doi:10.1038/ncomms3052.

Wendler, J.E., Wendler, I., Huber, B.T., 2013. Revision and evaluation of the systematic affinity of the calcareous dinoflagellate calcitarch Genus Pithonella based on exquisitely preserved Turonian material from Tanzania. Journal of Paleontology 87, 1077–1106.

Wonders, A.A.H., 1992. Cretaceous planktonic foraminiferal biostratigraphy, Leg 122, Exmouth Plateau, Australia, In: Haq, B.U., von Rad, U., et al. (Eds.), Proceedings of the Ocean Drilling Program, Scientific Results. Ocean Drilling Program, College Station, TX, pp.587–599.

Zepeda, M.A., 1998. Planktonic foraminiferal diversity, equitability and biostratigraphy of the uppermost Campanian–Maastrichtian, ODP Leg 122, Hole 762C, Exmouth Plateau, NW Australia, eastern Indian Ocean. Cretaceous Research 19, 117–152.

Zheng, X.-Y., Jenkyns, H.C., Gale, A.S., Ward, D.J., 2013. Changing ocean circulation and hydrothermal inputs during Ocean Anoxic Event 2 (Cenomanian–Turonian): Evidence from Nd-isotopes in the European shelf sea. Earth and Planetary Science Letters 375, 338–348.

Zheng, X.-Y., Jenkyns, H.C., Gale, A.S., Ward, D.J., Henderson, G.M., 2016. A climatic control on reorganization of ocean circulation during the mid-Cenomanian event and Cenomanian–Turonian oceanic anoxic event (OAE 2): Nd isotope evidence. Geology 44, 151–154.

Manuscript received: July 4, 2016
Revised version accepted: November 8, 2016

Appendix 1: Taxonomic Notes

In the following section morphologic features and stratigraphic distributions are described to clarify taxonomic concepts of select species illustrated in Fig. 5 and in Plates 1–6. The classification scheme follows Loeblich and Tappan (1988) except when specified. Presence/absence data for TDP Site 31 and ODP Site 762 are included in Tables 2–3. Abbreviations include: USNM = U.S. National Museum; UCMP = University of California Museum of Paleontology.

Genus *Archaeoglobigerina* Pessagno, 1967
Archaeoglobigerina cretacea Pessagno, 1967: Plate 1, Figures 3, 4, 9, 10
Globigerina cretacea d'Orbigny, 1840, p. 34, pl. 3, figs. 12–14 (lower Campanian, France).
Globotruncana cretacea (d'Orbigny), Banner and Blow, 1960, p. p. 8–10, p. 7, figs. 1a–c [lectotype], (lower Campanian, France).
Archaeoglobigerina cretacea (d'Orbigny), Pessagno, 1967, p. 317, pl. 70, figs. 3–8, pl. 94, figs. 4–5 (Santonian-Campanian, Texas).
Remarks. The specimen chosen by Banner and Blow (1960) as the lectotype of *A. cretacea* is more globular with a more broadly rounded peripheral margin and less well developed double keels than the *A. cretacea* specimens from TDP 31. The LO of this species is within the *F. maslakovae* Zone at Site 762 but it first appears stratigraphically higher, in the *M. sinuosa*/*Hu huberi* Zone at TDP 31.

Archaeoglobigerina spp.: Plate 1, Figures 7, 8
Remarks. Specimens identified as *Archaeoglobigerina* spp. are tentatively considered as transitional forms between an unknown ancestral species and *Archaeoglobigerina cretacea*. Further documentation is needed to verify the taxonomic status of those groups of specimens.

Genus *Contusotruncana* Korchagin, 1982
Contusotruncana fornicata (Plummer, 1931): Plate 2, Figures 9, 10
Globotruncana fornicata Plummer, 1931, p. 130, pl. 13, figs. 4–6.
Remarks. The oldest sensu stricto form of *C. fornicata* occurs within the middle *M. sinuosa*/*Hu. huberi* Zone at TDP 31 (14.29 mbs Sample 31-10-1, 19–39 cm) and ODP Site 762 (785.13 mbsf; 762-70X-1, 11–13 cm). Transitional forms, which differ by having a flatter spiral surface (e. g., Pl. 2, Fig. 9), extend into the lower *F. maslakovae* Zone at TDP 31 (39.60 mbs; 31-24-1, 50–70 cm) but were not identified at Site 762.

Genus *Dicarinella* Porthault, 1970
Remarks. Species included in this genus are restricted to forms with depressed radial sutures on the umbilical side.

Dicarinella concavata (Brotzen, 1934): Plate 3, Figures 9–10
Rotalia concavata Brotzen, 1934, p. 66, pl. 39, fig. b (Campanian–Santonian, Israel).
Globotruncana concavata (Brotzen), Kuhry, 1970, p. 299–300, 302, pl. 2, figs. 16–18 [lectotype], (Campanian–Santonian, Israel).
Dicarinella concavata (Brotzen), Robaszynski et al., 1979, p. 71–78, pl. 54, figs. 1–2, pl. 55, figs. 1–2 (upper Turonian–Coniacian, Morocco, Tunisia).
Remarks. This species is distinguished from its descendent species *D. asymetrica* (Sigal, 1952) by the absence of a periumbilical ridge surrounding the umbilicus. Transitional forms between the two species show a dense concentration of pustules that nearly form a periumbilical ridge in the final chambers (Pl. 3, Fig. 10). The species is rare in its early range but its large size and distinctive appearance make it a reliable biomarker for placement of the base of the upper Turonian *D. concavata* Zone.

Dicarinella canaliculata (Reuss, 1854): Plate 2, Figs. 1–3
Rosalina canaliculata Reuss, 1854, p. 70, pl. 26, fig. 4 (Upper Cretaceous, Austria).
Marginotruncana canaliculata (Reuss), Pessagno, 1967, p. 302–303, pl. 74, figs. 5–8 [neotype], (upper Turonian–Coniacian, Texas).
Dicarinella canaliculata (Reuss), Robaszynski et al., 1979, p. 67–70, pl. 53, figs. 1–3 (upper Turonian–Coniacian, Austria, France).
Remarks. Tanzanian specimens (Pl. 2, Figs. 2–3) show close similarity to the Pessagno's (1967) neotype (new SEM images Pl. 2, Fig. 1). It is characterized by having relatively flattened umbilical and spiral sides, umbilical sutures that are mostly depressed (but slightly raised on some specimens), and a double keel separated by a

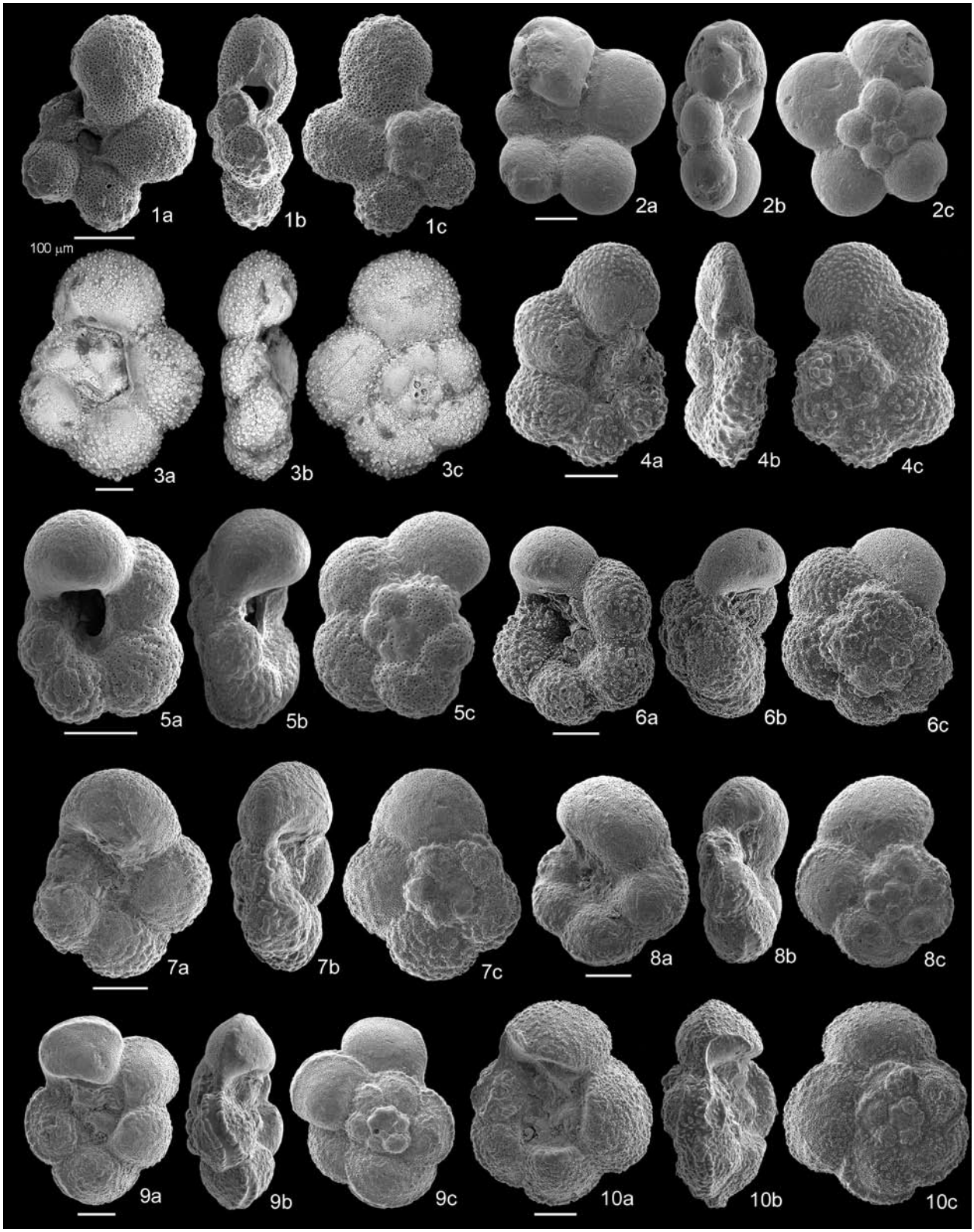

Plate 1. *Muricohedbergella amabilis* (Loeblich and Tappan, 1961), *M. flandrini* (Porthault, 1970), *Whiteinella archaeocretacea* Pessagno, 1967, *W. aprica* (Loeblich and Tappan, 1961), *W. brittonensis* (Loeblich and Tappan, 1961), *Archaeoglobigerina cretacea* (d'Orbigny, 1840), and *Archaeocretacea* sp. from Tanzania Drilling Project sites and holotype images. Figs. 1a–c: *M. amabilis*, TDP 31-19-1, 2–20 cm. Figs. 2a–c: *M. flandrini*, TDP 31-10-1, 19–39 cm. Figs. 3–4, *W. archaeocretacea*; Figs. 3a–c: holotype, USNM #689255; Figs. 4a–c: TDP 30-46-1, 27–45 cm. Figs. 5a–c: *W. aprica*, TDP 31-28-1, 25–35 cm. Figs. 6a–c: *W. brittonensis*, TDP 31-6-1, 80–104. Figs. 7–8, *Archaeoglobigerina* sp.; Figs. 7a–c: TDP 31-26-1, 40–60 cm; Figs. 8a–c: TDP 31-18-2, 20–40 cm. Figs. 9, 10, *A. cretacea*; Figs. 9a–c: TDP 31-14-2, 5–25 cm; Figs. 10a–c: TDP 31-18-2, 20–40 cm. All scale bars = 100 µm.

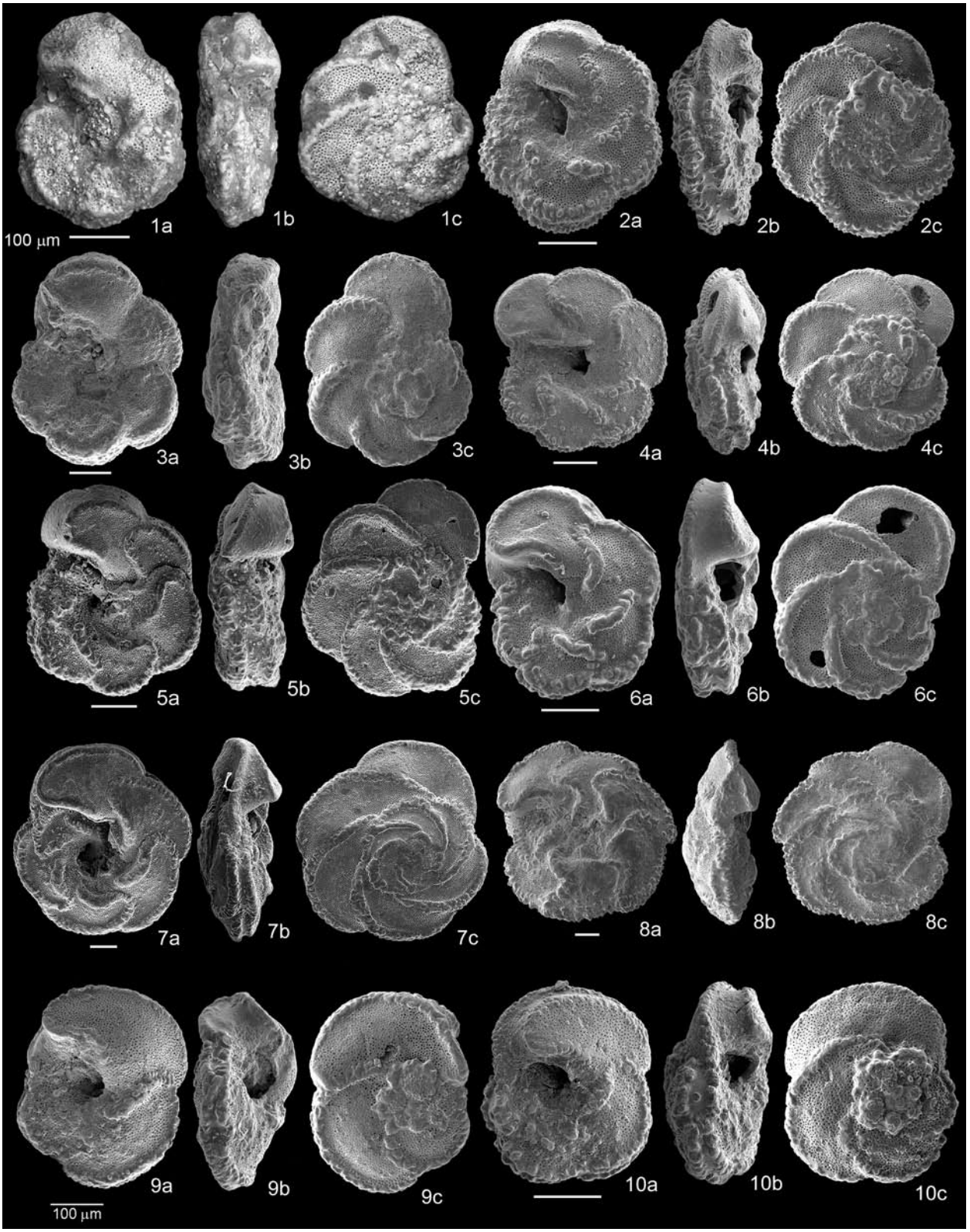

Plate 2. *Dicarinella canaliculata* (Reuss, 1854), *Marginotruncana coldreriensis* (Gandolfi, 1957), *M. sinuosa* (Porthault, 1970), *M. undulata* (Lehmann, 1963), and *Contusotruncana fornicata* (Plummer, 1931) from Tanzania Drilling Project sites and neotype images. Figs. 1–3, *D. canaliculata*; Figs. 1a–c: Neotype, USNM #689260; Figs. 2a–c: TDP 31-19-1, 2–20 cm; Figs. 3a–c: TDP 31-17-1, 2–22 cm. Figs. 4a–c, *M.* cf. *coldreriensis*, TDP 31-21-2, 74–94 cm. Figs. 5–6, *M. pseudolinneiana*; Figs. 5a–c: TDP 31-9-1, 34–51 cm; Figs. 6a–c: TDP 31-19-1, 20–28 cm. Figs. 6a–c, *M. sinuosa*, TDP 31-5-1, 7–29 cm. Figs. 8a–c, *M. undulata*, TDP 31-1-1, 34–50 cm. Figs. 9a–c, *C.* cf. *fornicata* (transitional form), TDP 31-21-2, 74–94 cm. Figs. 10a–c, *C. fornicata*, TDP 31-7-1, 73–92 cm. All scale bars = 100 µm.

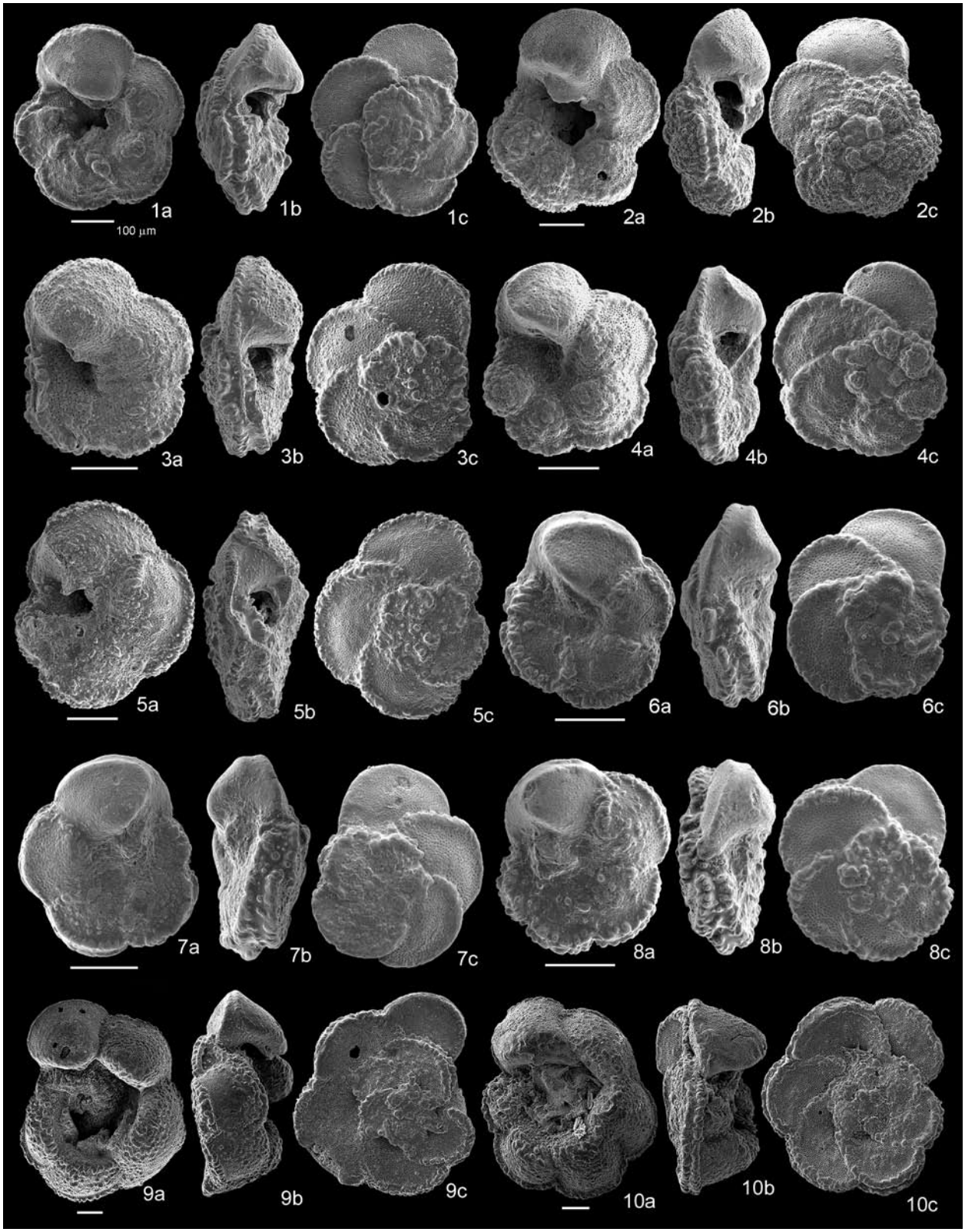

Plate 3. *Dicarinella hagni* (Scheibnerová, 1962) and *D. concavata* (Brotzen, 1934) from Tanzania Drilling Project sites. Figs. 1–8, *D. hagni*: Figs. 1a–c, TDP 22-49-1, 58–72 cm; Figs. 2a–c, TDP 31-19-1, 2–20 cm; Figs. 3a–c, TDP 31-31-1, 40–60 cm; Figs. 4a–c, TDP 31-5-1, 7–29 cm; Figs. 5a–c, TDP 31-31-1, 40–60 cm; Figs. 6a–c, (dwarf form), TDP 22-45-2, 50–67 cm; Figs. 7a–c, (dwarf form), TDP 30-46-2, 41–60 cm; Figs. 8a–c, (dwarf form), TDP 30-46-2, 41–60 cm; Figs. 8a–c, (dwarf form), TDP 22-45-2, 50–67 cm. Figs. 9–10 Figs. 9a–c: *D. concavata*, TDP 31-7-1, 3–20 cm; Figs. 10a–c: *D. concavata* (transitional to *D. asymetrica*), TDP 31-3-1, 38–60 cm. All scale bars = 100 µm.

moderately wide band on all chambers. The LO of this species is in the upper *H. helvetica* Zone at Site 762 but its LO is higher, within the lower *F. maslakovae* Zone, at TDP 31.

Dicarinella hagni (Scheibnerová, 1962): Plate 3, Figs. 1–8
Praeglobotruncana hagni Scheibnerová, p. 1962, p. 219, text-fig. 6a–c (middle Turonian, Czech Republic).
Dicarinella hagni (Scheibnerová), Robaszynski et al., 1979, p. 79–86, pl. 56, figs. 1–2, pl. 5, figs. 1–2 (Turonian, France, Angola).
Remarks. Typical forms included in this species (Pl. 3, Fig. 1) have a biconvex test with 5–6 chambers in the final whorl, umbilical sutures that are radial and usually depressed but are sometimes slightly raised (e. g., Pl. 3, figs. 4a, 5a, 6a, 8a), and a narrowly spaced double keel. Some authors (e. g., Falzoni et al. 2016a) include four-chambered forms (Pl. 3, Fig. 5) in *Dicarinella roddai* (Marianos and Zingula, 1966), but we did not distinguish the latter species because of continuous intergradation of the *hagni* sensu stricto and *roddai* end member morphotypes. Small "dwarf" forms are also included within the *D. hagni* plexus in the TDP sites because of their morphologic similarity to the sensu stricto morphotypes.

At TDP 31 and ODP Site 762 *D. hagni* abruptly disappears at the same level as the extinction of *H. helvetica*, but at the former site it reappears briefly in one sample within the *F. maslakovae* Zone.

Dicarinella imbricata (Mornod, 1950)
Globotruncana imbricata Mornod, 1950, p. 589–590, fig. 5 (IIIa–d).
Dicarinella imbricata (Mornod, 1950), Caron, 1976, p 332–335, figs. 3a–c.
Remarks. The first occurrence of *D. imbricata* in the upper Turonian (lowermost *F. maslakovae* Zone) at TDP 31 is delayed compared to other studies (e. g., Caron 1985, Premoli Silva and Sliter 1995, Falzoni et al. 2016a). Within its range and it is rare and occurs sporadically.

Dicarinella marianosi (Douglas, 1969): Plate 5, Figures 7–10
Globotruncana marianosi Douglas, 1969, p. 341, pl. 2, figs. 3a–c, text-figure 5a–c (Turonian, California, USA).
Dicarinella elata Lamolda, 1977, p. 471–472, pl. 1, fig. 1, pl. 2, fig. 3, text-figs. 3, 4 (lower Turonian, northern Spain).
Remarks. This species was originally placed the genus *Globotruncana* by Douglas (1969) and was described as having a single keel and depressed umbilical sutures. Although Robaszynski et al. (1979) placed this species in *Marginotruncana* it is here moved to *Dicarinella* because of the absence of raised sigmoidal sutures, which Porthault considered a key feature for inclusion within *Marginotruncana*. Because the holotypes of *D. marianosi* and *Dicarinella elata* Lamolda, 1977 are nearly identical (Pl. 5, Figs. 7, 8) and share the same stratigraphic range they are here considered as junior synonym. Tanzanian specimens (Pl. 5, Figs. 9, 10) show variation in the number of chambers in the final whorl and presence of one keel or two narrowly spaced keels that merge into a single keel on the final chambers.

Genus *Falsotruncana* Caron, 1981
Falsotruncana maslakovae Caron, 1981: Plate 4, Figures 3–4
Falsotruncana maslakovae Caron, 1981, p. 66–67, pl. 2, figs. 1–2 (upper Turonian, Tunisia).
Remarks. This is a distinctive species that is distinguished by its flat test profile, petaloid test outline, extra-umbilical primary aperture, and beaded double keels that are separated by a wide, poreless keel band. At TDP 31 its LO is immediately above the extinction of *H. helvetica* whereas at ODP Site 762 its LO is at the top of the *H. helvetica* Zone.

Genus *Globigerinelloides* Cushman and Ten Dam, 1948
Globigerinelloides asper (Ehrenberg, 1854)
Phanerostomum asperum Ehrenberg, 1854, p. 23, pl. 30, figs. 26a.
Not *Phanerostomum asperum* Ehrenberg, 1854, p. 23, pl. 30, figs. 26b.
Globigerinelloides asper (Ehrenberg, 1854), Masters, 1980, p. 96–97, Fig. 1, Pl. 1, figs. 1–5.
Remarks. The species concept of Masters (1980) is followed in the present study. At TDP 31 the taxon first occurs at the base of the *M. sinuosa*/*Hu. huberi* Zone and is very rare and sporadic in its range to the top of the Turonian sequence.

Genus *Helvetoglobotruncana* Reiss, 1957
Helvetoglobotruncana microhelvetica Huber and Petrizzo, n. sp.: Plate 5, Figures 1–6
Description. Test small, inequally biconvex, with a maximum diameter of 200–270 μm and maximum breadth 100 to 130 μm, normal perforate (pore size 1.2 to 2.4 μm), nearly planoconvex, subcircular in equato-

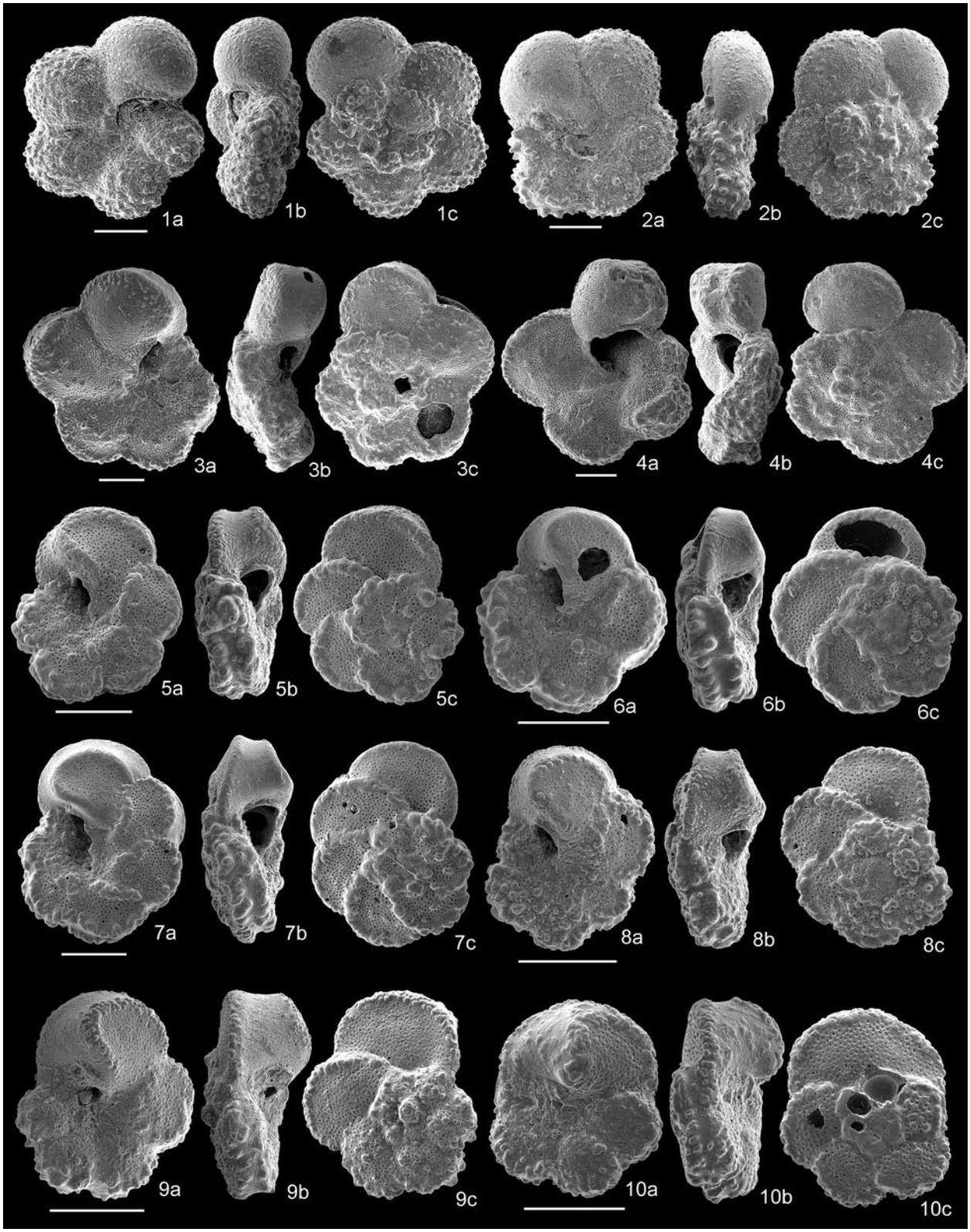

Plate 4. *Muricohedbergella hoelzli* (Hagn and Zeil, 1954), *Falsotruncana douglasi* Caron, 1981, *F. maslakovae* Caron, 1981, and *Marginotruncana caronae* Peryt, 1980 from Tanzania Drilling Project sites. Figs. 1a–c: *M. hoelzli*, TDP 31-25-1, 30–50 cm; Figs. 2a–c: *F. douglasi*, TDP 31-25-1, 30–50 cm; Figs. 3a–c: *F. maslakovae* TDP 31-21-2, 74–94 cm; Figs. 4a–c: *F. maslakovae* TDP 31-19-1, 2–20 cm; Figs. 5a–c: *M. caronae*, TDP 31-26-1, 40–60 cm; Figs. 6a–c: *M. caronae*, TDP 31-26-1, 40–60 cm; Figs. 7a–c: *M. caronae*, TDP 31-19-1, 2–20 cm. Figs. 8a–c: *M. caronae*, TDP 31-21-3, 28–46 cm; Figs. 9a–c: *M. caronae*, TDP 31-25-1, 30–50 cm; Figs. 9a–c: *M.* cf. *caronae* (transitional form), TDP 31-29-3, 71–93 cm. All scale bars = 100 μm.

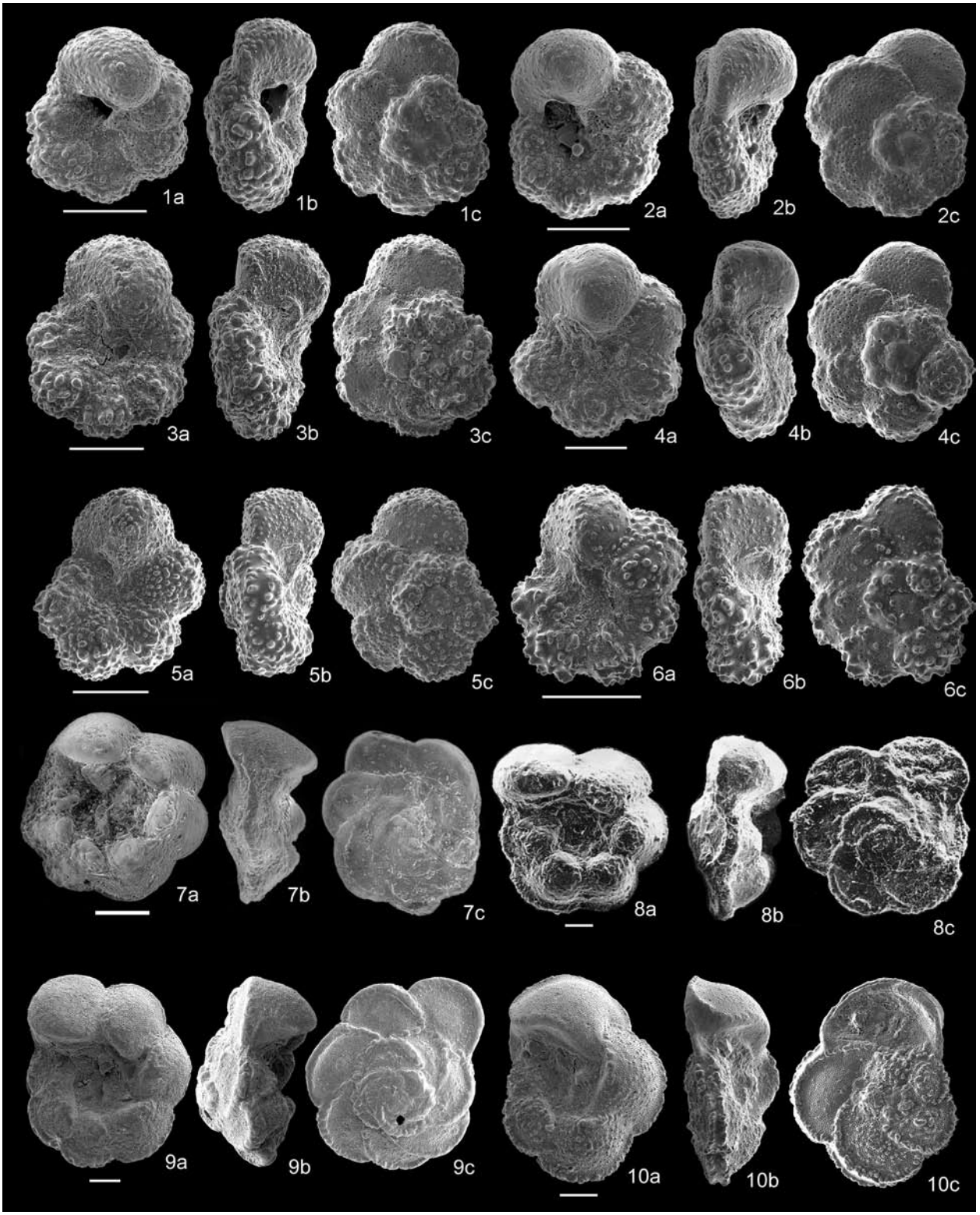

Plate 5. *Helvetoglobotruncana microhelvetica* Huber and Petrizzo, n. sp., *Dicarinella marianosi* (Douglas, 1969), and *Marginotruncana paraconcavata* (Porthault, 1970) from Tanzania Drilling Project sites and holotype images. Figs. 1–6, *H. microhelvetica*: Figs. 1a–c: holotype USNM #637700, TDP 31-28-1, 5–25 cm; Figs. 2a–c: paratype USNM #637701, TDP 31-28-1, 5–25 cm; Figs. 3a–c: paratype USNM #637702), TDP 24-4-2, 98–108 cm; Figs. 4a–c: TDP 31-60-1, 47–67 cm; Figs. 5a–c: TDP 22-43-1, 95–113 cm; Figs. 6a–c: TDP 30-19-1, 38–56 cm. Figs. 7–9, *D. marianosi*: Figs. 7a–c: Holotype UCMP #49003 – CWRUH 013; Figs. 8a–c: holotype of *D. elata* (Lamolda 1977), BIPA #1029, considered junior synonym of *D. marianosi*. Figs. 9a–c: TDP31-57-1, 70–90 cm. Figs. 10a–c, *D. marianosi*, TDP 31-11-1, 0–20 cm. All scale bars = 100 μm.

rial outline; equatorial periphery weakly lobate; peripheral margin imperforate except final chamber, which may or may not be perforate; 12–14 chambers in adult tests increase gradually in size as added, with 5–6 in the final whorl; umbilical chambers inflated, chamber surfaces with randomly scattered, fine to moderate-sized pustules, umblical sutures radial and depressed; spiral chambers petaloid, chamber surfaces slightly inflated, with slight convexity toward the peripheral margin, weakly pustulose to smooth with weak alignment of pustules along the peripheral chamber margin, spiral sutures initially depressed and radial, later with weakly aligned pustules; in edge view final chamber offset with respect to spiral coil surface and final chamber face is slightly concave and angled backwards from the peripheral margin; aperture a circular arch that is mostly extra-umbilical in position and bordered by a narrow lip.

Remarks. This species is distinguished from *H. helvetica* (Bolli, 1945) by its smaller size, presence of a more weakly developed pustulose keel on the peripheral margin, greater convexity of the dorsal chambers surfaces, and a smaller, more circular umbilical-extraumbilical aperture. The maximum test diameter of *H. microhelvetica* mostly ranges between 210 and 280 μm whereas that of *H. helvetica* mostly ranges from 350–600 μm. Transitional forms between these two species (e. g., Huber and Petrizzo 2014, Fig. 7a–c) occur in some samples.

Test size. Maximum test diameter: holotype 212 μm, illustrated paratype and hypotypes 209 to 264 μm; maximum breadth: holotype 125 μm, illustrated paratype and hypotypes 97 to 128 μm.

Type locality and repository. Holotype USNM 637700 (Pl. 5, Fig. 1) and paratypes USNM 637701–637702 (Pl. 5, Figs. 2–3) deposited at the Smithsonian National Museum of Natural History and selected from Tanzania Drilling Project Site 31 (10° 1 49.80 S, 39° 38 44.00 E), Sample TDP 31-28-1, 5–25 cm (46.25 meters below surface) in the upper *H. helvetica* Zone of the Lindi Formation.

Etymology. Prefix "micro" used with *helvetica* to reflect its smaller size and close phylogenetic relationship to *H. helvetica*.

Phylogenetic relationships. Similarity to *H. helvetica* suggest they are closely related, but presence of an unconformity that truncates the lower range of both species prevents determination of which is the ancestral species.

Stratigraphic range. Restricted to the late early through middle Turonian *H. helvetica* Zone.

Geographic distribution. Identified at all Tanzanian Drilling Project boreholes that recovered sediments from the *H. helvetica* Zone but has not been found at any other location outside Tanzania.

Genus *Huberella* Georgescu, 2007

Huberella huberi Georgescu, 2007

Huberella huberi Georgescu, 2007, p. 214, pl. 2, figs. 1–6, pl. 3, fig. 1 (upper Turonian, DSDP Site 150, Caribbean).

Remarks. The LO of this species has been recorded in the upper Turonian at DSDP Sites 95, 150, and 465 (Georgescu 2007). At TDP 31 its LO is at 27.30 mbs (TDP 31-18-2, 20–40 cm) and it occurs consistently through the *D. concavata* Zone (Haynes et al. 2015). It is here defined as a zonal marker for the upper Turonian because of its distinctive morphology, consistent stratigraphic appearance, and wide geographic distribution.

Genus *Marginotruncana* Hofker, 1956

Remarks. We follow Porthault's (1970) emendation of this genus to include only species with elevated sigmoidal sutures on the umbilical side.

Marginotruncana cf. *M. caronae* Peryt, 1980

Marginotruncana caronae Peryt, 1980, p. 60, pl. 15, figs. 1a–c. Falzoni et al., 2016, p. 82–83, Fig. 11, 1–2 (upper Turonian, central Poland).

Remarks. This species is distinguished from co-occurring marginotruncanids based on its plano-convex test profile, fewer number of chambers (4.5 to 5 chambers in the final whorl), slight inflation of spiral chamber surfaces, and greater convexity of the adumbilical chamber surfaces. Only the spiral view of the holotype and edge and spiral views of two different paratypes were illustrated by the author and the SEM images are high in contrast such that some details are difficult to interpret. The paratype showing an umbilical view appears to have umbilical sutures that are weakly depressed and mostly radial, suggesting placement in *Dicarinella* may be more appropriate than in *Marginotruncana*.

Falzoni et al. (2016a) extended the range of *M. caronae* into the upper Cenomanian in their study of the Clot Chevalier section in the Vocontian Basin (SE France). Their illustrated specimens appear to have radial, weakly depressed umbilical sutures bordering the ultimate and penultimate chambers, but the penultimate suture appears to be raised and slightly sigmoidal on at least one specimen (Falzoni et al. 2016a,

Fig. 11–2a). The umbilical chambers of their specimens are not as inflated as the species Peryt's (1980) primary type specimens.

Tanzanian specimens identified in the present study as *M. caronae* differ from the type species and specimens illustrated by Falzoni et al. (2016a) by their smaller size and presence of raised sigmoidal umbilical sutures between most chambers. We apply a broad concept for this highly variable species but we acknowledge that further comparison of specimens from all three localities is needed to clarify whether they are conspecific.

In central Poland *M. caronae* was described from upper Turonian through lower Santonian sediments. At TDP 31 and ODP Site 762 the LO of *M. caronae* is recorded at the top of the *H. helvetica* Zone and it occurs in most samples through the *D. concavata* Zone. Absence of specimens in the middle and lower *H. helvetica* Zone for both sites is puzzling given its distribution in the Vocontian Basin.

Marginotruncana angusticarenata (Gandolfi, 1942)
Globotruncana linnei (d'Orbigny) *A. angusticarenata* Gandolfi, 1942, p. 126, 15, 153, pl. 4, figs. 17, 30, text-fig. 46 (3a–c).
Marginotruncana angusticarenata (Gandolfi, 1942), Pessagno, 1967, p. 300–301, pl. 65, figs. 14–19, pl. 98, figs. 5, 9–11.
Remarks. The LO of this species at TDP 31 is in the upper *F. maslakovae* Zone and it occurs sporadically until the *D. concavata* Zone where it occurs consistently. At TDP 39 it ranges through the *D. asymetrica* Zone.

Marginotruncana cf. *coldreriensis* (Gandolfi, 1957): Plate 2, Figure 4
Globotruncana renzi Gandolfi, 1942, pl. 3, fig. 1A–C (lower Turonian, Switzerland).
Globotruncana coldreriensis Gandolfi, 1957, pl. 9, fig. 7AeC (lower Turonian, Switzerland).
Marginotruncana cf. *coldreriensis* (Gandolfi, 1942), Falzoni et al., 2016, p. 83–85, fig. 11, 3a–c (lower Turonian, SE France).
Remarks. The complicated taxonomic history and distinguishing features of this species were summarized by Falzoni et al. (2016). We follow the latter authors in distinguishing this species from *M. renzi* Gandolfi by the presence of less inflated umbilical chambers bordered by more distinctly sigmoidal umbilical sutures and by having a more convex spiral side. We advocate continued use of open nomenclature for the species until a neotype for the species is selected and until clear distinction of well-preserved *renzi* and *coldreriensis* is made from study of a sample series containing both species.

Marginotruncana pseudolinneiana Pessagno, 1967: Plate 2, Figures. 5, 6
Marginotruncana pseudolinneiana Pessagno, 1967, p. 310, pl. 65, figs. 24–27, pl. 76, figs. 1–3 (upper Coniacian to lower Santonian, Austria).
Remarks. This species is characterized by having a planar spiral side, a planar to slightly convex umbilical side and paired keels that are separated by a wide keel band and it is generally a relatively large in size ($>$ 350 μm). Small forms (200 to 350 μm) are relatively common in the early part of its range in the upper Turonian at TDP 31, whereas larger forms predominate higher in the section.

Genus *Muricoglobigerina* Huber and Leckie, 2011
Muricoglobigerina flandrini (Porthault, 1970): Plate 1, Figure 2
Hedbergella flandrini Porthault, 1970, p. 64–65, pl. 10, figs. 1–3.
Remarks. This species was originally described from mid-Coniacian through lower Santonian sediments in southeastern France for forms having a compressed test with a lobate outline, a rounded equatorial peripheral margin, and five chambers in the final whorl. At TDP 31 it first occurs in the middle of the *M. schneegansi*/*Hu. huberi* Zone (upper upper Turonian), whereas it occurs older sediments assigned to the *F. maslakovae* Zone (lower upper Turonian) at ODP Site 762. This species appears similar to *M. amabilis* (Loeblich and Tappan, 1961), which also has a compressed test with a lobate equatorial outline (see Pl. 1, Fig. 1), but *M. flandrini* is distinguished by having a more rounded peripheral margin, a smoother test surface, and smaller wall pores (*M. flandrini* pore diameters are $<$ 2.0 μm and average 1.6 μm; *M. amabilis* pore diameters are $>$ 3.5 μm and average 4.0 μm).

Praeglobotruncana Bermúdez, 1952
Praeglobotruncana gibba Klaus, 1960: Plate 6, Figure 10
Praeglobotruncana var. *gibba* Klaus 1960, p. 304–305, holotype designated in Reichel, 1950, pl. 16, fig. 6, pl. 17, fig. 6.
Remarks. The higher spire used to distinguish *P. gibba* from its ancestor *P. stephani* is a transitional feature that sometimes makes the two species difficult to distinguish.

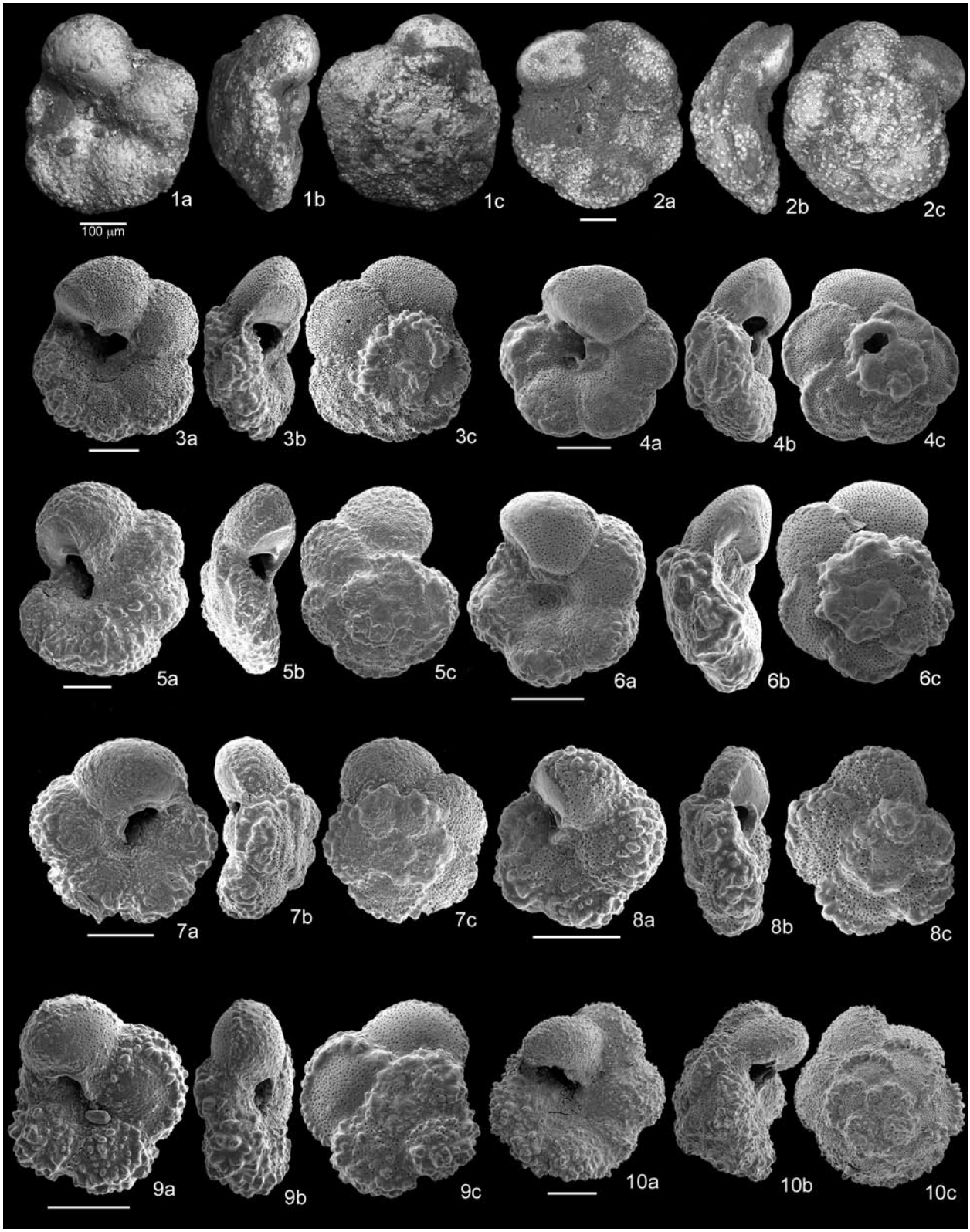

Plate 6. *Praeglobotruncana stephani* (Gandolfi, 1942) and *P. gibba* Klaus, 1960, from Tanzania Drilling Project sites and holotype of *P. hilalensis* Barr, 1972. Figs. 1, 3–9, *P. stephani*: Figs. 1a–c, holotype; Figs. 3a–c: TDP 29-10-2, 32–51 cm; Figs. 4a–c: TDP 31-28-1, 25–35 cm; Figs. 5a–c: TDP 31-63-1, 29–49 cm; Figs. 6a–c: dwarf specimen, TDP 31-17-1, 2–22 cm; Figs. 7a–c: dwarf specimen, TDP 31-21-1, 45–65 cm; Figs. 8a–c: dwarf specimen, TDP 31-20-1, 16–36 cm; Figs. 9a–c: dwarf specimen, TDP 31-54-1, 70–90 cm. Fig. 2, *P. hilalensis*, holotype, USNM #167852. Fig. 10, *P. gibba*, TDP 22-8, 33–55 cm. All scale bars = 100 µm.

Praeglobotruncana stephani (Gandolfi, 1942):
Plate 6, Figures 1, 3–9
Globotruncana stephani Gandolfi, 1942, p. 130, 137, pl. 3, figs. 4, 5, pl. 6, figs. 4, 6, pl. 9, figs. 5, 8 (upper Albian, Switzerland).
Praeglobotruncana stephani (Gandolfi), Robaszynski et al., 1979, p. 47–50, pl. 48, figs. 1–3 (upper Albian, Switzerland).

Remarks. This species has been characterized as having a continuous gradation of morphologies between the lower spired, smaller, and more lobate *P. delrioensis* (Plummer) and the higher spired, larger, and more circular *P. gibba* Klaus, 1960 (Pl. 6, Fig. 10) and it has been described under a number of species names that are now considered as junior synonyms (Loeblich and Tappan, 1961). It was originally described as having aligned pustules that form a single keel, but the emendation of the species by Falzoni et al. (2016) allows for development of a double row of pustules in more advanced specimens. The species is distinguished from *P. hilalensis* Barr, 1972 (Pl. 6, Fig. 2) by having a more lobate peripheral outline, and less convex spiral side, and a less narrowly defined peripheral keel.

High variability is also observed in the Turonian TDP populations, with some forms showing close similarity with the holotype (Pl. 6, Figs. 1, 3) and others showing significant variation in in test size and convexity as well as in the angularity and expression of a narrow vs. broad band of pustules along the peripheral margin (Pl. 6, Figs. 4–9). An ecophenotypic control on the test size may be indicated by the presence of only small or dwarfed forms of the species in samples from above the top of the *H. helvetica* Zone (Fig. 4).

Appendix 2: Alphabetical Listing of Species

Below is an alphabetical listing of all planktonic foraminiferal species included in the range charts but not included in the taxonomic discussion above.

Helvetoglobotruncana helvetica (Bolli, 1945)
Helvetoglobotruncana praehelvetica (Trujillo, 1960)
Huberella praehuberi Georgescu, 2007
Marginotruncana coronata (Bolli, 1945)
Marginotruncana angusticarenata (Gandolfi, 1942)
Marginotruncana schneegansi (Sigal, 1952)
Marginotruncana sinuosa Porthault, 1970: Plate 2, Figure 7
Marginotruncana tarfayensis (Lehman, 1963)
Marginotruncana undulata (Lehman, 1963): Plate 2, Figure 8
Marginotruncana sigali (Reichel, 1950) s.l.
Muricohedbergella hoelzli (Hagn and Zeil, 1954)
Planoheterohelix globulosa (Ehrenberg, 1840)
Planoheterohelix paraglobulosa (Georgescu and Huber, 2009)
Planoheterohelix postmoremani Georgescu and Huber, 2009
Planoheterohelix praenuttalli Haynes, Huber and MacLeod, 2015
Pseudotextularia nuttalli (Voorwijk, 1937)
Whiteinella aprica (Loeblich and Tappan, 1961)
Whiteinella baltica Douglas and Rankin, 1969
Whiteinella brittonensis (Loeblich and Tappan, 1961)

Below is an alphabetical listing of all calcareous nannofossil species included in the range charts and discussion above.

Calcicalithina alta Perch-Nielsen 1979
Chiastozygus spissus Bergen in Bralower & Bergen, 1998
Eiffellithus casulus Shamrock and Watkins, 2009
Eiffellithus digitatus Shamrock and Watkins, 2009
Eiffellithus eximius (Stover, 1966) Perch-Nielsen, 1968
Eiffellithus perchnielseniae Shamrock and Watkins, 2009
Eiffellithus turriseiffellii (Deflandre *in* Deflandre and Fert, 1954) Reinhardt, 1965
Eprolithus moratus (Stover, 1966) Burnett, 1998
Helicolithus turonicus Varol and Girgis, 1994
Liliasterites angularis Svábenická and Stradner *in* Stradner and Steinmetz, 1984
Lithastrinus septenarius Forchheimer, 1972
Marthasterites furcatus (Deflandre *in* Deflandre and Fert, 1954) Deflandre, 1959
Micula adumbrata Burnett, 1997
Micula cubiformis Forchheimer, 1972
Micula staurophora (Gardet, 1955) Stradner, 1963
Quadrum gartnerii Prins and Perch-Nielsen *in* Manivit et al., 1977
Radiolithus planus Stover, 1966
Reinhardtites biperforatus (Gartner, 1968) Shafik, 1979
Rhagodiscus achylostaurion (Hill, 1976) Doeven, 1983
Rhombaster svabenickiae Bergen *in* Bralower & Bergen, 1998
Stoverius achylosus (Stover, 1966) Perch-Nielsen, 1986
Stoverius coronatus (Bukry, 1969) Perch-Nielsen, 1984
Tranolithus minimus (Bukry, 1969) Perch-Nielsen, 1984